DISSERTATION

Antibiotic use during pregnancy increases allergic asthma severity in murine offspring: Establishing a causal association and identifying potential mechanisms

Pränatale Antibiotikaeinnahme erhöht den allergischen Asthmaschweregrad bei Mäusenachkommen: Nachweis eines kausalen Zusammenhangs und Ermittlung potenzieller Mechanismen

zur Erlangung des akademischen Grades
Doctor rerum medicinalium (Dr. rer. medic.)

vorgelegt der Medizinischen Fakultät
Charité – Universitätsmedizin Berlin

von
Moumen Mahmoud-Alzain Alhasan

Erstbetreuung: PD Dr. Conrad, Melanie

Datum der Promotion: 28. Februar 2025

Table of contents

List of tables

List of figures

List of abbreviations

Abbr.	Meaning
AHR	Airway hyperreactivity
BAL	Bronchoalveolar lavage
BSA	Bovine serum albumin
CD	Cluster of differentiation
COD	Coefficient of determination
CT	Cycle threshold
CpG	5'-Cytosine-phosphate-Guanine-3'
DC	Dendritic cell
DOHaD	Developmental Origins of Health and Disease
EDTA	Ethylenediaminetetraacetic acid
ELISA	Enzyme-linked immunosorbent assay
Eub	Eubacterial
FACS	Fluorescence-activated cell sorting
FCεRIα	Fc receptor, IgE, high affinity I, alpha polypeptide
FDA	U.S. Food and drug administration
FID	Flame ionization detector
FITC	Fluorescein isothiocyanate
FOXP3	Forkhead box protein 3
FSC	Forward scatter
G	Gestation day
G-CSF	Granulocyte colony-stimulating factor
HDAC	histone deacetylase
H&E	Hematoxylin and eosin staining.
IFN	Interferon

Ig	Immunoglobulin
IL	Interleukin
ILC	Innate lymphoid cell
IP	Intraperitoneally
IPQ	Isotopic pattern quality
KC	Keratinocyte chemoattractant
LAGeSo	Landesamt für Gesundheit und Soziales
LG	Lines of goblet cells
LnG	Lines of non-goblet cells
LPS	Lipopolysaccharide
LV	Line of blood vessel
MCP	Monocyte chemoattractant protein
MFI	Mean fluorescence intensity
MS	Mass spectrometry
NCR	Natural cytotoxicity receptor
newCAST	New computer-assisted stereological toolbox
NK	Natural killer
Nu.G	Number of goblet cells
OVA	Ovalbumin
PAS	Periodic acid-schiff
PBS	Phosphate-buffered saline
PcoA	Principal component analysis
PCR	polymerase chain reaction
PCR-DGGE	PCR-based denaturing gradient gel electrophoresis
PG	Points of Goblet cells
PI	Point of inflammation

PMA	phorbol 12-myristate 13-acetate
PN	Postnatal day
qPCR	Quantitative polymerase chain reaction
RANTES	Regulated upon Activation, Normal T cell Expressed, and Secreted
RBC	Red blood cells
Rn	Newtonian resistance
RORγt	Retinoid-related orphan receptor gamma t
RPM	Revolutions per Minute
RR	Relative risk
RT	Room temperature
SC	Subcutaneous
SCFA	Short-chain fatty acid
SDS	Sodium dodecyl sulfate
SEM	Standard error of the mean
SI-LP	Small intestine lamina propria
SiglecF	Sialic acid-binding Ig-like lectins 5
S/N	Signal-to-nose ration
SPF	Specific pathogen free
SSC	Side scatter
T-bet	T-Box protein expressed in T cells
Th	T helper
TNF	Tumor necrosis factor
Vol.G	Volume of goblet cells
Vol.Inf	Volume of inflammation

Abstract in Deutsch

Einleitung: Asthma ist eine sowohl genetisch als auch durch die Umwelt beeinflusste Lungenerkrankung, die sich durch Husten, Keuchen und Atemnot äußert. Der Zusammenhang zwischen der Einnahme von Antibiotika während der Schwangerschaft und dem erhöhten Asthmaschweregrad bei Kindern wurde in vielen Studien vorgeschlagen. Allerdings sind die Mechanismen jedoch noch nicht gründlich untersucht worden.

Zielsetzung: Das Ziel in diesem Projekt ist, ein Mausmodell zu etablieren, um die Auswirkungen der pränatalen Antibiotikaexposition auf die Asthmaentwicklung bei Nachkommen zu untersuchen. Außerdem soll die Wirkung der Dysbioseübertragung auf die Immunsystem- und Asthmaentwicklung untersucht werden.

Methoden: Trächtige Mäuse wurden mit Vancomycin oder Wasser behandelt, dann wurden die Nachkommen einem Asthma-Protokoll unterzogen. Der Asthmaschweregrad wurde bei Nachkommen ermittelt (durch Die Bestimmung der Leukozytenzahl der bronchoalveoläre Lavage, Zytokin- und Serumantikörpermessungen, Lungenhistologie und bronchiale Hyperreaktivität-Test). RNA-Sequenzierung und Gaschromatographie wurden eingesetzt, um die Darmmikrobiom-Zusammensetzung und die Konzentration kurzkettiger Fettsäuren zu erforschen. Dünndarm, Blut und Lunge der Nachkommen wurden immunphänotypisiert, und die Darmentzündung und das Leaky-Gut wurden untersucht. Schließlich wurde der mütterliche Darm und die Milchzusammensetzung während der Stillzeit untersucht.

Ergebnisse: Asthma-Analyse: Pränatal-Antibiotika-Nachkommen zeigten einen schwereren Asthmagrad als Pränatal-Kontrolle-Nachkommen (erhöht: BAL-Eosinophilen, Serum-Gesamt-IgG1, OVA-IgG1 und OVA-IgE, Lungenentzündung und Atemwegswiderstand). Mikrobiota-Analyse: Die Vancomycin-Behandlung war mit einer Darmdysbiose bei Müttern und Nachkommen verbunden. Gram-negative *Bacteroides* und *Escherichia* waren angereichert, während die Produzenten kurzkettiger Fettsäuren (SCFA), Ruminococcus und Clostridium, dezimiert waren. Dies ging mit verringerten fäkalen SCFA-Konzentrationen, einer erhöhten Darmentzündung bei den Nachkommen, Leaky-Gut und der Verbreitung von Lipopolysacchariden in den Blutkreislauf einher.

Durchflusszytometrie: Die Darmdysbiose der Nachkommen war mit einem entzündlichen ILC3-Phänotyp im Darm verbunden. Das Blut wies einen erhöhten Anteil an RORγt+ T-Helferzellen (Th-Zellen) und eine erhöhte Eosinophilen-Aktivierung auf, und auch in der

Lunge war der Anteil an RORγt+ Th-Zellen im frühen Leben und nach der Asthma-Induktion erhöht.

Schlussfolgerung: Die pränatale Antibiotikaexposition war mit einer Darmdysbiose, verminderten SCFA-Konzentrationen und Entzündungen im Darm säugender Mäuse verbunden, was zu einer Disposition von LPS im Serum führte. Dies ging mit einem erhöhten Anteil an RORγt+ Th-Zellen im Blut und in der Lunge während des frühen Lebens einher. Wir stellen die Hypothese auf, dass dieser Prozess zu dem in unserem Modell beobachteten erhöhten Schweregrad des Asthmas beiträgt.

Abstract in English

Introduction: Asthma is a pulmonary disease influenced by both genetics and the environment, that manifests with cough, wheezing and breathing difficulties. Many studies have linked antibiotic use during pregnancy to increased asthma severity in children; however, the underlying mechanisms have not been thoroughly investigated.

Objective: This project aims to establish a mouse model to study the impact of prenatal antibiotic exposure on offspring asthma development. Further, we will investigate how the mother-offspring transfer of antibiotic-induced gut microbial dysbiosis influences immune system development and the severity of allergic asthma.

Methods: Pregnant mice were treated orally with vancomycin or water (control), then the offspring were subjected to an ovalbumin experimental asthma protocol. Asthma severity was assessed in allergic offspring (bronchoalveolar lavage (BAL) differential cell counts, cytokine and serum antibody measurements, lung histology and airway reactivity). 16sRNA sequencing and gas chromatography were used to longitudinally examine fecal gut microbiome composition and short chain fatty acid concentrations in mothers and offspring. Offspring small intestine, blood and lung were immunophenotyped by flow cytometry, and intestinal inflammation and barrier permeability were assessed (through lipocalin-2, lipopolysaccharide and FITC-Dextran assays). Finally, immunohistochemistry was performed on the maternal intestine during lactation, and breast milk composition was assessed.

Results: **Asthma phenotype:** Allergic offspring from vancomycin treated mothers showed a more severe asthma phenotype than allergic offspring from control mothers (increased: BAL eosinophils, serum total IgG1, OVA IgG1 and OVA IgE, lung inflammation and airway resistance). **Microbiota analysis**: Maternal vancomycin treatment was

associated with gut dysbiosis in mothers and offspring. Gram-negative *Bacteroides* and *Escherichia* were enriched, whereas short-chain fatty acid (SCFA) producers *Ruminococcus* and *Clostridium* were depleted. This was associated with decreased fecal SCFA concentrations, increased intestinal inflammation in the offspring, compromised gut barrier integrity and lipopolysaccharide dissemination to the circulation.

Flow cytometry: Offspring intestinal dysbiosis was associated with an inflammatory ILC3 phenotype in the intestine. Blood from dysbiotic offspring showed increased RORγt^+ T helper cell percentages and eosinophils activation, and the lungs also held increased RORγt^+ Th cell percentages in early life and after asthma induction.

Conclusion: Prenatal antibiotic exposure was associated with gut dysbiosis, decreased SCFA concentrations and inflammation in the gut of suckling mice, leading to disposition of LPS in the serum. This was accompanied by increased RORγt^+ Th cell percentages in the blood and lung during early life. We hypothesize that this process contributes to the increased asthma severity seen in our model.

1. Introduction

1.1. Asthma definition, manifestations and etiology

Allergic asthma is a chronic inflammatory disease of the airways, which is increasing in prevalence worldwide, especially in children in industrialized countries [1,2]. In 2023 update of the Global burden of chronic respiratory diseases and risk factors, it was estimated that more than 260 million people have asthma, which is responsible for over 460,000 deaths worldwide [3] Affecting 1 in 10 children and 1 in 12 adults, asthma is manifested by cough, wheezing and airway contraction with accumulated mucous and shortness of breath [4].

Allergic asthma occurs when the immune system becomes intolerant toward aeroantigens such as pollen, household dust mites or animal hair, and is characterized by type 2 airway inflammation.[2]. During an asthma exacerbation, dendritic cells phagocytose airborne allergens and migrate to the lymph nodes where they present allergen to naïve T cells, stimulating their differentiation to CD4+ Th2 cells. Simultaneously, lung epithelial and tuft cells produce alarmins such as thymic stromal lymphopoietin (TSLP), IL-25 and IL-33, which contribute to the differentiation and activation of Th2 cells and type 2 innate lymphoid cells (ILC2). These cell types then produce IL-4, IL-5, IL-9 and IL-13, as well as other cytokines, which further promote type 2 inflammation, shown in Figure 1 [2,5].

Type 2 inflammatory cytokines contribute to allergic lung inflammation in several different ways. IL-4 and IL-13 stimulate B cell class switching to IgE-producing plasma cells, and the binding of IgE to the FcεRI on the lung basophils and mast cells stimulates release of inflammatory compounds. IL-5 mediates eosinophil recruitment to the airways where they degranulate releasing major basic protein (MBP), eosinophil cationic protein (ECP), and eosinophil peroxidase (EPO) that damage the lung epithelial cells and stimulate the release of alarmins in a positive feedback loop [2]. Finally, IL-4, IL-9 and IL-13 also induce goblet cell mucus production, which accumulates and further contributes to constriction of the airways shown in Figure 1[2,5]. Shortness of breath is brought on by airway constriction, due to both mucous secretion and fluid leakage from inflamed airways. This leakage happens due to increased vascular permeability mediated by histamine and leukotrienes [2,6]. Long-term persistent inflammation in the lung causes disease chronification and remodeling of the airways, which worsens lung condition and significantly affects quality of life [2].

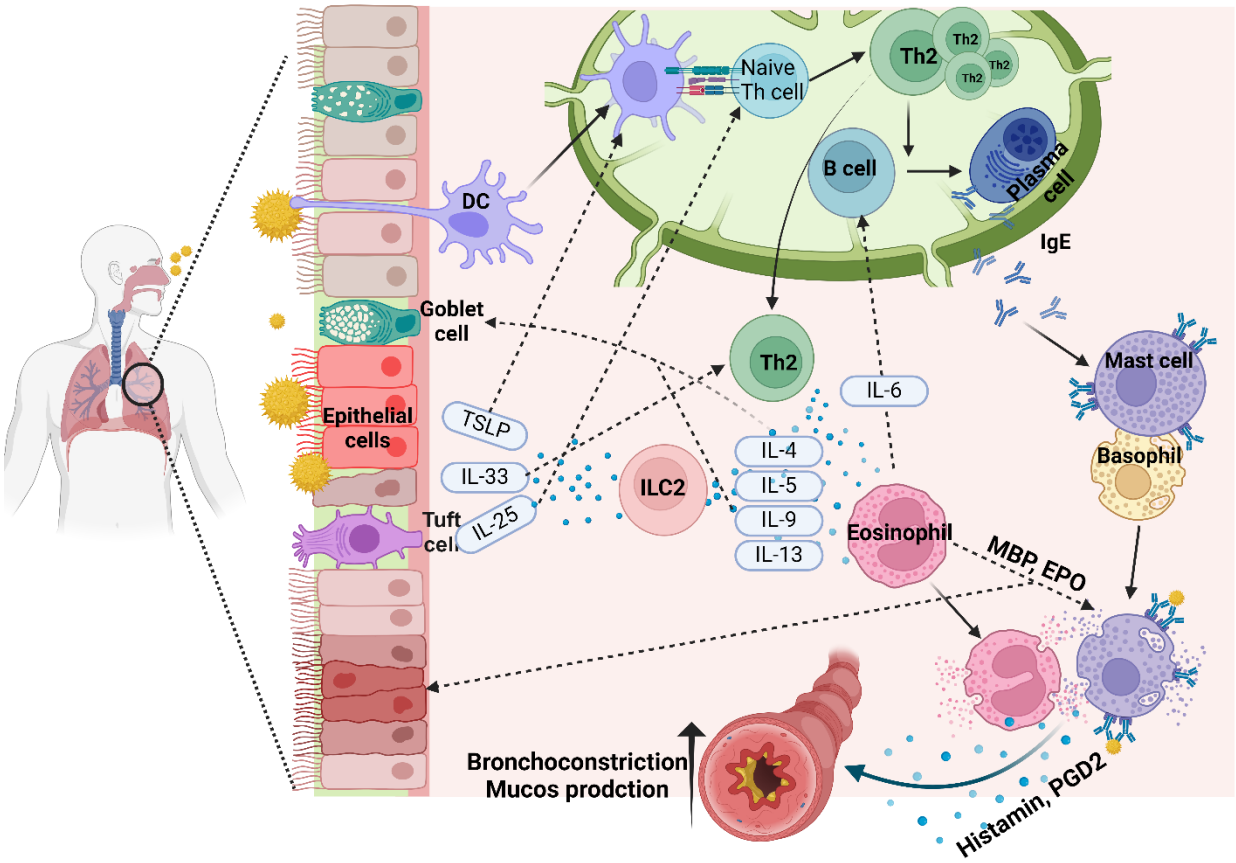

Figure 1. Allergic asthma mechanisms.

When an allergen enters the lower airways, it is sampled by dendritic cells and presented to T cells, which stimulates their differentiation to Th2 cells and initiation of a type 2 inflammatory reaction. This reaction can be also stimulated via ILC2s that are stimulated by epithelial signals. Both Th2 cells and ILC2s produce multiple Type2 inflammatory cytokines that induce the production of IgE, and recruit eosinophils, basophils and mast cells to the lung. Mediators produced by these cells are responsible for asthma inflammation mucus overproduction, leading to symptoms of cough, wheeze and airways constriction [own representation]. Figure created with BioRender.com.

Asthma is a complex multifactorial disease controlled by our genes, lifestyle and the environment. Though hereditary factors play a major role in asthma development [7], recent research has demonstrated that environmental factors can also strongly affect asthma susceptibility, especially when they occur prenatally or during early life. For instance, both human and mouse studies show that helminth infections [8,9], living on a farm [10–12] and prenatal exposure to farm bacteria during fetal development [13] are protective factors against asthma. On the other hand, pre- and postnatal exposure to antibiotics [14–16], excessively hygienic living conditions [17], C-section delivery [18,19] a westernized lifestyle [17,20] and several other factors are linked to the increased risk for asthma in children, shown in Figure 2. The environment in which we develop can either protect against or increase the risk for having asthma in childhood.

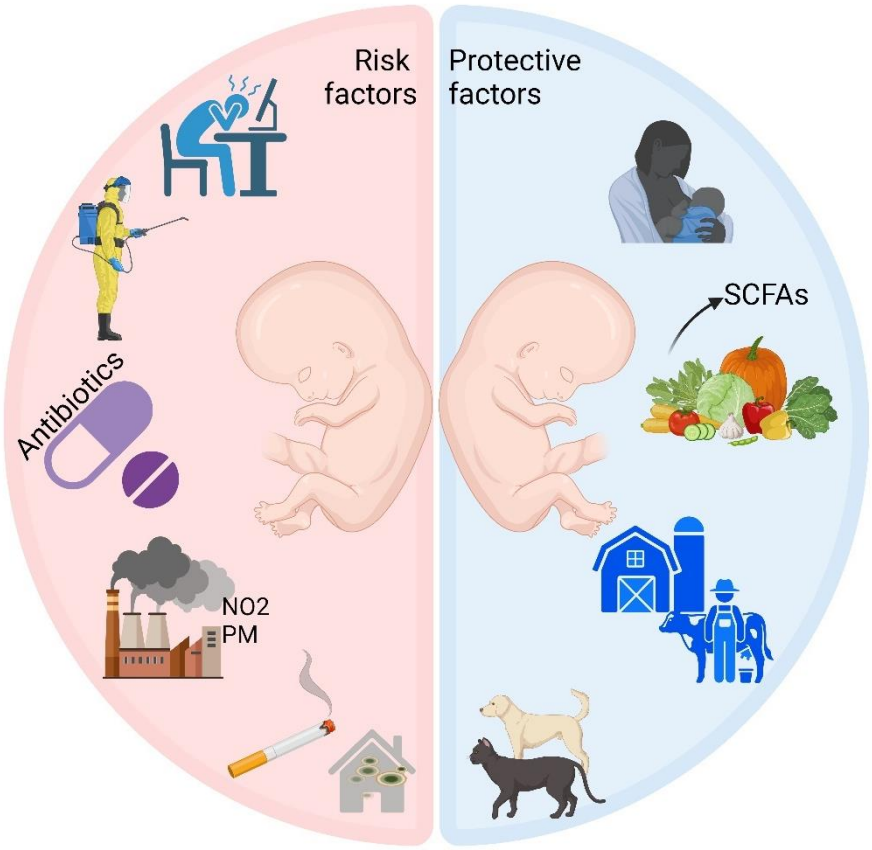

Figure 2 The impact of the environmental factors during early-life on allergic asthma development in children.

Maternal exposure during pregnancy to stress, pesticides, antibiotics, air pollution (e.g. nitrogen dioxide NO2 and particulate matter PM) or smoke is associated with increased asthma risk in children. Protective factors against asthma during the perinatal time period include breastfeeding, fiber rich food, exposure to a traditional farming environment and having pets [own representation]. Figure created with BioRender.com.

1.2. The Developmental Origins of Health and Disease hypothesis (DOHaD)

In the mid-80s, Barker observed that maternal malnutrition during the second and third trimester of pregnancy was associated with increased morbidity and mortality in the next generation due to coronary heart diseases in adulthood [21]. This led to the Fetal Origins hypothesis, which states that improper nutrition during fetal development and low birth weight, could contribute to increased blood pressure in adulthood and/or the induction of metabolic disorders later in life [22]. Parallels were made to this, by the epidemiologist David Strachan in 1989, through his work on bacterial exposure in early life and the development of allergic diseases. Strachan observed that a larger family size was associated with a lower risk of allergic rhinitis during childhood [23]. Bach et al. (2002) indirectly confirmed this correlation when they reported that an observed decrease in incidence in infectious diseases from 1950-2000 was accompanied by an increased incidence in

allergic diseases [24]. In their pursuit to discover the mechanisms behind this correlation, Romagnani et al. (2004) proposed that bacterial exposures in early life could potentiate Th1 cells to suppress Th2 immunity[25], whereas Yazdanbakhsh and Wills-Karp (2001) proposed that the decreased bacterial exposure in early life (for instance, due to a small family size) could affect tolerance mechanisms by reducing regulatory T helper cell (Treg) populations and the production of the cytokine interleukin (IL)-10 [17,26]. Eventually, the Fetal Origins and Hygiene hypotheses provided the basis for the Developmental Origins of Health and Disease (DOHaD) hypothesis, which postulates that exposure to environmental factors during the fetal and neonatal time periods can positively or negatively affect immune system development and contribute to disease susceptibility in later life [27–29].

1.3. Antibiotic use during pregnancy and offspring asthma risk

Since the development of the first antibiotic called Salvarsan in Paul Ehrlich's lab 100 years ago, the human life span has increased by an average of 23 years [30]. Antibiotics can be chemically synthesized as well as naturally produced by different bacteria and fungi, and the 25 clinically used antibiotic classes work either by stopping growth (bacteriostatic antibiotics) or by killing the bacteria (bactericidal antibiotics). According to the global antibiotic consumption report 2021, the global antibiotic consumption rate was 14.3 doses per 1000 population per day in 2018. This was accompanied by a 46% increase in antibiotic use between 2000 and 2018. These numbers indicate that antibiotics are being overprescribed, which could have long-term consequences for global health [31].

Pregnant women are more susceptible to infection due to hormonal changes and physiological alterations designed to prevent the rejection of the allogenic fetus [32]. As a result, antibiotic use during pregnancy is very common, with 8 out of 10 prescriptions written for antibiotics, and approximately 25% of pregnant women receiving at least one antibiotic course during pregnancy [33,34]. Epidemiological studies have linked the use of antibiotics during pregnancy with increased susceptibility towards asthma and allergic diseases in children. Initial human cohort studies, in the UK [35] and Denmark [36] drew attention to the correlation between prenatal antibiotic exposure and increased asthma prevalence in children. These initial studies were followed by many others, and while the majority of studies linked antibiotic use during pregnancy with the increased asthma risk in children [37–44] some studies attributed this risk to an increased maternal propensity for infections rather than to antibiotic use itself [45]. Other researchers implied that the observed increase in asthma risk was due to confounding by factors shared by siblings [38,46].

The use of mouse models is an ideal approach to confirm the epidemiological evidence for prenatal antibiotic exposure and asthma susceptibility, as they enable the study of underlying mechanisms and disease pathology. Earlier animal work showed that treatment of mice with the antibiotic vancomycin during pregnancy and lactation, as well as treatment of the offspring, resulted in increased asthma severity [47,48]. However, though the importance of this work is clear, there was still a need for a model to causally link maternal antibiotic use that occurs only during gestation with increased offspring asthma risk.

1.4. Early life intestinal colonization and immune system development

Infants are first exposed to intestine colonizing bacteria during birth, via the transfer of the maternal intestinal and vaginal flora [49]. Vaginal delivery supplies the infant gut microbiota with many facultative anaerobic bacteria, for instance from the genera *Escherichia* and *Staphylococcus*. These bacteria contribute to the intestinal environment in a manner that facilitates further colonization by anaerobic organisms such as *Bacteroides* and *Bifidobacterium* [50]. Finally, breastfeeding and environmental exposures further contribute to diversification and fortification of particular bacterial clades in the infant intestine [51].

The maturation of the intestinal microbiota takes approximately three years in humans [52,53]. During this sensitive period, the relative abundance of different bacterial species and their diversity can be affected by environmental changes that can have a long-term impact on gut microbiome composition for (for example: visiting day care, diet or antibiotic use)[54–56]. During early life, the type and composition of bacteria encountered in the intestine during particular developmental stage “the windows of opportunity” contributes significantly to immune system development and disease susceptibility later in life [28].

The healthy mature intestinal microbiota is composed of approximately 2,000 bacterial species totaling up to 10^{13} bacteria[57] These bacteria provide the body with many crucial services including: fiber digestion, prevention of intestinal infections and maintenance of the intestinal barrier, thus contributing to overall health and gut homeostasis [58]. Additionally, bacterial colonization of the neonatal gut is essential for proper immune system function [59] and can alter the developing neonatal immune system in the following ways.

1) Direct interaction of intestinal immune cells with gut bacteria.: For example, induction of RORγt T cells by segmented filamentous bacteria [60] or tolerogenic priming of dendritic cells by *Clostridium leptum* [61,62].

2) Indirect immune stimulus via exposure to bacterial components. For example, exposure to polysaccharide A can protect against gut inflammation by stimulating IL-10 production by T cells [63], and exposure to sphingolipids from anaerobic bacterial membranes has been shown to reduce the invariant natural killer T cell population in the colon and protect against the colitis [63]. In addition to this, lipopolysaccharide (LPS) from gram-negative bacteria induces the differentiation of naïve Th cells into IL-17 producing RORγt+ T helper 17 (Th17) cells that activate cytokine production by dendritic cells and monocytes [64,65]. Finally, released bacterial DNA (5'-cytosine-phosphate-guanine-3' or CpG) in the intestine can promote B cell activation and Th17 cell differentiation while preventing the differentiation of Tregs [66,67].

3) Indirect effects on the immune system through the production of metabolites. The gut microbiota is known for its ability to transform nutrients into metabolites, which subsequently have a broad impact on human health [68]. For instance, SCFA production from indigestible dietary fiber enhances tolerance mechanisms in the immune system. Butyrate can stimulate the differentiation of naïve T cells into Tregs [69] , potentiate proliferation of type 1 and 3 innate lymphoid cells (ILC1s and ILC3s), suppress proliferation of type 2 ILCs (ILC2s) and attenuate the migration and activation of the eosinophils [70–72]. In addition to this, both propionate and butyrate were found to activate intrinsic apoptosis pathways in eosinophils, and acetate was shown to increase Treg populations in the colon in a GPR43 dependent manner [73]. Finally, SCFAs can suppress the immune response via inhibition of histone deacetylase (HDAC) enzymes. This leads to inhibition of IL-8 production, and ILC2 proliferation at the same time supporting the generation of the immunosuppressant lymphocytes such as Tregs and Bregs [74–76].

The gut microbiota plays a major role in homeostasis and overall health, such that alteration of microbiota composition, called dysbiosis, can detrimentally affect individual health [77]. Gut dysbiosis in early life can disturb the maturation of secondary intestinal lymph structures (e.g., Peyer's patches and the germinal centers)[78] and it can also change the migration and homing behavior of gut leukocytes such as eosinophils, ILCs and T helper cells (TH cells) [79,80].

1.5. Gut dysbiosis in early life and offspring asthma development: The gut-lung axis.

Though links between the gut and lung have been reported for over 20 years, the gut-lung-axis is just beginning to be intensely studied [81]. Using 16sRNA qPCR and next

generation sequencing techniques, researchers have identified characteristic differences in gut bacterial clades between asthmatic and healthy children. Asthmatic children exhibited in their gut higher abundances of *Escherichia and Enterobacteriaceae*, and lower abundances of *Bifidobacterium, Blautia, Clostridium, and Ruminococcus*, [82,83]. By examining the gut microbiota of children exposed to antibiotics perinatally, one can see the similarities with the microbiota profile detected in asthmatic children (low abundance of and *Bacteroides*, *Bifidobacterium*, *Roseburia, Ruminococcus*, and high abundance of the *Proteobacteria*, *Enterobacter*, *Escherichia-Shigella*, and *Enterobacteriaceae*) [84,85].

Despite the knowledge gained from epidemiological studies, the link between the gut microbiota and asthma development remained unknown. To examine the mechanisms involved, Russell et al. (2012) designed the first mouse model, in which pre- and postnatal treatment of mothers and their offspring with the antibiotic vancomycin resulted in depletion of gut bacteria in the phylum *Firmicutes*, such as *Lachnospiraceae*, *Ruminococcaceae* and *Clostridiales,* accompanied by increased asthma severity in the offspring [47]. Deeper analysis of the gut microbiome in this model revealed an enrichment of the *Enterobacteriacae* in fecal samples from dysbiotic offspring, accompanied by a reduction in alpha diversity [16], which was later also reported in human cohort study [85].

Though this model provides proof of concept for perinatal (maternal and offspring) exposure to antibiotics and increased asthma severity, the question regarding how **maternal antibiotic use during pregnancy** influences offspring asthma outcomes remains to be answered. Additionally, though existing mouse models have made a connection between gut microbial dysbiosis in early life and increased asthma severity, the mechanisms contributing to this phenomenon as well as the connection between the gut and the lung remained poorly understood.

In summary, despite the knowledge gathered from human cohorts and mouse models, there is still little information regarding how antibiotic use during pregnancy affects the gut microbiome of mother and offspring, and how gut dysbiosis in early life alters immune tolerance mechanisms such that the offspring are more susceptible to asthma.

1.6. Objectives

The aim of this dissertation is to utilize a series of mouse studies to answer the open questions mentioned above through achieving the following objectives.

Objective 1: Mouse model establishment and proof of concept. Antibiotic use during pregnancy and increased asthma severity in the offspring.

Aims are:

- To establish a mouse model for studying the effects of 3 different concentrations of prenatal antibiotic treatment on pregnancy and on asthma severity in offspring.
- To establish and assess asthma-related inflammatory parameters, including histological inflammation score, bronchoalveolar lavage (BAL) differential cell counts, serum antibodies titers and cytokine levels.
- To preliminarily analyze the gut microbiota of both mothers and offspring.
- To measure SCFA concentrations in the offspring caecum.

Objective 2: Antibiotic Treatment During Pregnancy model - Immune phenotyping of the offspring gut-lung axis and assessment of airway reactivity

Aims:

- Examine the effect of prenatal antibiotic use on airway reactivity in offspring
- Perform deep analysis of the transfer of gut dysbiosis from mother to offspring
- Examine the dysbiosis impact on maternal intestinal physiology and breast milk composition during lactation.
- Examine the dysbiosis impact on offspring gut barrier integrity and inflammation.
- Immunophenotype the offspring gut, blood and lung in early life and after asthma induction (adulthood) to assess immune system development.

2. Methods

2.1. Objective 1: Mouse model establishment and proof of concept. Antibiotic use during pregnancy and increased asthma severity in the offspring.

2.1.1. Animals

Twelve-week-old BALB/c mice were obtained from Janvier Labs (Le Genest-Saint-Isle). All mice were housed in specific pathogen-free conditions (SPF) under 12/12-hour day/night cycles, with food and water provided ad libitum. All animal experiments were approved and performed following the local German guidelines and authorities (Landesamt für Gesundheit und Soziales; LAGeSo).

2.1.2. Experimental design

To establish this proof-of-concept model, mouse mating was performed by pairing three females with one male, and the formation of a vaginal plug after mating was considered gestation day (G)0. Daily from G8-G17, pregnant mice were fed a 40 µl mixture orally via micropipette, containing 25 µl of freshly prepared vancomycin (Sigma-Aldrich) dissolved in water (for a total concentration of 10, 20 or 40 mg/kg), plus 15 µl ORA-Sweet (Perrigo). Control animals received 25 µl water plus 15 µl of ORA-Sweet. Mice were assessed visually to confirm consumption of the entire dose before being returned to the cage. Protocol shown in Figure 3.

Offspring were born, then at postnatal day (PN)21 female offspring were weaned and subjected to an experimental asthma protocol, consisting of subcutaneous (SC) injection of ovalbumin (OVA) VI (10 µg in 200 µl) (Sigma-Aldrich) on PN21, PN28 and PN35. This was followed by an aerosol challenge with 1% nebulized OVA V (Sigma-Aldrich) for 20 minutes on PN46, PN47 and PN48. At PN49 mice were sacrificed after a lethal dose of 200 mg/kg ketamine (Merial) and 30 mg/kg xylazine (VMD Livestock) for asthma phenotype analysis (Figure 3).

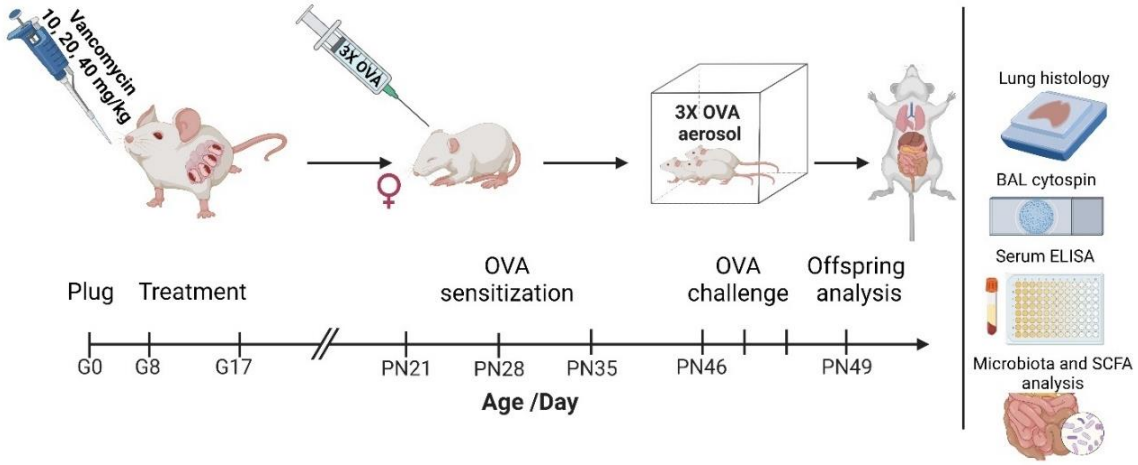

Figure 3. Experimental design - Establishment of an antibiotic treatment during pregnancy model that results in increased offspring asthma severity

Mice were mated, then from G8 to G17 pregnant animals were treated orally either with vancomycin (10, 20 or 40 mg/kg) or water. Female offspring were weaned at PN21, then subcutaneously sensitized with OVA at PN21, PN28 and PN35. At PN46, PN47 and PN48, mice were challenged with OVA aerosol and then at PN49 they were sacrificed for tissue analysis [own representation]. Figure created with BioRender.com.

2.1.3. Asthma phenotype analysis

2.1.3.1. Serum collection

Blood samples were obtained from the retro-orbital sinus of lethally anaesthetized animals and left to clot at room temperature for one hour. Following this, the samples were centrifuged at 2000 revolutions per minute (rpm) for 10 minutes and the resulting serum was divided into aliquots and stored at -80°C for subsequent analysis.

2.1.3.2. Bronchoalveolar lavage (BAL) collection and cytospin preparation

To collect BAL, a 20G safety cannula (Vasofix) was inserted through a tracheotomy and the lung was washed once with 1 ml of cOmplete Protease Inhibitor Cocktail (Roche), prepared with one tablet in 50 ml of phosphate buffered saline (PBS – Gibco). Following this, BAL cells were counted using a Neubauer Chamber (Hecht Assistant), then centrifuged at 350xg at 4°C for 10 minutes. The resulting supernatant was stored at -80°C for subsequent analysis. To prepare cytospins, the cell pellet was resuspended in 1 ml of PBS / 1% bovine serum albumin (BSA – Sigma) and two cytospins were prepared by mixing 100 µl of the cell suspension with 300 µl of PBS and centrifuging them onto Super Frost Plus slides (R.Langenbrinck) with a Cytospin III centrifuge (Tharmac) at 700 rpm for 5 minutes. After drying at room temperature for 24 hours, cells were stained using a Differential Quik Stain Kit (Polysciences) according to manufacturer's instructions and 200 leukocytes were counted in a blinded manner.

2.1.3.3. Lung histology and quantification of inflammation

Following the BAL procedure, the lungs were fixed using 4% formalin. After 24 hours at room temperature, the fixed lungs were embedded in agar (Merck) and sliced into 2 cm thick sections using the device shown in Figure 4, before being embedded in paraffin. 4 µm sections were cut and stained using periodic acid-Schiff (PAS) or hematoxylin and eosin (H&E) staining.

Next, lung leukocyte infiltration and goblet cell mucous production were quantified using the meander random sampling tool in the newCAST software (Visiopharm). This was done by superimposing 100 random squares with a grid of lines and cross symbols over

the image. Points of inflammation (PI) or points of goblet cells (PG) were counted when a cross symbol intercepted a leukocyte or goblet cell, respectively. The lines of goblet cells (LG) or non-goblet cells (LnG) were counted depending on whether a line crossed the bronchial epithelium. If a line crossed a blood vessel, it was considered a line blood vessel (LV). Using these counts and the equations mentioned in Figure 4, the normalized volume of inflammation (Vol. Inf), number of goblet cells (Nu. G) and volume of goblet cells (Vol. G) were calculated cells (Vol. G) were calculated.

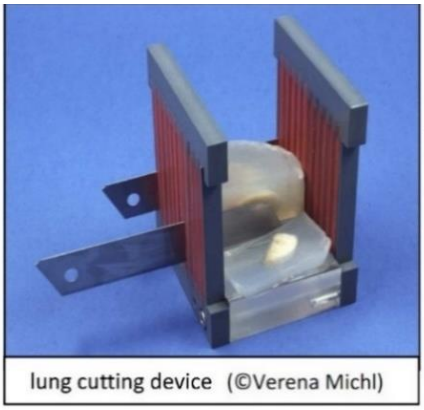

$$\text{Vol. Inf} = (\Sigma PI) \times 9.395 / (\Sigma LG + \Sigma LV)$$

$$\text{Nu.G} = (\Sigma LG \times 100) / (\Sigma LG + \Sigma LnG)$$

$$\text{Vol. G} = (\Sigma PG \times 9.395) / (\Sigma LG + \Sigma LnG)$$

Figure 4. Lung cutting device and equations used for lung inflammation quantification.

The lung was embedded in agar and then cut into 2 cm thick sections in the device via inserting blades in the openings. After cutting, the lung was embedded in paraffin and 4 µm sections were prepared for PAS and HE staining [own representation].

2.1.3.4. Antibody measurement via enzyme-linked immunosorbent assay (ELISA)

A sandwich ELISA method was used to measure the concentrations of total immunoglobulin (Ig)G1, OVA-specific IgG1, OVA-specific IgE and IgA. To measure total IgG1, a Nunc MaxiSorp plate (BioLegend) was coated with 50 µl of 0.5 mg/ml anti-IgG1 (Pharmingen) and incubated for 2 hours at room temperature. The plate was then washed with wash buffer (PBS plus 1% tween-20 (Sigma)) and blocked with 150 µl of PBS plus 1% BSA for 2 hours. Serum samples were diluted 1:10000 in PBS and an IgG1 standard series (250 – 1.95 ng/ml, Pharmingen) was prepared using the wash buffer. Next, 50 µl of the diluted sample or standard was added to the plate and incubated overnight at 4°C. After washing, 50 µl of biotinylated anti-mouse IgG1 (2.5 µg/ml, Pharmingen) was added to the plate and incubated for 2 hours at room temperature. After washing, 50 µl of 0.1 µg/ml streptavidin peroxidase (Sigma) was added and the plate was incubated for 30 minutes in the dark at room temperature. After a final wash, 100 µl of tetramethylbenzidine (TMB, Sigma) was added to the plate and the reaction was stopped with 50 µl of 2M sulfuric acid (Sigma) then measured at 450 nm on the plate reader Infinite® 200 PRO (Tecan).

OVA IgG1 and OVA IgE measurements were performed the same as previously described with the exception that the plate was coated with 50 µl of 20 mg/ml OVA VI (Sigma) diluted in coating buffer (NaHCO3 8.4 g/l) with a dilution factor of 1:50,000 for OVA IgG1 and 1:1,000 for OVA IgE. Standard series were prepared using anti-OVA IgG1 (500 – 3.90 ng/ml, Sigma) or anti-OVA IgE (2,000 – 1.56 ng/ml, Serotec). Next, diluted samples were added and incubated overnight at 4°C. After incubation, 50 µl of biotinylated anti-mouse antibodies IgG1 or IgE (0.5 mg/ml, Pharmingen) were added, and the procedure was continued as documented for total IgG1.

The IgA ELISA was performed in the same manner as above; however, the Nunc MaxiSorp plate was coated with 100 µl of anti-IgA antibody (1 µg/ml, Southern Biotech) then was blocked using 2% BSA for 2 hours. A 50 µl standard series was prepared using the IgA standard (BD) (2000 – 0.91 ng/ml) and loaded to the plate alongside 50 µl of diluted samples (milk 1:7000, feces 1:2000 and serum 1:800). After incubating the plate for 2 hours and washing, 50 µl of secondary antibody (Abcam) was added. Lastly, the plate was washed and the substrate ABTS was added and measured at 405 nm wavelength.

2.1.3.5. Cytokine measurement

Cytokines from BAL, serum and sorted lung ILC2s were analyzed using a mouse 23-plex Luminex kit (Bio-Rad) according to the manufacturer's instructions. Cytokines measured included: IL-1α, IL-1β, IL-2, IL-3, IL-4, IL-5, IL-6, IL-9, IL-10, IL-12p40, IL-12p70, IL-13, IL-17A, Eotaxin, Granulocyte colony-stimulating factor (G-CSF), Granulocyte-macrophage colony-stimulating factor (GM-CSF), Interferon gamma (IFN-γ), Keratinocyte chemoattractant (KC), Monocyte Chemoattractant Protein-1 (MCP-1), Macrophage Inflammatory Protein-1 Alpha and beta (MIP-1α and MIP-1β), Regulated upon Activation, Normal T cell Expressed, and Secreted (RANTES), Tumor necrosis factor (TNF-α). In short, the standard series was prepared using standard diluent, then 50 µl of magnetic beads were added to each well. Standards or samples (50 µl) were added to the plate and incubated in the dark for 30 min at room temperature. After washing, 25 µl of detection antibodies were added and incubated at room temperature for 30 min, then the plate was washed and incubated for 10 minutes with 50 µl of streptavidin-phycoerythrin. After washing, the samples were resuspended in 125 µl of assay buffer and measured on a Bio-Plex Multiplex Immunoassay System (Bio-Rad).

2.1.3.6. Airway reactivity assessment

To measure airway reactivity, a FlexiVent device (Scireq) was used. Mice were anaesthetized intraperitoneally (IP) with 100 µl of 10 mg/ml, ketamine (Merial) und 1 mg/mL Xylazin (VMD Livestock), and involuntary breathing was stopped by IP injection of 100 µl of 2 mg/ml Pancuronium IP (Insra) diluted 1:10. Airway reactivity was measured via tracheotomy with increasing concentrations of methacholine (0.625, 1.25, 2.5, 5, 10, 20, 40, 80 mg/ml – Sigma) using the parameters shown in Table 1. The "Forced Oscillation Technique" was performed at a 2.5 Hz ventilation rate to measure airway resistance and compliance, according to the manufacturer's manual. Data of the Newtonian resistance (Rn), compliance (Crs) and elastance (Ers) of the respiratory system were exported and analyzed. Only measurements with a coefficient of determination (COD) of over 0.9 were accepted.

Table 1: FlexiVent presetting and script for the airway reactivity test.
[Established in Dr. Markus Mall lab].

		Min	Max
FX1 Channel calibration	Pcyl (Cylinder pressure)	-80.0 cm H2O+- 5 cmH2O	+80.0 cm H2O+- 5 cmH2O
	Pao (Airway opening pressure)	-80.0 cm H2O+- 5 cmH2O	+80.0cm H2O+- 5 cmH2O
Tube calibration	Perturbation	Deep inflation	
	R_L (Shunt resistance)	>2000 cm H2O.s/ml	
	Perturbation	Snap-Shot-150	
	R_t (Tube resistance)	<0.5 cm H2O.s/ml	
Methacholine challenge script			
Nebulizer		3 sec	
SnapShot-150/ Quick Prime-3		12 cycles	
Deep Inflation		2 times	

2.1.4. Gut microbiome analysis through quantitative polymerase chain reaction qPCR

Sample collection and preparation

For assessment of the fecal microbiome, fecal pellets were collected from mothers and their offspring at the following time points: mothers – before mating, at G17 and at weaning (PN21), and offspring at weaning and after asthma induction at PN49. Feces was snap-frozen in liquid nitrogen and stored at -80°C. qPCR was performed in collaboration

with Dr. Markus Heimesaat's lab according to the following protocol. Samples were reconstituted in 400 µl of sterile PBS, then homogenized by adding 25 µl of 20 mg/ml lysozyme (Sigma) and incubated on a Thermos-shaker (Biosan) for 30 min at 37°C. Each sample received 20 µl of Proteinase K (20 mg/ml, Roth) and 400 µl of lysis buffer (10 ml 0.1 M Tris HCl + 15 ml 1.0 M NaCl + 20 ml 0.1 M Ethylenediaminetetraacetic acid (EDTA) + 5 ml 10% sodium dodecyl sulfate (SDS)), then the mixture was incubated with shaking for 60 min at 56°C on the Thermos-shaker. After enzymatic and chemical decomposition was accomplished, 300 mg of zirconium beads (OPS Diagnostics) and 150 µl of phenol (Roth) was added, then mechanical decomposition was performed using a Speed Mill (Analytik Jena) (2 X 40 seconds).

16s rRNA qPCR – DNA extraction, precipitation, purification and titration.

Digested fecal samples received 150 µl of chloroform-isoamyl alcohol (24:1, Roth) and after centrifugation, the clear top phase was transferred into a new tube and the procedure repeated. To precipitate the DNA, 100 µl of precipitation solution (0.1M EDTA + 3M Na acetate + 20 mg/ml glycogen + 1.3 ml 100% ethanol) was added, then samples were stored at -20°C until further analysis. Later, samples were centrifuged for 30 min at 13000 rpm at 4°C and the supernatant was discarded. Pellets were dried using a Speed Vac centrifuge (Heraeus) for 15 min, then resuspend in 100µl of sterile distilled water. This solution was shaken for 10 minutes, then purified using a QIAquick PCR Purification Kit (Qiagen) according to manufacturer's instructions. DNA concentration was assessed using a Quant-iT PicoGreen ds DNA assay kit (Invitrogen), and samples were equilibrated to a final DNA concentration of 5 ng/µl with distilled water.

qPCR analysis of fecal microbiota

The following bacterial clades – *Bifidobacterium*, *Bacteroides–Prevotella*, *Clostridiumcoccoides–Eubacterium rectale*, *Clostridium leptum*, *Enterococcus*, *Gammaproteobacteria/ Enterobacteriaceae*, *Lactobacillus and Staphylococcus* – were analyzed in feces samples using PCR-based denaturing gradient gel electrophoresis (PCR-DGGE). Briefly, the DNA was first amplified using a thermocycler and then cloned in a liquid culture medium through the plasmid-based TOPO-Cloning technique (Invitrogen) with the primers listed in Table 2. DNA of the standard bacteria and samples was normalized to a concentration of 1 ng/µl, then a series of 10-fold dilutions (ranging from 2108 to 2.108 copies) of the standard bacteria was prepared to create a standard curve. The Quant-iT PicoGreen dsDNA assay kit (ThermoFisher) was used, and each sample was mixed with 20 µl of the

master mix and subjected to the amplification program, specified in Table 3. Cycle threshold (CT) was set as depending on the eubacterial V3 amplicon (Eub) and the frequencies of each group were determined by calculating the proportion of each bacterial strain compared to the Eub. The analysis was done by using the established genetic fingerprints shown in [86].

Table 2: Primer sequences for fecal microbiota analyses.
[Established in Dr. Markus Heimesaat lab].

Primer	Specificity	Forward sequence (5′–3′)	Reverse sequence (5′–3′)
Universal	Domain Bacteria	CGGTGAATACGTTCCCGG	TACGGCTACCTTGTTACGACTT
Bifidobacterium	Genus	CGGGTGAGTAATGCGTGACC	TGATAGGACGCGACCCCA
Bacteroides–Prevotella	Group	GGTGTCGGCTTAAGTGCCAT	CGGACGTAAGGGCCGTGC
Clostridiumcoccoides–Eubacterium rectale	Group	AGTTT(C/T)ATTCTTGCGAACG	AGTTT(C/T)ATTCTTGCGAACG
Clostridium leptum	Subgroup	GCACAAGCAGTGGAGT	CTTCCTCCGTTTTGTCAA
Lactobacillus	Group	AGCAGTAGGGAATCTTCCA	CGCCACTGGTGTTCYTCCATATA
Enterobacteriaceae	Genus	CATTGACGTTACCCGCAGAAG	CTCTACGAGACTCAAGCTTGC
Enterococcus	Genus	CCCTTATTGTTAGTTGCCATCATT	ACTCGTTGTACTTCCCATTGT
Staphylococcus	Genus	ACGGTCTTGCTGTCACTTATA	TACACATATGTTCTTCCCTAATAA
Mouse Intestinal Bacteroides	Genus	CCAGCAGCCGCGGTAATA	CGCATTCCGCATACTTCTC

2.1.5. Short-chain fatty acid (SCFA) analysis

Analysis of SCFAs were performed in collaboration with the Department of Gastrointestinal Microbiology at the German Institute of Human Nutrition (Potsdam-Rehbruecke) and with the company Microbiome Insights Inc (Vancouver). Analysis of acetate, propionate, butyrate and valerate in mouse feces, cecum and breast milk was performed by using gas chromatography. Briefly, samples were diluted, centrifuged and mixed with an internal standard (2-ethyl butyric acid), 0.36 M HclO4 and 1 M NaOH before overnight lyophilization. The samples were then redissolved with 400 µl of acetone and 5 M of formic acid, centrifuged and 1 ml of the supernatant was injected into an HP 5890 series II gas chromatograph (Hewlett-Packard) equipped with an either HP-20 M column (BGB analytic) or Thermo TG-WAXMS A GC and a flame ionization detector (FID).

Table 3: PCR Protocol for qPCR analysis of fecal microbiota samples.
[Established in Dr. Markus Heimesaat lab].

Material (concentration)	Amount	Vendor
AmpliTaq DNA polymerase (2.5 IU/ml)	0.4 µl	Applied Biosystems
Aqua Dest	12.6 µl	Sigma-Aldrich
Bovine serum albumin (20 mg/ml)	0.1 µl	Fermentas
Buffer I (10X)	2 µl	Applied Biosystems
MgCl2 (25 mM)	2 µl	Applied Biosystems
PCR nucleotide mix (10 mM dNTP)	0.4 µl	Roche
Sample DNA extract (1 ng/µl).	2 µl	
Specific primer (30 mM)	0.4 µl	Tib MolBiol
SYBR Green I (1:200 dilution)	0.1 µl	Invitrogen

Amplification thermocycles

Step	Temperature	Time
Initial denaturation	95°C	2 min
40 cycles	95°C	10 s
Annealing	60°C	10 s
Elongation	72°C	30 s
Fluorescence acquisition	80°C	End of a cycle
Melting curves	60°C to 95°C	rate of 0.058C/s

2.2. Objective 2: Model replication and immune phenotyping of offspring gut, blood and lung

2.2.1. Experimental design

Next, the antibiotic treatment model was repeated for deep assessment of the effect of antibiotic treatment during pregnancy on 1) The transfer of gut dysbiosis from mother to offspring. 2) Maternal intestinal growth and breast milk composition at PN15. 3) the immune system development along the gut-lung-axis in early life and after asthma induction 4) The gut barrier integrity. Pregnant mice were treated with the dosage 20 mg/kg vancomycin, as described in section 2.1.2. At PN15, breast milk and maternal intestines were collected, in addition to offspring blood, intestine and lung, shown in Figure 5. In a second group of animals, offspring were subjected to the OVA asthma induction protocol detailed in section 2.1.2. Feces were also collected from mothers and offspring at the time points mentioned in model establishment section (Figure 5).

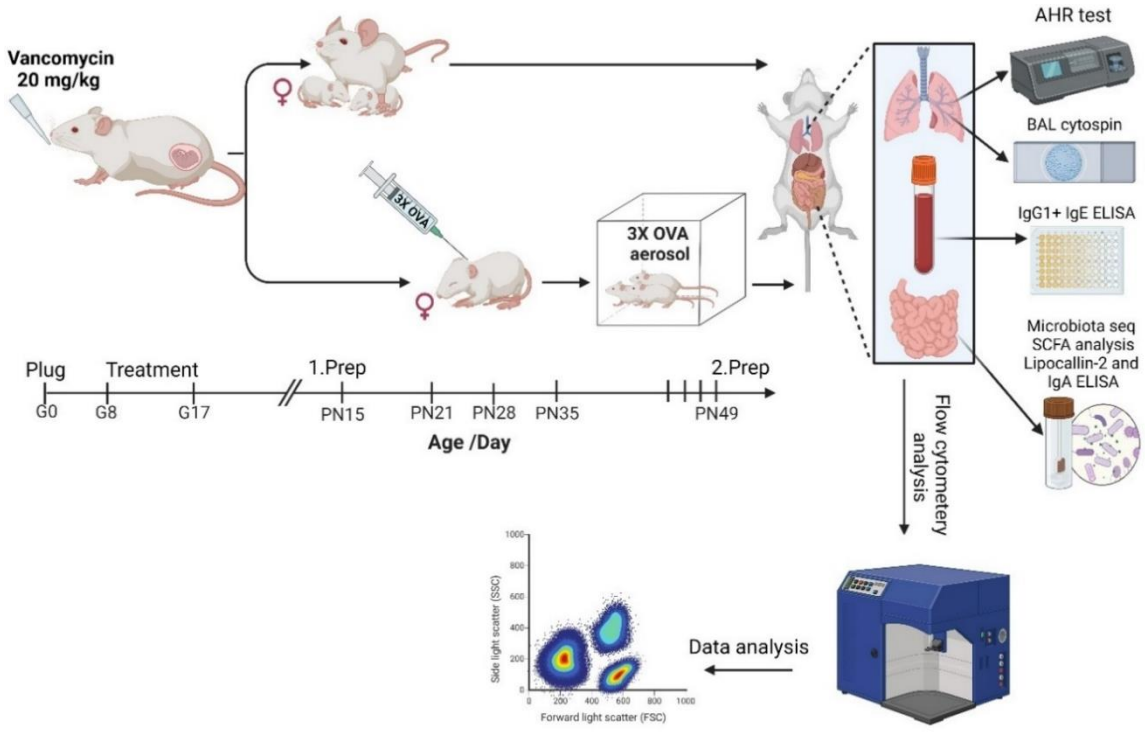

Figure 5. Experimental design for the Antibiotic Treatment During Pregnancy model: mechanism assessment.

Vancomycin (20 mg/kg) was administered to pregnant mice from G8-17, control mice received water. On PN15, one group of mothers and offspring were sacrificed, and maternal milk, blood and intestine samples were harvested as well as offspring blood, intestine and lung. An additional group of offspring was subjected to an asthma protocol starting from PN21 consisting of SC sensitization with OVA at PN21, PN28 and PN35 and OVA challenge at PN46, PN47 and PN48. The offspring were either subjected to airway reactivity test or euthanized on PN49 for analysis of blood, intestine and lung [own representation]. Figure created with BioRender.com.

2.2.2. 16S rRNA gene amplicon sequencing

To perform a deeper analysis of maternal and offspring gut microbiome changes, collected fecal samples were sequenced using 16S rRNA sequencing (Microbiome Insights). The process involved creating cDNA from the sample using a PowerSoil for King-Fisher kit (MO Bio) and amplifying targeted gene fragments of the 16S ribosomal RNA (16S rRNA) of the V4 region using coded primers (fwd: GTGCCAGCMGCCGCGG-TAA, rev: GGACTACHVGGGTWTCTAAT). The amplicons were then sequenced using the MiSeq 2000 bi-directional Illumina and the library was prepared using the TruSeq DNA Sample Prep v2 Kit (Illumina). The quantity and quality of the DNA were checked with Qubit (ThermoFisher).

The Operational Taxonomic Units (OTUs) were clustered at 97% similarity using the software MOTHUR [87] , resulting in 8631 OTUs from 31554 quality-filtered reads. The reads were classified using the Greengenes v. 13_8 database and the relative abundance of the most abundant OTUs was plotted at each taxonomic rank. Any duplicates of chloroplast, mitochondria and archaea were removed, alpha diversity was determined using the Shannon index and beta diversity was determined using Bray/Curtis indices (visualized as a Principal component analysis (PcoA) to show the differences between samples). Only OTUs with a count of more than 3 in 10% of samples were used for the test.

2.2.3. Murine milk collection and analysis

A breast milk collection protocol was adapted from Gómez-Gallego et al [88]. In brief, PN15 offspring were separated from their mothers for a period of 6 hours to allow the accumulation of milk. The mothers were anesthetized using an IP injection of 150 µl of 10 mg/ml ketamine (Merial) und 1 mg/mL Xylazin (VMD Livestock), then 1 IU/50µl oxytocin (Sigma) was injected SC to stimulate milk secretion. Using a human breast milk pump and a custom-built, vacuum-sealed collection device (Charité Facilities Management) shown in Figure 6, it was possible to collect between 500 µl and 1000 µl of milk. After collection, samples were centrifuged for 20 minutes at 1500xg, then the upper fat layer was collected for SCFA measurement (detailed in Section 2.1.5) and the middle layer

was collected for cytokine measurement using a 23-plex Luminex assay (Bio-Rad) detailed in Section 2.1.3.5 and IgA antibody measurement using ELISA, detailed in Section 2.1.3.4.

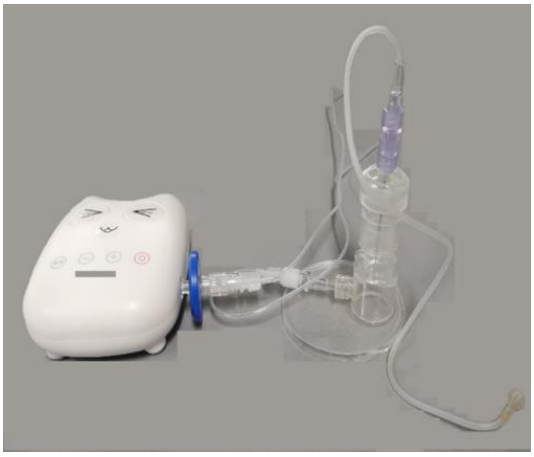

Figure 6. Milk pump design.
Lactating mother mice were anaesthetized, then, oxytocin was SC injected 5 min before the procedure to stimulate milk secretion. Breast milk was then harvested using the milk pump and a special collector manufactured at the Charité Facility Management [own representation].

2.2.4. Maternal intestinal tissue collection and analysis

To investigate the changes to the maternal small intestine during lactation at PN15, the distal part of the small intestine was wrapped in a Swiss roll formation, then fixed in 4% paraformaldehyde (Sigma) for 6 hours. The tissue was then dehydrated overnight in 30% sucrose (Sigma) in PBS. After drying the tissue, it was placed in Peel-A-Way embedding molds (Sigma) filled with optimal cutting temperature compound (Sakura) and frozen in a dry ice/ethanol slurry. Using a Cryostat CM1850 (Leica) the blocks were cut to 7 µm thickness with 100 µm space between the sections.

After drying the slides overnight, immunofluorescence staining of the intestinal epithelial cells was performed. Samples were incubated with antigen retrieval solution (Dako) in a water bath at 95°C, tissues were permeabilized with 0,5% Triton X-100 (Sigma) and then non-specific antigen binding locations were blocked using 2% donkey serum (ThermoFisher) in PBS. The following primary antibodies were added: Ki-67 (rabbit, Abcam) and EpCAM (rat, BioLegend) then the following secondary antibodies were used for detection; donkey anti-rabbit (Alexa Fluor 488, ThermoFisher) and donkey anti-rat (DyLight 550, ThermoFisher). 4′,6-diamidino-2-phenylindole (DAPI, Sigma) was used to stain the nucleus. Pictures were taken at 10x magnification Using an Axio Observer 7 light microscope (Zeiss), to measure the villus height and crypt depth 40x pictures were taken for counting proliferating epithelial cells (Ki-67^{+}). Proliferating epithelial cells were counted and the height-depth of a villus-crypt were also measured by drawing a line from the bottom of the crypt to the top of the villus using the software Fiji.

2.2.5. Offspring intestinal inflammation analysis

2.2.5.1. Lipocalin-2 ELISA

To assess intestinal inflammation in PN15 mothers and their offspring, fecal lipocalin-concentrations were measured using ELISA. Samples were collected and weighed (as detailed in Section 2.1.4), then homogenized in 1 ml of 0.05 % Tween/PBS and centrifuged at 12000 rpm for 10 minutes. Supernatants were then diluted 1:100 and measured using a LEGEND MAX™ mouse NGAL (Lipocalin-2) ELISA kit (BioLegend) according to manufacturer's instructions.

2.2.5.2. Intestinal permeability assay with FITC-Dextran

A FITC-Dextran assay was performed on PN15 and PN49 offspring to investigate the impact of early life dysbiosis on small intestine barrier integrity. Female PN15 and PN49 offspring from prenatal-antibiotic treated or prenatal-control mothers were fasted for 1.5 hours and then gavaged with 500 mg/kg 4 kDa FITC-Dextran (Sigma). Food and water were removed after the gavage for additional 1.5 hours (5 hours for adult mice) then animals were anesthetized, and blood was collected. Serum from these mice was diluted 1:4, then loaded on black 96-well plate. The FITC signal was measured with an Infinite Pro plate reader at excitation wavelength 485 nm and emission wavelength of 530 nm.

2.2.6. Offspring immunophenotyping

Next, to immunophenotype the PN15 and PN49 offspring intestine, blood and lung samples were collected and processed, as described in the following sections. Markers used to identify all described cell populations are shown in Table 4. For all immunophenotyping, samples were acquired with a Fortessa x20 flow cytometer (BD) and cell populations were analyzed using the software FlowJo™ (v.9 and 10, BD Life Sciences).

Table 4: Pan cellular markers used to define targeted cells.
[own representation].

Pan cellular markers.		
Myeloid cells		
Cell type	**pan marker**	**subpopulations**
Basophils	CD49b+, FcεRIα	
Dendritic cells	CD11c+, MHCII+	CD11b+, CD64+
Eosinophils	CD11b+ SiglecF+	CD11c+
Macrophages	CD11b hi, Ly6C-	CD64+, CD11c-, Siglec F+
Monocytes	CD11b hi, Ly6C+	CD64+
Neutrophils	CD11b+, Ly6G+	

Lymphoid cells		
Cell type	**pan marker**	**subpopulations**
T cells	CD3+	CD4+, CD8+
Memory T cell	CD4+/CD8+,	Central memory CD44+, CD62L+ Effector memory CD44+, CD62L-
T helper cells	CD4+	T-bet+\GATA3+\ RORγt+, Foxp3+
Innate lymphoid cells		
Cell type	**pan marker**	**subpopulations**
ILCs	Lin-, CD127+	ILC1, ILC2, ILC3
ILC1	T-bet+	EOMES +
ILC2	GATA3+	IL17RB, ST2, KLRG1,
ILC3	RORγt+	NKp46, T-bet, CCR6
NK	Lin-, CD127-, EOMES +	

2.2.6.1. Intestine flow cytometry analysis

Small intestine lamina propria leukocytes were obtained and processed as mentioned in [89]. In short, the small intestine was extracted, rinsed, cleaned, cut into small pieces and digested with cell dissociation solution (for composition please see [89]). After digestion, tissue was smashed using a 70 µm cell strainer (Corning) and then washed with Dulbecco's modified Eagle medium (Gibco) buffer. Isolated cells were purified via Percoll gradient (80% plus 40% - Sigma), then washed and resuspended in FACS buffer. After washing, cells were resuspended in a mixture of antibodies mentioned in Table 5 for 30 minutes, then washed and resuspended in 200 µl of FACS buffer. For intracellular staining, the Foxp3 kit (eBioscience) was used according to the manufacturer's instructions. The gating strategy is shown in Figure 7.

Table 5: **Antibodies used in intestinal flow cytometry analyses.**
[own representation]

Intestine ILCs panel			
Antigen (clone)	**Fluorophore**	**Dilution factor**	
CD3e (145-2C11)	Biotin	600	
CD5 (53-7.3)	Biotin	1000	
CD19 (MB19-1)	Biotin	100	
Ly6C/G (RB6-8C5)	Biotin	600	Lineage
TCRβ (H57-597)	Biotin	200	
TCRγδ (GL3)	Biotin	500	
Streptavidin	BV650	600	
CCR6 (140706)	BV421	100	
CD4 (L3T4)	BUV496	100	
CD25 (PC61)	PE-Cy7	200	
CD45 (30-F11)	APC-fire 750	400	
CD127 (A7R34)	PE-Dazzle	100	

Eomes (Dan11mag)	AF488	100
GATA3 (L50 823)	BUV395	100
IL-17RB(MUNC33)	eFluor 660	100
Ki67 (SolA15)	AF700	100
KLRG1 (2F1)	BV711	300
Live dead	Aqua Zombie	1000
NKp46 (29A1.4)	PerCp-eFluor 710	100
RORgt (Q31-378)	BV786	100
ST2 (RMST2-29	SuperBright 600	100
T-bet (eBio4B10)	PE	100
Thy1.2 (53-2.1)	BUV737	500

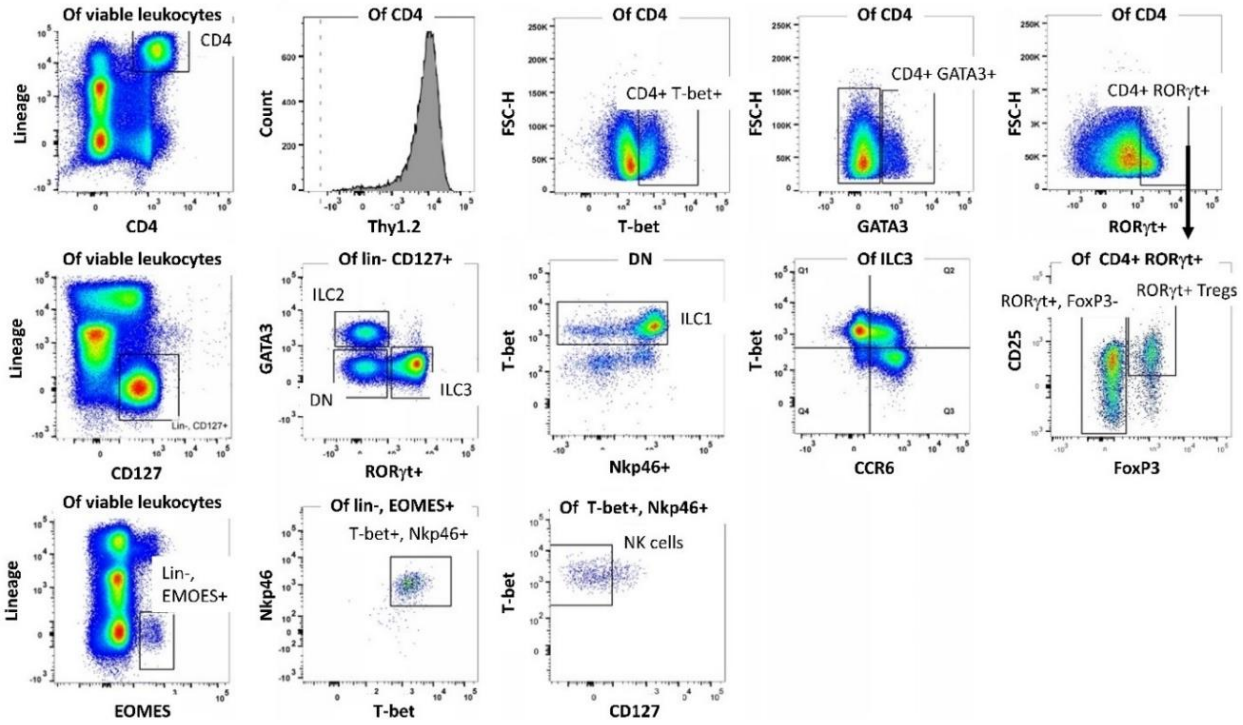

Figure 7. Small intestine lamina propria flow cytometry gating strategy.
After removing doublets and dead cells CD4+ T cells were gated from Lineage+ cells and checked for the expression of CD90.2+ (Thy1.2+). CD4+ T cells were separated into the subpopulations T-bet+, GATA3+ and RORγt+ cells. ILCs were defined as Lineage, CD127+, with ILC2s expressing GATA3+, ILC3s expressing RORγt+ and further divided into 3 populations (Q1: CCR6-, T-bet+, Q2: CCR6+, T-bet+, Q3: CCR6+, T-bet-). From the double negative cells, ILC1s were defined as T-bet+. NK cells were defined as Lin-, Eomes+, NKp46+, T-bet+ and CD127- [90].

2.2.6.2. Blood flow cytometry analysis

Blood samples obtained from the retro orbital sinus of were subjected to red blood cell (RBC) lysis using RBC lysis buffer (eBioscience). After washing and centrifuging at 350xg for 5 minutes, cell pellets were resuspended in PBS. Leukocytes were counted with a Neubauer chamber, and 10^6 cells were obtained for the staining protocol. First, cells were

stained with a viability dye (BioLegend) for 30 min at room temperature (RT) then washed with FACS buffer (PBS, 2 mM EDTA (Corning), 0.2% BSA (SERVA)). For further staining, cells were stained in the antibody mixture mentioned in Table 6 and then processed as mentioned in intestinal flow cytometry section. The gating strategy is shown in Figure 8.

Table 6: List of antibodies used in flow cytometry analysis to identify myeloid, lymphoid and effector T helper cells.
[own representation]

Myeloid cells panel		
Antigen (clone)	**Fluorophore**	**Dilution factor**
CD11b (M1/70)	PE-Cy7 or (lung BV711)	100
CD11c (N418)	AF-488 (lung PE-Cy7)	50
CD64 (B56)	APC	50
Live-dead dye	Aqua Zombie (lung eFlur780)	500
Ly6C(HK1.4)	Pacific Blue (lung PerCP-Cy5.5)	200
Ly6G (1A8/RB6-8C5)	PerCP (lung FITC)	50
MHCII (M5/114.115.2)	Brilliant Violet 650	100
Siglec F (E50-2440)	PE	50
Additional antibodies for Lung myeloid cells panel		
CD45 (30-F11)	AF700	200
CD49b (DX5)	APC	200
F4/80(BM8)	BV510	200
FcεRIα (Mar-01)	PB	200
Lymphoid cells panel		
Antigen (clone)	**Fluorophore**	**Dilution factor**
B220 (RA3.6B2)	PerCP-Cy5.5 (B710)	100
CD3 (17A2)	APC-eF780 (R780)	100
CD4 (YTS)	FITC (B530)	200
CD8 (53-6.7)	Pacific Blue (V450)	100
CD44 (IM7)	PE-Cy7 (YG780)	300
CD62L (MEL-14)	APC (R670)	800
Live-dead dye	Aqua Zombie (V525)	500
Effector T helper cells panel		
Antigen (clone)	**Fluorophore**	**Dilution factor**
CD3 (17A2)	APC-eF780 (R780)	100
CD4 (RM4-5)	PE-Cy7 (YG780)	100
CD25 (PC61)	Alexa Fluor 488 (B530)	100
Foxp3 (FjK-16s)	eF450 (V450)	400
GATA3 (TWAJ)	PerCPeF710 (B710)	100
Live-dead dye	Aqua Zombie	500
RORgt (Q31-378)	PE (YG586)	100
T-bet (4B10)	eF660 (R670)	100

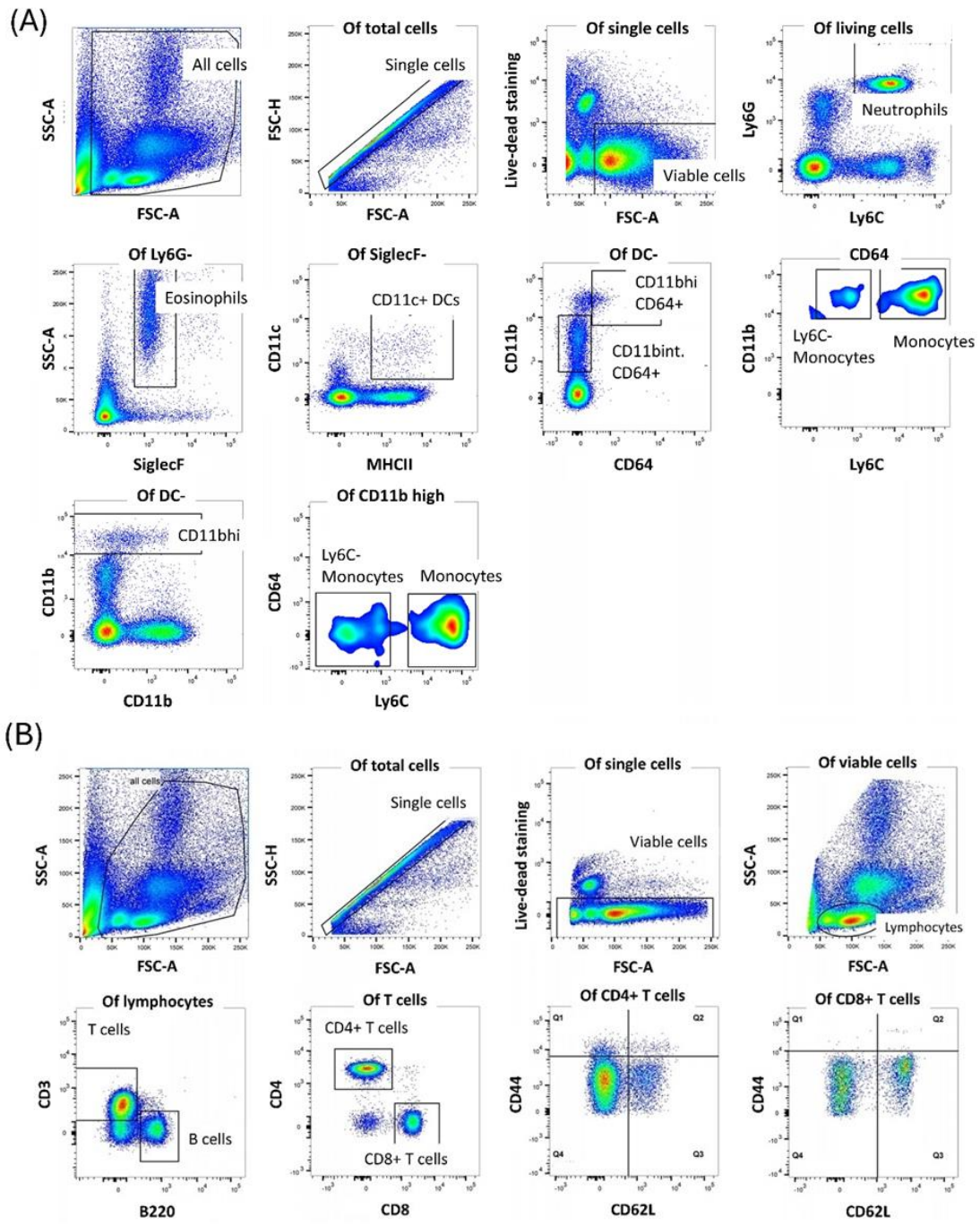

Figure 8. Blood myeloid and lymphoid cell gating strategy.
(A) After selecting the cells and removing doublets and dead cells, neutrophils were defined as Ly6G+ cells. From Ly6G- the population, eosinophils were defined as SiglecF+, SSC-A high. From the remaining cells, MHCII+, CD11c+ dendritic cells (DCs) were detected. After excluding DCs, Ly6C- Monocytes and Ly6C+ monocytes were examined within the CD64+ and CD11b high populations. (B) After excluding the debris and doublets, viable cells were selected, and lymphocytes were gated using forward and side scatter. T cells were separated from B cells using CD3 and B220 respectively. CD4+ and CD8+ T cells were investigated for memory cell markers. Q1: CD44+, CD62L- T cells (effector memory cells). Q2: CD44+ CD62L+ T cells (central memory T cells). Q3: CD44-, CD62L+ T cells (naïve T cells) [own representation].

2.2.6.3. Lung flow cytometry analysis

Lungs were extracted, weighed and cut in small pieces, then digested for 1 hour at 37°C in the following solution (5 mL of RPMI + 5% fetal bovine serum (ThermoFisher) + 1 mg/mL collagenase (Sigma) + 0.02 mg/mL Dnase I (Roche)). Tissue was smashed using a 100 µm cell strainer (Corning) with a syringe plunger (B. Braun) and cells were stained with the antibody mixture mention in either in Table 6 and 7. From here, cells were processed as mentioned in intestinal flow cytometry section. The lung flow cytometry gating strategy is shown in Figure 9.

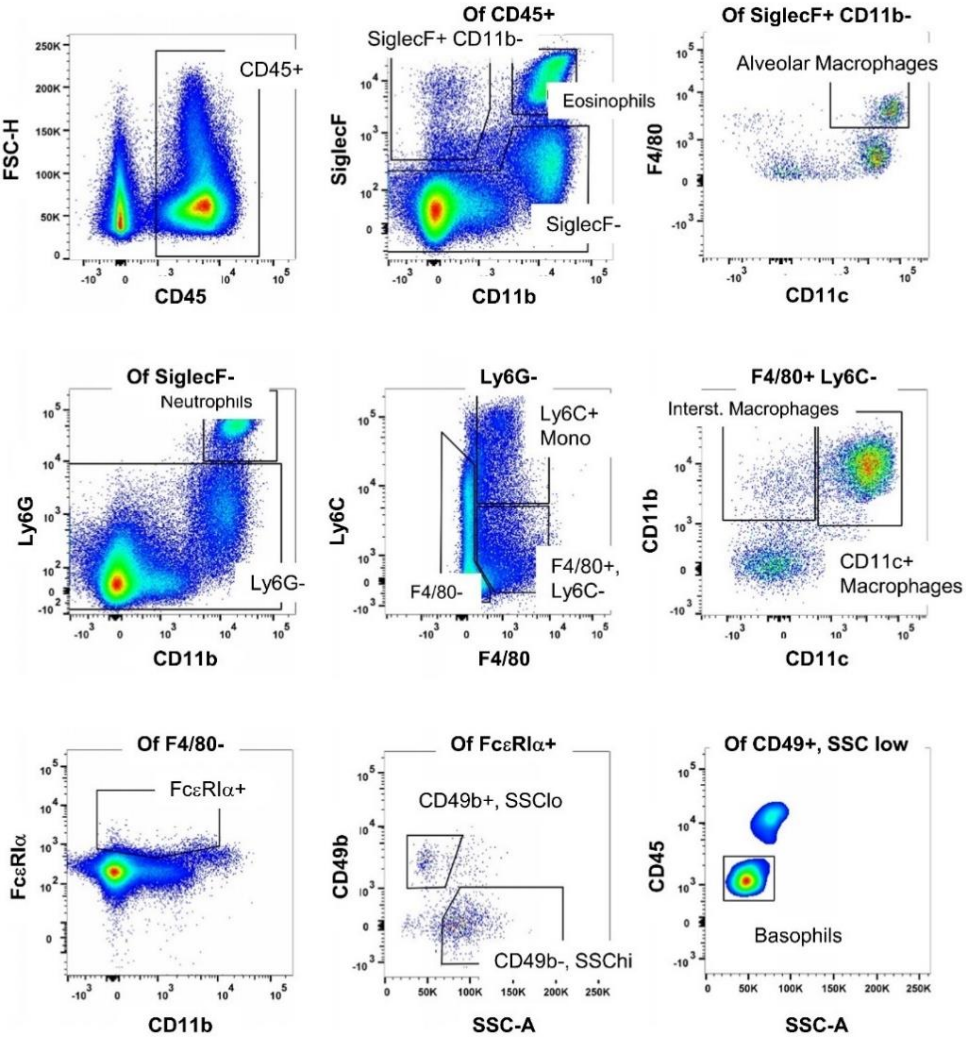

Figure 9. Lung myeloid cell gating strategy.
After removal of duplicates and dead cells from CD45+ leukocytes, eosinophils (CD11b+ SiglecF+) were gated. Alveolar macrophages were defined by the markers CD11b-, SiglecF+, CD11c+ and F4/80+. Ly6G+ neutrophils were gated from the SiglecF- population. Ly6C+ monocytes were gated from Ly6G- population. Macrophages were defined as Ly6C-, F 4/80+ then were divided into two groups CD11c+ or CD11c- which represent the interstitial macrophages. Basophils were gated from F4/80-, FcεRIα+, CD49b+, SSC-A low and CD45 low [own representation].

Table 7: List of antibodies used in flow cytometry analysis to identify lung ILC2s.
[own representation]

Lung ILC2s panel			
Antigen (clone)	**Fluorophore**	**Dilution factor**	
B220 (RA3-6B2)	Biotin	1000	
CD3 (145-2C11)	Biotin	600	
CD4 (GK1.5)	Biotin	200	
CD11b (M1/70)	Biotin	1000	
CD11c (N418)	Biotin	100	
CD19 (MB19-1)	Biotin	100	
FceRI (36951)	Biotin	200	Lineage
Gr1 (RB6-8C5)	Biotin	600	
TCRb (H57-597)	Biotin	200	
TCRγδ (GL3)	Biotin	500	
TER119 (TER-119)	Biotin	600	
Streptavidin	V500	200	
CD45 (30-F11)	AF700	200	
CD90.2 (53-2.1)	FITC	200	
CD127 (A7R34)	ef450	100	
GATA3 (TWAJ)	eFluor660	100	
KLRG1 (2F1)	BV711	500	
Live-dead dye	eFluor780	1000	
RORgt (B2D)	PE	100	
ST2 (U29-93)	BUV395	100	

2.2.6.4. Lung ILC2 sorting and cytokine measurement.

To assess ILC2 cytokine production in the lung of allergic offspring, half of the lung was processed as shown above in the lung flow cytometry protocol, and leukocytes were stained for ILC2 defining surface markers (CD45, lineage (TER119, B220, CD19, CD11c, FcεRIα, TCRβ), CD90, CD127, CD25). Cells were sorted using a BD FACSAria. A purity check was performed for each sample and the sorting gating strategy was performed as shown in Figure 10. After sorting, 2000 cells were lysed using a cell lysis buffer (Invitrogen) and cytokines were measured with Luminex, as described in section 2.1.3.5

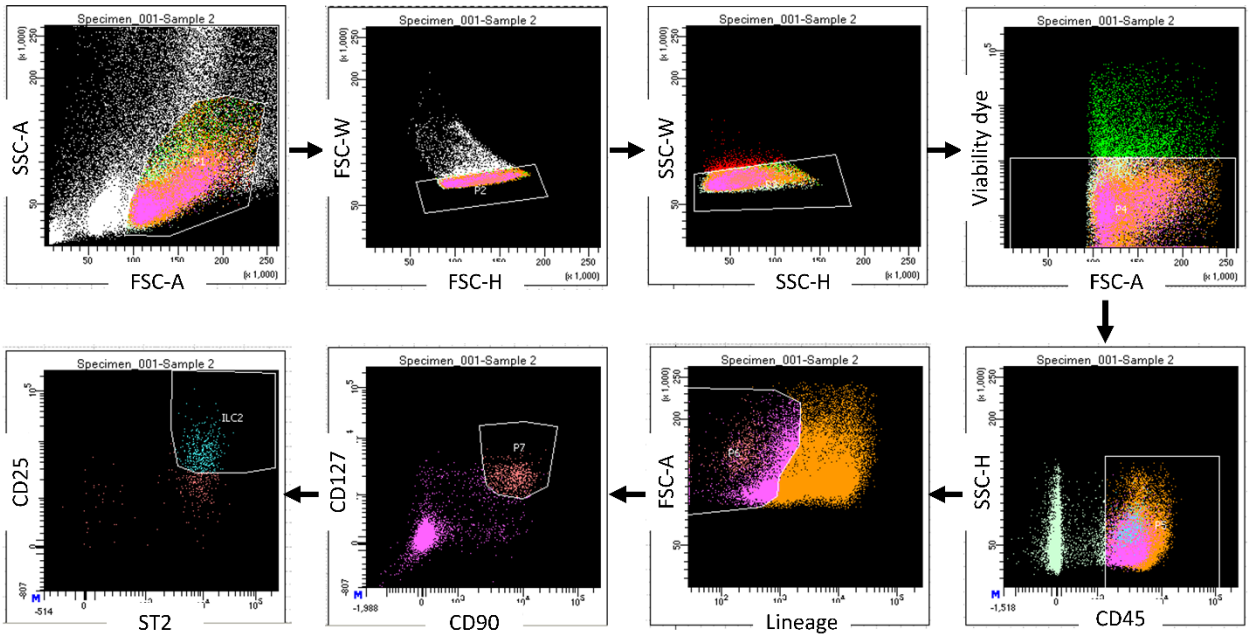

Figure 10. ILC2 sorting strategy.
Lymphocytes were selected based on forward scatter-Aria (FSC) and side scatter (SSC). The process of removing doublets was carried out in two steps, using FSC-H versus FSC-W and then SSC-H versus SSC-W. Dead cells were filtered out by utilizing a viability dye and the leukocytes were identified as CD45+. After excluding cells that were lineage-positive, ILC2s were selected by via the surface markers CD127+/CD90+/ST2+/CD25+ [own representation].

2.3. Statistical analysis

Data was tested for normal distribution with the Shapiro-Wilk normality test. In the case of parametric data, one-way ANOVA (in case of multiple groups comparisons) or Student's t-test was performed for comparison of two groups. In the case of non-parametric data, a Kruskal-Wallis (with Dunnett's multiple comparison test) was applied in case of multi-group comparisons, and a Mann-Whitney U test was applied for two-group comparison. Outlier analysis was performed using Cook's distance. Statistical tests were performed with GraphPad Prism (V.8 and 9, Dotmatics).

3. Results

3.1. Objective 1: Mouse model establishment and proof of concept. Prenatal Antibiotic treatment and increased asthma severity in the offspring.

3.1.1. Model establishment.

To establish a proof-of-concept model for antibiotic treatment during pregnancy and increased offspring asthma risk, we treated pregnant mice daily with vancomycin, corresponding to low, medium and high doses in humans (Figure 11A and B). Pregnant dams were treated orally with vancomycin mixed with 15µl of ORA-Sweet syrup. All mice consumed the mixture voluntarily, allowing stress free treatment of the animals (Figure 11C). Fecundity analysis demonstrated that maternal vancomycin treatment did not affect the litter size or sex proportion of the pups (Figure 11D), however the 20 and 40 mg/kg concentrations were associated with lower offspring weight (Figure 11E).

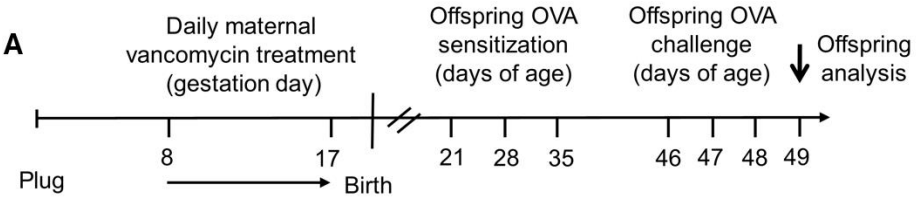

B

Group	Maternal vancomycin treatment	Offspring allergy
1 (Control)	0 mg/kg (MC)	OVA
2	10 mg/kg (MV10)	OVA
3	20 mg/kg (MV20)	OVA
4	40 mg/kg (MV40)	OVA

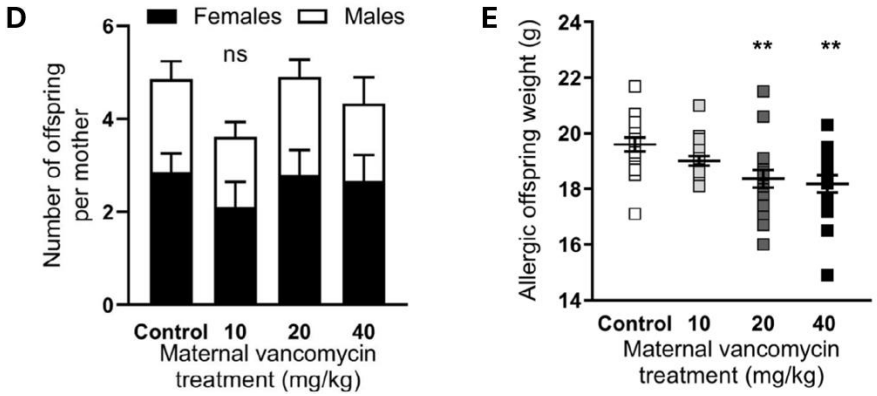

Figure 11. Establishment of a mouse model for prenatal antibiotic treatment and assessment of asthma severity in the offspring.

A-B Experimental design and treatment groups. **C** Oral administration technique **D** Litter size and male/female offspring proportion. **E** Weight of 7-week-old allergic offspring. Means ± SEM are shown n>16. Significance is represented by *P < .05, **P < .01, ***P < .001, one-way ANOVA or Kruskal-Wallis test comparing the control group against 10, 20, and 40 mg/kg vancomycin groups [91].

When female offspring from vancomycin-treated mothers were exposed to an experimental asthma protocol, they showed a maternal-vancomycin-dose-dependent worsening of asthma compared to offspring from control mothers. Though no differences were observed in serum IgG1, OVA-specific IgG1 or OVA-specific IgE (Figure 12A), lung histology revealed increased inflammation, evidenced by increased eosinophil influx as well as increased goblet cell percentage and volume in the 20 and 40 mg/kg groups (Figure 12B and C). Analysis of the BAL revealed a significantly higher leukocyte influx, mainly composed of eosinophils and macrophages (Figure 12D). Regarding BAL cytokines, Although the allergic reaction was stronger in the Prenatal-Antibiotic offspring, assessment of the BAL showed a decrease in 12 cytokines (IL-1b, IL-4, IL-5, IL-9, IL-12p70, eotaxin, G-CSF, GM-CSF, MCP-1, MIP-1a, MIP-1b and RANTES) in the 20 mg/kg and 40 mg/kg groups compared to the control (Table 8 [91]).

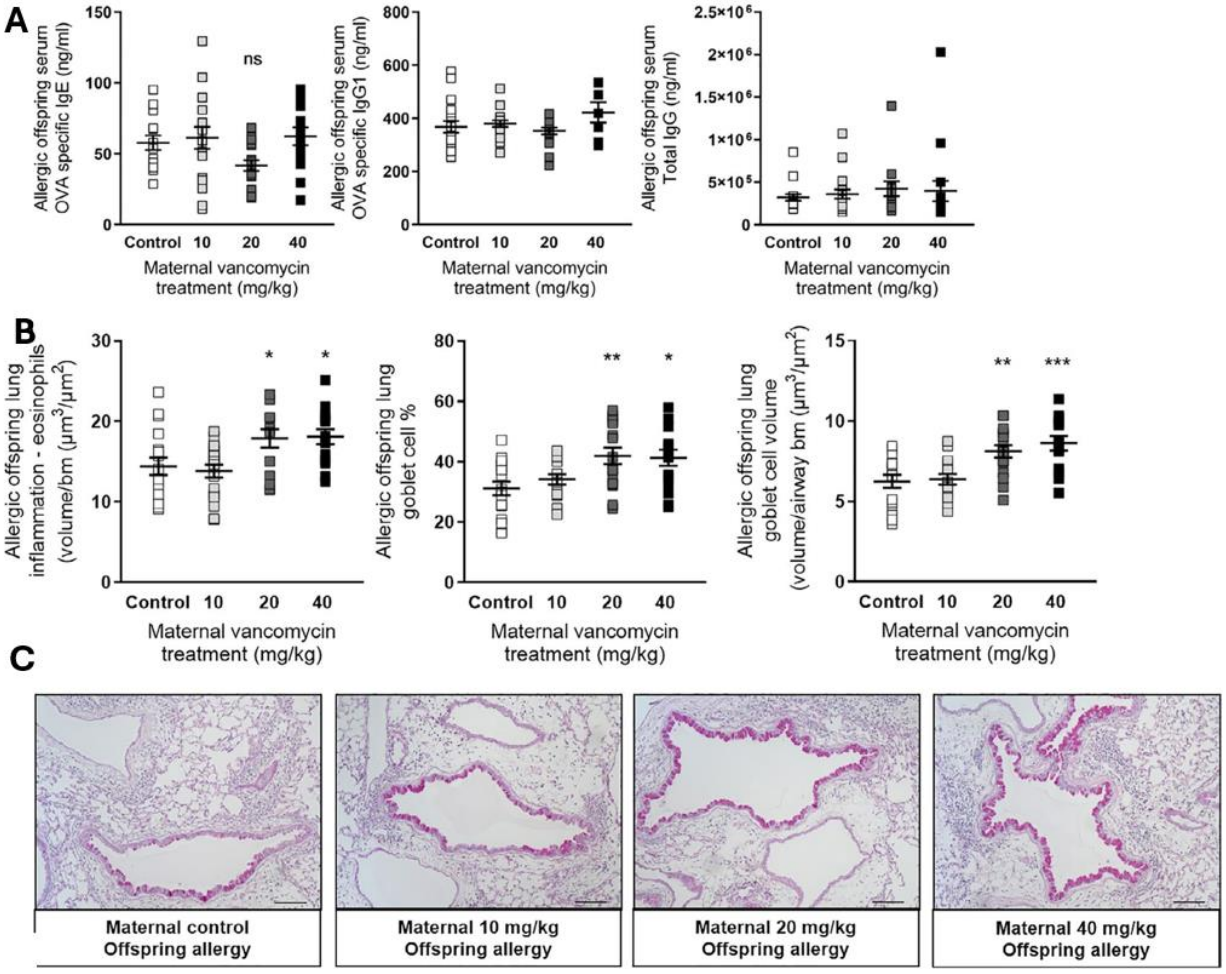

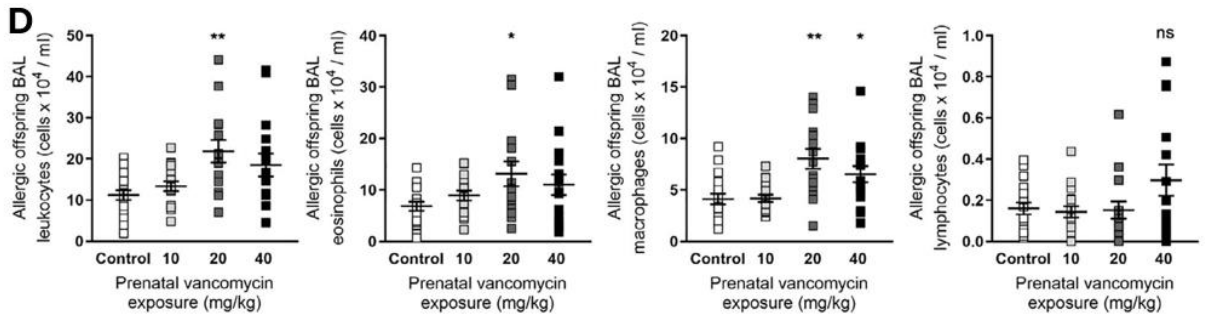

Figure 12. Analysis of the asthma phenotype in offspring from vancomycin treated mothers. **A** Serum total IgG1, OVA-specific IgG1 and OVA-specific IgE antibodies. **B** Lung inflammation quantification eosinophil number, goblet cell percentage, goblet cell volume. **C** Representative lung histology images (Scale bar = 100 µm). **D** Differential cell count in the bronchoalveolar lavage. n>16. Significance is represented by *P < .05, **P < .01, ***P < .001, one-way ANOVA or Kruskal-Wallis test was performed comparing the control group against the 10, 20, and 40 mg/kg vancomycin groups [91].

Table 8: Measurement of 23 cytokines in the BAL of Prenatal-Antibiotic and Prenatal-Control allergic offspring.

Means ± SEM are shown, control (n >16). Significance is represented by *P < .05, **P < .01, ***P < .001 one-way ANOVA or Kruskal-Wallis test with Dunnett's multiple comparisons test were performed [91].

	Maternal control	Maternal 10 mg/kg	Maternal 20 mg/kg	Maternal 40 mg/kg
	n = 18	n = 18	n = 13	n = 16
Concentration (pg/mL)	Mean (SEM)	Mean (SEM)	Mean (SEM)	Mean (SEM)
IL-1α	7.2 (0.4)	8.5 (0.9)	9.0 (0.8)	9.0 (1.0)
IL-1β	48.0 (4.9)	36.1 (4.0)	**22.0 (5.3)****	**25.4 (5.6)***
IL-2	164.8 (18.1)	6.4 (0.4)	6.6 (0.4)	6.8 (0.7)
IL-4	165.4 (17.5)	142.9 (16.4)	**82.9 (16.9)***	145.0 (4.2)
IL-5	164.8 (18.1)	146.2 (11.4)	**103.2 (17.2)***	130.7 (13.4)
IL-6	9.7 (2.9)	10.3 (1.6)	9.7 (1.6)	8.2 (1.4)
IL-9	42.0 (6.0)	**20.9 (5.5)***	26.4 (7.8)	**9.7 (4.4)*****
IL-12p40	52.6 (4.2)	43.4 (2.8)	40.1 (3.8)	44.4 (4.2)
IL-12p70	12.4 (1.0)	11.1 (0.7)	**7.7 (0.8)****	**9.1 (1.3)***
IL-13	111.1 (13.4)	83.6 (9.3)	81.5 (12.1)	92.2 (9.6)
Eotaxin	161.6 (7.2)	141.0 (7.0)	135.6 (11.2)	**113.0 (16.9)****
G-CSF	8.4 (0.8)	7.9 (0.9)	**5.3 (0.9)***	**5.5 (0.9)***
GM-CSF	10.0 (0.6)	8.5 (0.3)	**6.5 (0.6)*****	**3.3 (6.5)*****
KC	213.2 (27.5)	230.8 (29.1)	240.7 (34.7)	207.3 (26.5)
MCP-1	28.9 (5.9)	16.2 (2.8)	**4.7 (3.0)*****	**6.1 (2.7)*****
MIP-1α	9.8 (0.9)	9.6 (0.6)	**5.1 (0.1)*****	7.7 (0.9)
MIP-1β	4.3 (0.4)	3.8 (0.2)	**2.4 (0.3)*****	**2.6 (0.2)*****
RANTES	6.5 (0.4)	5.8 (0.2)	**4.7 (0.3)****	**5.3 (0.4)***
TNFα	20.9 (1.3)	19.6 (1.0)	17.1 (1.9)	22.6 (4.7)

3.1.2. Examination of the maternal and offspring intestinal microbiota.

After confirming the increased asthma severity in the Prenatal-Antibiotic offspring, we assessed the mother to offspring transfer of gut microbial dysbiosis by performing qPCR on collected fecal samples. Treatment with vancomycin resulted in an increase in the total gut bacterial load in both treated mothers (at G17) and their offspring at PN15 and PN49

(Figure 13A). This increase in the total bacterial load occurred mainly due to the enrichment of the gram-negative bacteria such as *Enterobacteriaceae* (Log 4 increase in G17 treated mothers and approximately Log 4 increased in PN15 offspring (Figure 13B), and *Bacteroidetes* (Log 2 in G17 treated mothers, and Log 1 in the PN15 and PN49 offspring Figure 13C). This was accompanied by the depletion of gram-positive bacteria, such as members of the *Clostridium leptum* group in both vancomycin treated mothers and their offspring (Figure 13D).

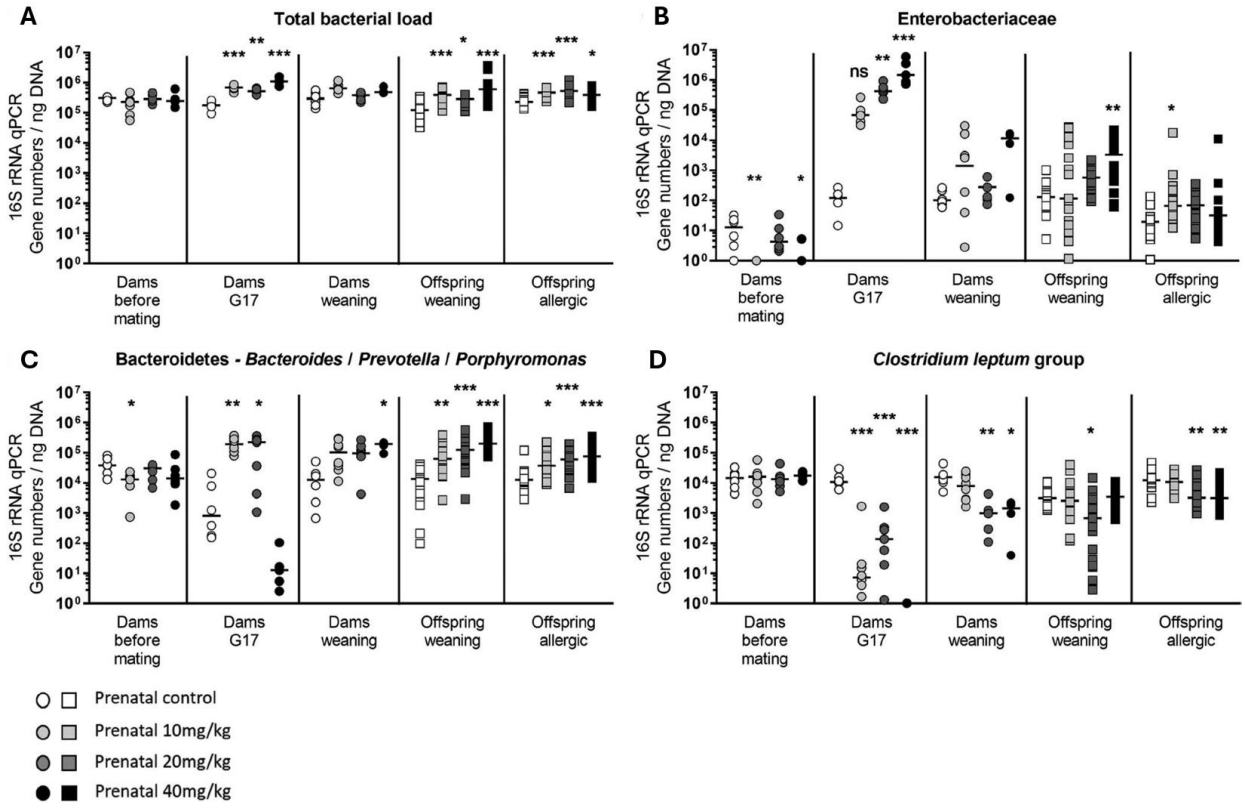

Figure 13. Vancomycin treatment during pregnancy results in transfer of gut microbial dysbiosis from mothers to their offspring.

A Total bacterial load. **B** *γ-proteobacteria-Enterobacteriaceae* quantification. **C** *Bacteroidetes—Bacteroides, Prevotella, and Porphyromonas* quantification. **D** *Clostridium leptum* quantification. N>6. Significance is represented by *P < .05, **P < .01, ***P < .001, one-way ANOVA or Kruskal-Wallis test was performed to compare control group against 10, 20, and 40 mg/kg vancomycin groups [91].

3.2. Objective 2: Prenatal Antibiotic Treatment model - Immune phenotyping of the offspring gut-lung axis and assessment of airway reactivity

3.2.1. The effect of maternal antibiotic use during pregnancy on airway reactivity in offspring with allergic asthma.

Next, we repeated the model using a vancomycin dosage of 20 mg/kg to assess the effects of maternal antibiotic use during pregnancy on allergic offspring airway hyperreactivity. Prenatal-Antibiotic exposed offspring had more severe airway hyperreactivity than

Prenatal-Control offspring, evidenced by higher Newtonian resistance after challenge with increasing concentrations of methacholine (Figure 14A). Analysis of BAL leukocyte composition revealed that offspring from the maternally treated group had a higher number of eosinophils and lymphocytes (Figure 14B). Assessment of serum antibody concentrations showed significantly increased concentrations of OVA-specific IgE, OVA-specific IgG1 and total IgG (Figure 14C).

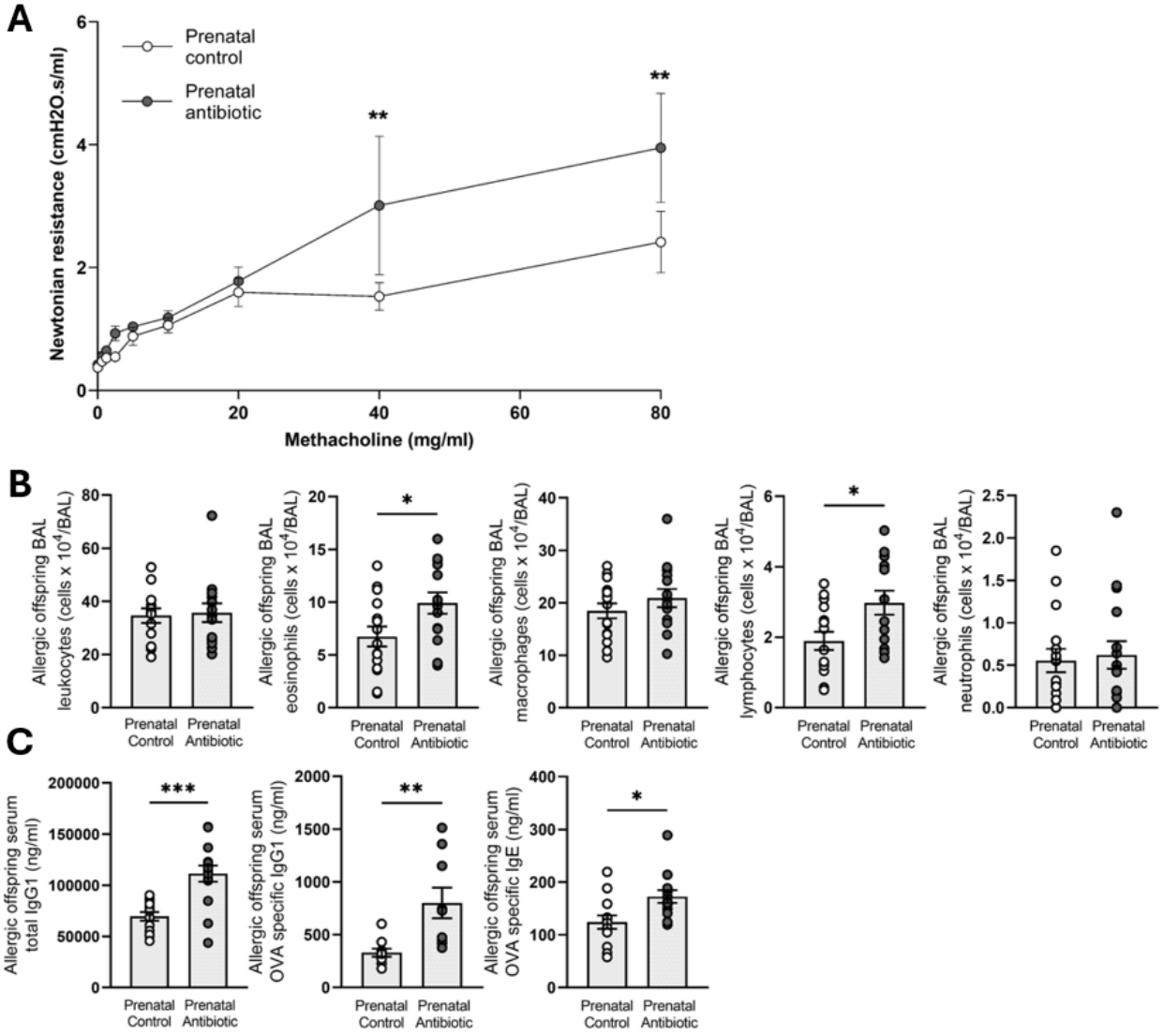

Figure 14. Assessment of airway hyperreactivity and asthma phenotype in allergic offspring from 20 mg/kg vancomycin treated mothers.

A Assessment of the airway hyperreactivity via measurement of Newtonian resistance after escalating dosages of methacholine (n=12). **B** BAL differential cell counts; Leukocytes, eosinophils, macrophages, lymphocytes and neutrophils (n=16). **C** Serum total IgG1, OVA specific IgG1 and OVA specific IgE (n ≥9). Significance is reported by *P < .05, **P < .01, ***P < .001, Student's t-test or Mann Whitney test, Figure adapted from [90].

3.2.2. Gut microbiome sequencing the mother and offspring feces and assessment of SCFA concentrations.

After confirming increased airway reactivity in allergic offspring from mothers treated with 20mg/kg vancomycin, we next performed a deeper analysis of the maternal and offspring gut dysbiosis. 16S rRNA sequencing was used to assess the fecal gut microbiota in mothers (before mating, at the end of the treatment at G17 and at weaning at PN21) and their offspring at (weaning and after asthma induction). As shown in Figure 15A-C and in Table 9, several bacterial genera including *Escherichia, Parabacteroides, Sutterella and Akkermansia* had higher relative abundance, not only in the feces from antibiotic treated mothers, but also in their offspring. In the offspring, *Bacteriodes* also had significantly higher abundance in the offspring, both at weaning and after asthma induction. On the other hand, the relative abundance of several bacterial families - such as *Lachnospiraceae, Rikenellaceae*, and genera - *Oscillospira and Ruminococcus* were reduced in both mothers and offspring. Both Prenatal-Antibiotic mothers and their offspring showed less a-diversity (Shannon index, Figure 15D) and principal component analysis of offspring β-diversity demonstrated that maternal antibiotic treatment had a larger effect on the gut microbiota than age difference or asthma induction (Figure 15E). Measurement of SCFAs in the feces (collected at the same time points as the microbiota analysis) showed significant reductions in acetate, propionate, butyrate and isovalerate in both Prenatal-Antibiotic mothers and their offspring at the end of pregnancy, which persisted until weaning (Figure 15F).

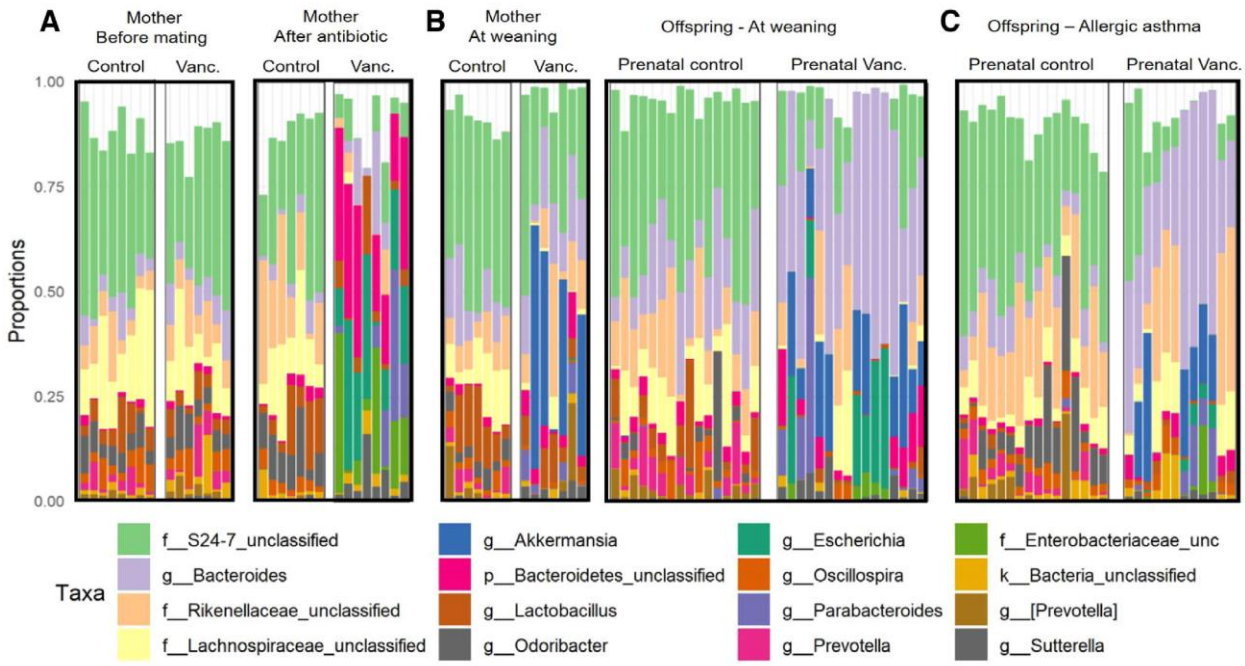

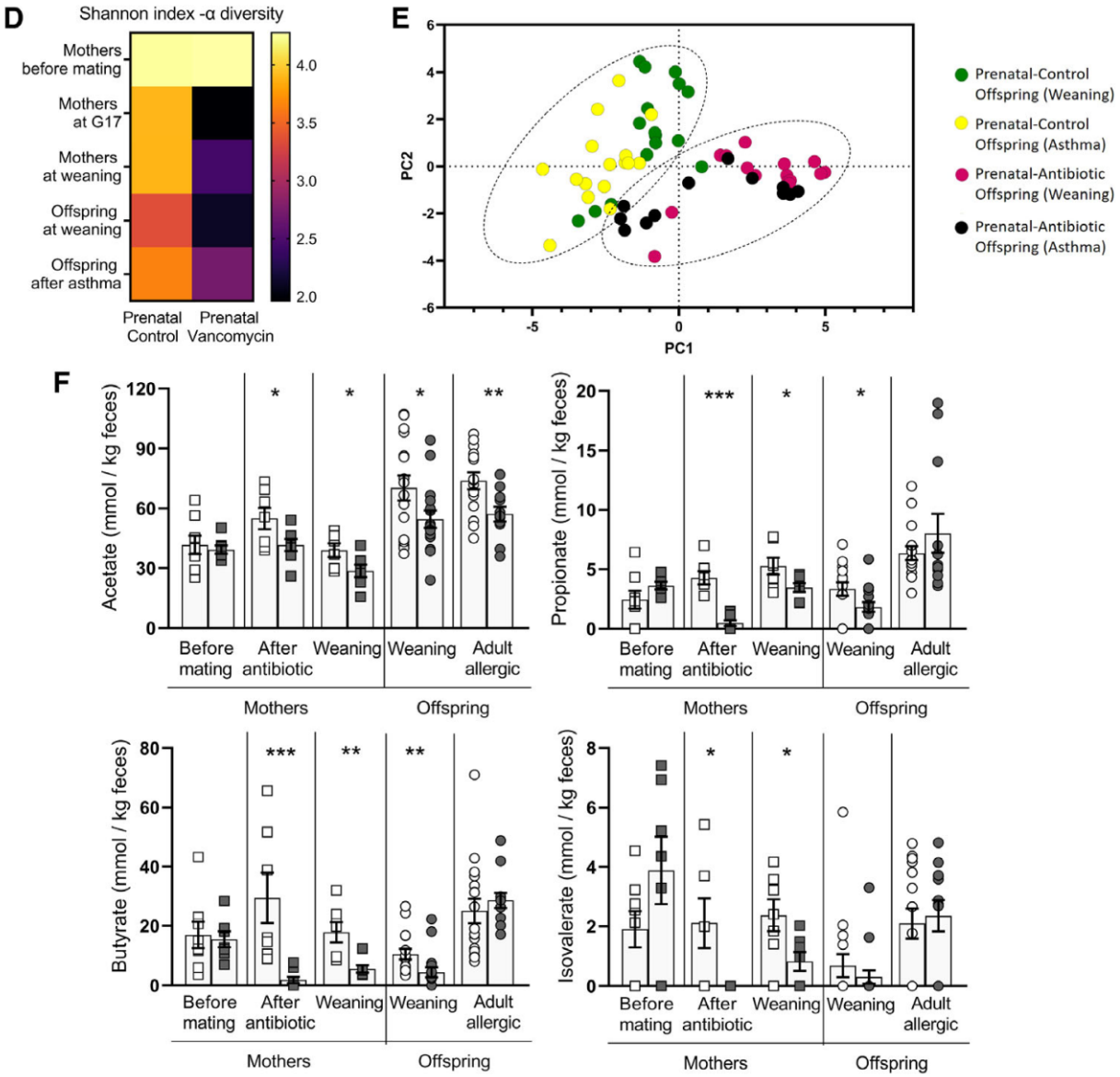

Figure 15. Fecal microbiota and SCFA analysis in mothers and offspring.

A-C Bar plots representing the relative abundance of bacteria clades. k - kingdom; p - phylum; f - family; g - genus. **D** α-diversity of the fecal gut microbiota in mothers and their offspring. **E** beta-diversity analysis of prenatal-control and prenatal-antibiotic offspring at weaning and after asthma induction. **F** Fecal short-chain fatty acid measurement in maternal and offspring feces: acetate, propionate, butyrate, and isovalerate. Means ± SEM are shown. Significance is represented by *P < .05, **p < .01, ***p < .001. Student's t-test or Mann–Whitney test was performed for the statical analysis [90].

Table 9: **Phylogenetic classification of changes in fecal bacterial composition in Prenatal-Control versus Prenatal-Antibiotic treated mothers and their offspring.**

Relative abundance was determined by 16S rRNA gen amplicon sequencing. Classification: k - kingdom; p - phylum; o – order; f - family; g - genus. Grey-highlighted cells represent the most abundant clades. Student's t-test or Mann-Whitney test was applied A blank cell = no difference between control and antibiotic-treated groups. *P < .05, **P < .01, ***P < .001. ****P < 0.0001 [90].

	Mother after antibiotics (G17)	Mother weaning (PN21)	Offspring weaning (PN21)	Offspring asthma (PN49)
g_Akkermansia		Inc*	Inc****	Inc**
g_Bacteriodes			Inc****	Inc****
p_Bacteroidetes	Inc***	Inc*		
g__Blautia		Inc*	Inc****	Inc*
f__Desulfovibrionaceae	Inc**			
f__Enterobacteriaceae	Inc*			
g__Escherichia	Inc**		Inc****	
g__Parabacteroides	Inc**	Inc*		Inc****
p__Proteobacteria	Inc**			
p_Proteobacteria	Inc****	Inc*	Inc****	
g__Sutterella	Inc***	Inc***	Inc**	Inc*
p_Verrucomicrobia		Inc*	Inc****	Inc**
o__Bacteroidales		Dec*	Dec****	Dec****
g__Bilophila	Dec**			
g__Butyricicoccus	Dec***	Dec**	Dec*	
g__Candidatus_Arthromitus	Dec***			Dec**
g__Clostridium	Dec***	Dec*	Dec*	
g__Clostridium	Dec***		Dec**	Dec**
g__Clostridium		Dec***	Dec**	Dec***
g__Coprobacillus	Dec**	Dec*		Dec**
g__Coprococcus	Dec***	Dec**	Dec****	Dec**
g__Dehalobacterium	Dec***	Dec***	Dec****	Dec**
g__Dorea	Dec***	Dec***	Dec*	
f__F16	Dec***		Dec**	Dec*
p__Firmicutes	Dec***	Dec*	Dec****	Dec**
p_Firmicutes	Dec****	Dec***	Dec***	
f__Lachnospiraceae	Dec***	Dec**	Dec**	
g__Lactobacillus			Dec*	
f__Mogibacteriaceae			Dec*	Dec**
g__Oscillospira	Dec***	Dec**	Dec***	
g__Odoribacter	Dec****	Dec****	Dec****	Dec****
g__Prevotella	Dec**	Dec***	Dec****	Dec****
g__Prevotella	Dec***		Dec****	Dec****
o__RF39	Dec ***	Dec*		Dec***
f__Rikenellaceae	Dec**		Dec*	
f__Ruminococcaceae	Dec****	Dec**	Dec****	Dec**
g__Ruminococcus	Dec****	Dec**	Dec**	Dec***
f__S24-7 p_(o_Bacteriodales)	Dec***	Dec*	Dec****	Dec***

3.2.3. The effect of antibiotic use during pregnancy on lactation, milk composition and the intestine of sucking mice.

The maternal intestine expands during lactation to provide more surface area for nutrient absorption [92,93]. To investigate if the maternal gut dysbiosis observed in our model could interfere with this process, we next examined maternal intestinal histology and milk composition during lactation. Analysis of PN15 lactating mothers demonstrated that

neither the intestinal length nor intestinal villus-crypt length was affected by antibiotic treatment (Figure 16A and B).

Next, we assessed the impact of vancomycin treatment on immunological components in the milk at PN15, using a 23-plex cytokine assay. Though we detected 6 cytokines (IL-1α, eotaxin, G-SCF, KC, RANTES, and TNF-α) in the breast milk, there were no differences observed between the antibiotic treated mothers and controls (Figure 16C). SCFA analysis in the breast milk demonstrated that through acetate, propionate, and butyrate were all measurable there were also no differences observed between groups (Figure 16D).

As it is known that gut microbial dysbiosis can induce changes in IgA composition [94], we next measured IgA concentrations in mothers and their offspring. Prenatal-Antibiotic mothers had significantly higher concentrations of IgA in the serum and milk (Figure 16E). Increased IgA concentrations were also detected in the serum and feces of their PN15 offspring (Figure 16F). We next assessed intestinal inflammation in mothers and their offspring. Measurement of the inflammation marker lipocalin-2 in feces demonstrated intestinal inflammation in both mothers and offspring from the Prenatal-Antibiotic group (Figure 16G). Finally, we demonstrated that maternal antibiotic use during pregnancy was also associated with a significant reduction in PN15 offspring weight when compared to offspring from control mothers (Figure 16H).

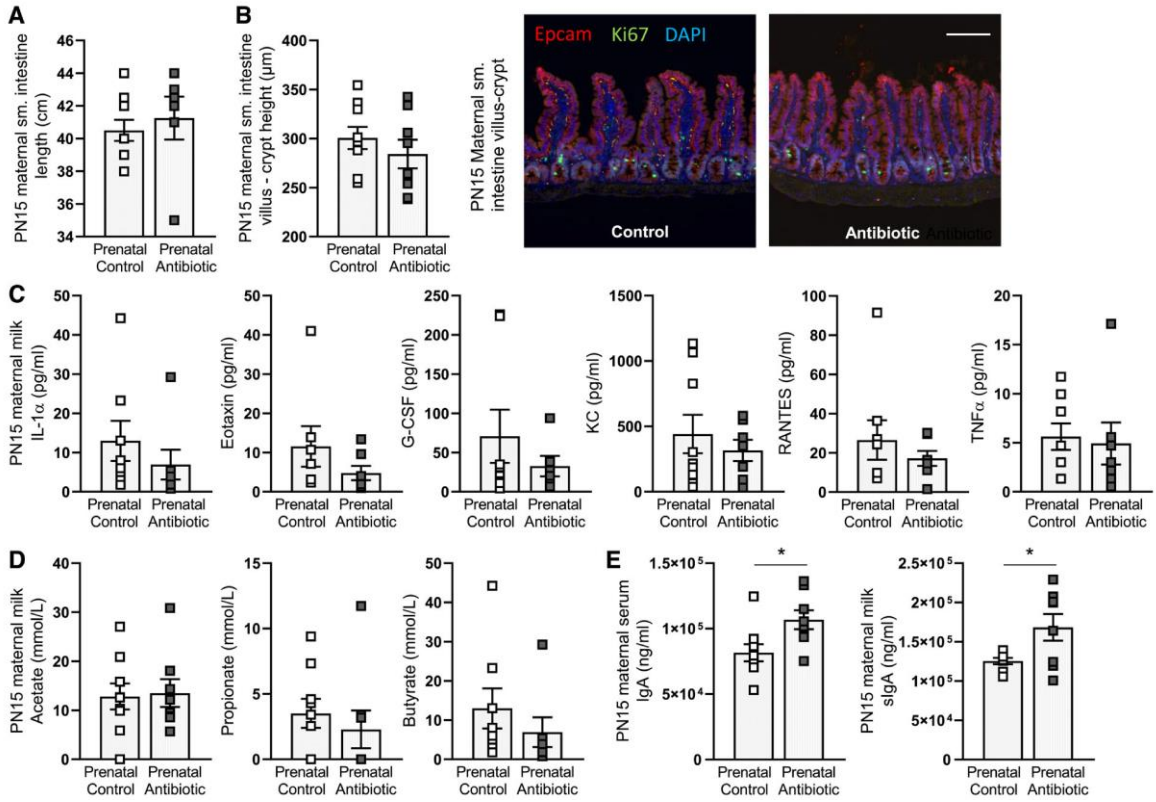

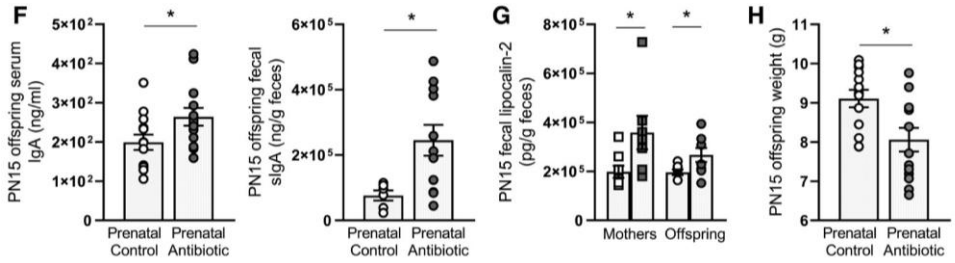

Figure 16. Prenatal antibiotic exposure induces intestinal inflammation and increases IgA concentrations in PN15 mothers and their offspring.

A PN15 maternal small intestine length. **B** PN15 maternal small intestine villus-crypt length (µm) and immunofluorescence staining of the small intestine using the markers Epcam, Ki67 and DAPI (scale bar = 100 µm). **C** Detectable cytokines in breast milk, namely: IL-1α, eotaxin, G-CSF, KC, RANTES, and TNF-α. **D** Measurable SCFAs in milk. **E** Maternal serum and breast milk IgA concentrations. **F** Offspring serum and fecal IgA concentrations. **G** Fecal lipocalin-2 levels. h PN15 offspring weight. Maternal and offspring samples, n>8. Means ± SEM are shown. Significance is reported by *P < .05, **P < .01, ***P < .001, Student's t-test or Mann Whitney test [90].

3.2.4. Assessment of offspring immune system development along the gut-lung axis

In order to understand how offspring intestinal dysbiosis could affect development of the mucosal immune system, flow cytometry analysis was performed on the small intestine lamina propria (SI-LP), blood and lung in early life at PN15 and at after allergic asthma induction at PN49.

3.2.4.1. Gut dysbiosis in early life disturbs small intestine mucosal immune cell composition and gut permeability.

The innate and adaptive mucosal immune system of the small intestine plays a major role in intestinal homeostasis [95]. Immunophenotyping of the SI-LP in early life showed that even though absolute leukocyte cell numbers did not vary between the groups, leukocyte cell percentages were significantly increased in Prenatal-Antibiotic offspring (Figure 17A). Analysis of $CD4^+$ T cells showed increased percentages in Prenatal-Antibiotic offspring in early life however, after asthma induction a significant reduction was observed in this cell type. (Figure 17B). $CD4^+$ T cell subpopulations revealed that the prenatal antibiotic exposure had no effect on the T-bet^+ or RORγt^+ Th cells in early life, however, the $GATA3^+$ cell population percentages were lower in the Prenatal-Antibiotic offspring compared to controls (Figure 17C). After asthma induction, all CD4+ T cell subpopulations (T-bet^+, $GATA3^+$ and RORγt^+ $FoxP3^{+/-}$) were decreased in the SI-LP (Figure 17C).

Regarding ILCs, a decrease in total ILC percentage was observed in both the PN15 and allergic groups. Investigation of ILC subpopulations revealed that ILC1 and ILC3 percentages were not affected at any time point, but ILC2s were increased in the SI-LP after asthma induction (Figure 17D). Further analysis of ILC3 subgroups revealed an increase

in the percentage of the inflammatory NCR^{-} (CCR6^{+} T-bet^{-}) and a reduction in anti-inflammatory NCR^{+} (CCR6^{-} T-bet^{+}) ILC3s (Figure 17e). These inflammatory changes in the intestine were accompanied by disruption of the intestinal barrier in early life as a gut permeability assay demonstrated significantly increased amounts of FITC-Dextran in serum from Prenatal-Antibiotic offspring (Figure 17F).

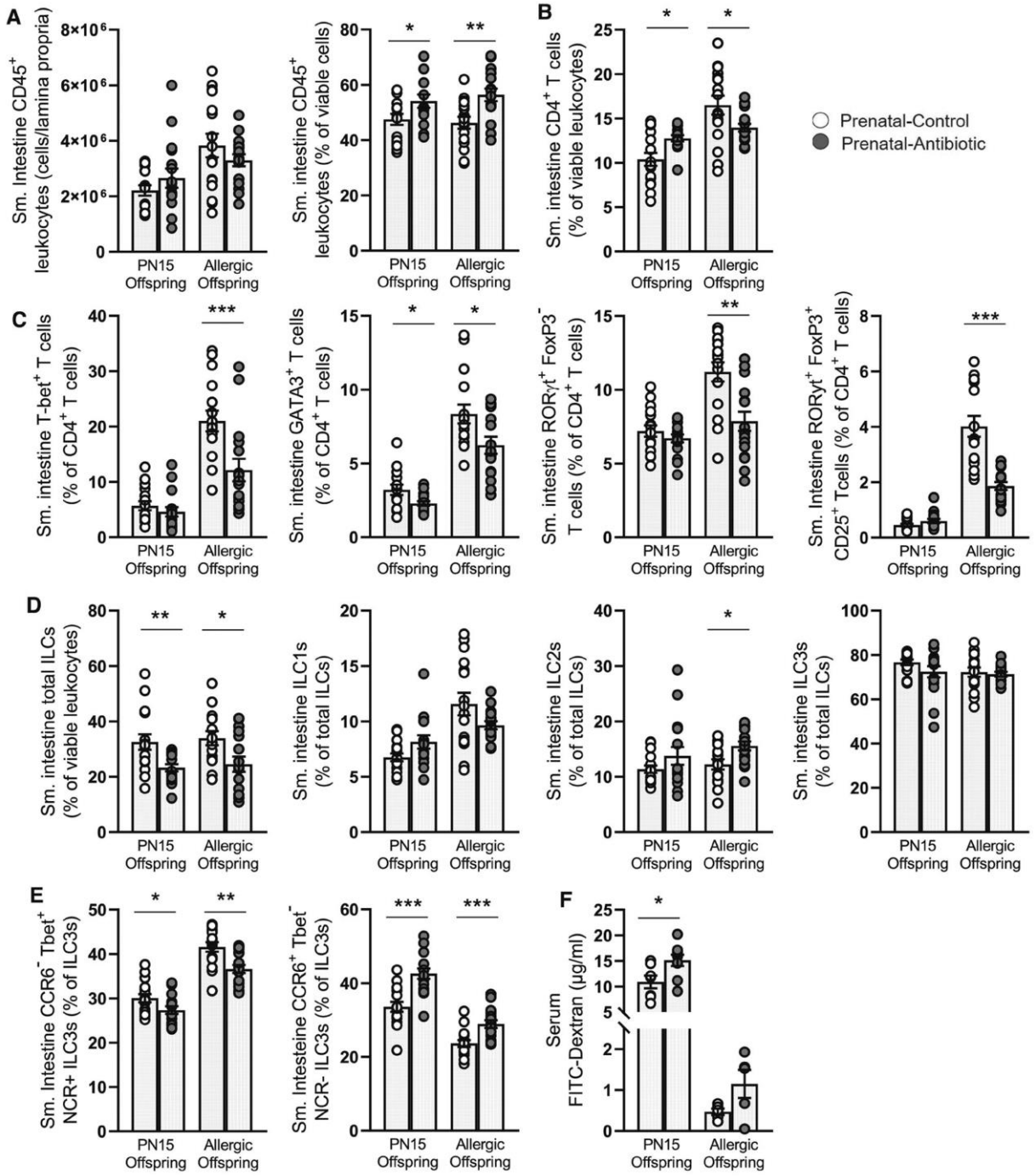

Figure 17. Prenatal antibiotic exposure alters ILC3s population and compromises intestinal barrier integrity in the offspring in early life.

A Absolute numbers and percentages of leukocytes. **B** CD4+ T helper cell percentages. **C** T helper cells subpopulations: T-bet+, GATA3+, RORγt + FoxP3-, RORγt+ FoxP3+ CD25+. **D** Percentages of total ILCs, ILC1s ILC2s and ILC3s. **E** ILC3s subpopulations NCR+ (CCR6- T-bet+) and NCR- (CCR6+ T-bet-). **F**

Serum concentration of 4 kDa FITC-dextran after oral gavage to PN15 and allergic mice. (A-E) n=16 and for (F), n ≥ 5. Means ± SEM are shown. Significance is reported by *P < .05, **P < .01, ***P < .001, Student's t-test or Mann Whitney test [90].

3.2.4.2. Dysbiosis, intestinal inflammation and reduced gut barrier integrity in early life are associated with increased blood LPS concentrations and RORγt Th cell percentages in the circulation.

To understand the communication between the gut and lung, we assessed several parameters in offspring blood. Prenatal-Antibiotic mothers and their PN15 offspring contained higher concentrations of LPS in the serum compared with controls, whereas adult asthmatic offspring showed no difference in serum LPS (Figure 18A). Flow cytometry analysis of the blood revealed leukopenia in Prenatal-Antibiotic offspring at PN15, which was resolved at the PN49 time point after asthma induction (Figure 18B). No differences in Ly6C^{hi} monocytes, neutrophils or eosinophils were observed at either time point (Figure 18C). Despite the unchanged percentages of the eosinophils, a significant increase in the expression of the activation markers sialic acid-binding Ig-like lectin 5 (SiglecF) and CD11b was observed in offspring, both in early life and after asthma induction (Figure 18d). Additionally, although no significant changes were detected in blood Th cells or T-bet^{+} and GATA3^{+} subpopulations at either time point (Figure 18E and F), CD4^{+} RORγt^{+} T cells were significantly increased both in early life and after asthma induction (Figure 18F). RORγt^{+} FoxP3^{+} cells were not detected in the blood and Tregs did not show any changes between the groups.

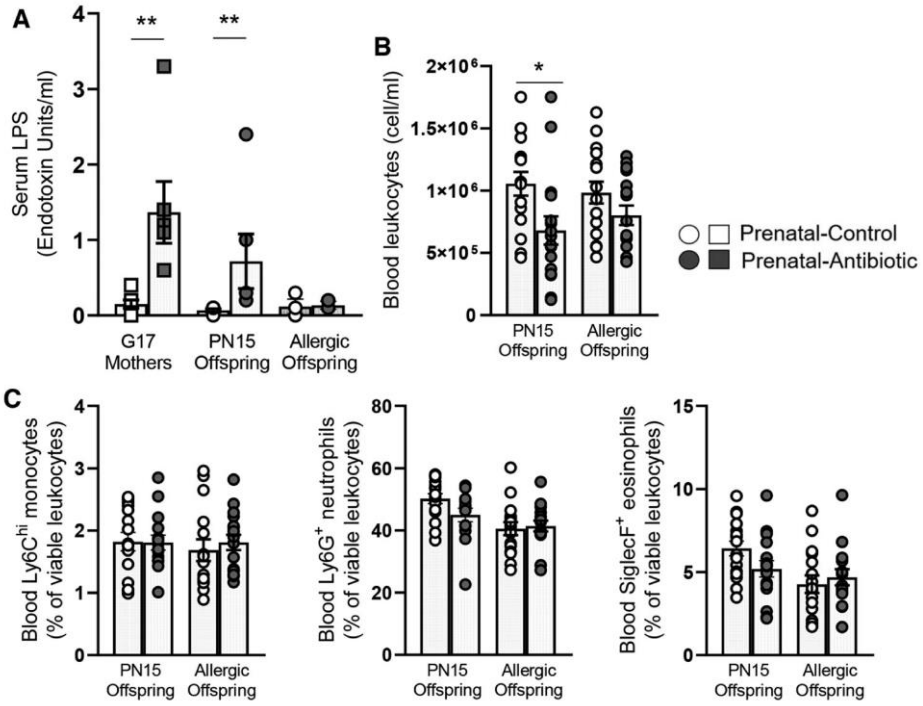

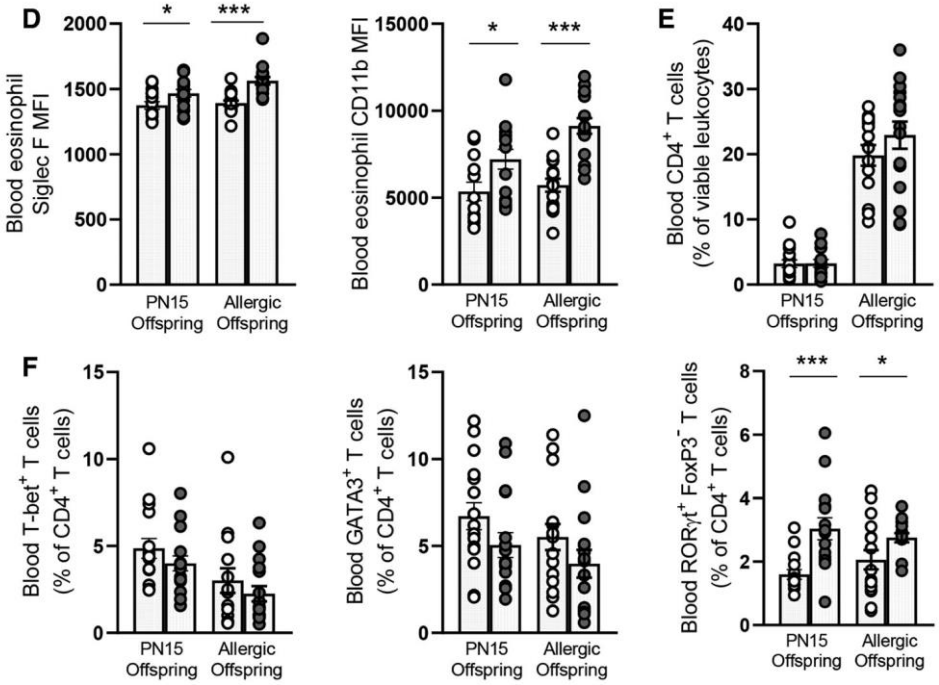

Figure 18. Increased LPS and RORgt+ FoxP3- Th cells in the blood of offspring from antibiotic treated mothers.

A LPS serum concentrations. **B** Blood leukocyte concentrations per ml blood. **C** Percentages of: Ly6Chi monocytes, Ly6G+ neutrophils and SiglecF+ eosinophils. **D** CD11b and SiglecF mean fluorescence intensity (MFI) of eosinophils. **E and F** Percentages of CD4+ T cells and its subsets: T-bet+, GATA3+, RORγt+ FoxP3-. Means ± SEM are shown. n=6 for n=16. Means ± SEM are shown. Significance is reported by *P < .05, **P < .01, ***P < .001, Student's t-test or Mann Whitney test [90].

3.2.4.3. Intestinal dysbiosis in early life is associated with accumulation of RORγt+ FoxP3+/- Th cells in the lung at PN15 and after asthma induction.

To examine the impact of intestinal dysbiosis on lung immune cell composition, flow cytometry analysis was performed in PN15 and allergic offspring (PN49). In early life the lungs of the Prenatal-Antibiotic offspring held higher numbers of leukocytes than controls, however the percentage of the $CD45^+$ leukocytes did not vary between the groups at either time point (Figure 19A). Although the total ILC percentage was not affected by maternal antibiotic use, ILC2 percentages were increased in the lung of allergic mice (Figure 19B). Prenatal-Antibiotic offspring lung tissue exhibited a lower percentage of neutrophils at PN15, whereas allergic lungs contained higher percentages eosinophils and $CD11c^+$ macrophages compared to allergic offspring from control mothers (Figure 19C). Examination of Th cells revealed that maternal antibiotic treatment had no impact on the lung $CD4^+$ T cells in the offspring, or T-bet^+ and $GATA3^+$ subpopulations. However, these animals had increased percentages of $ROR\gamma t^+FoxP3^-$ and $ROR\gamma t^+FoxP3^+$ T cells (Figure 19D).

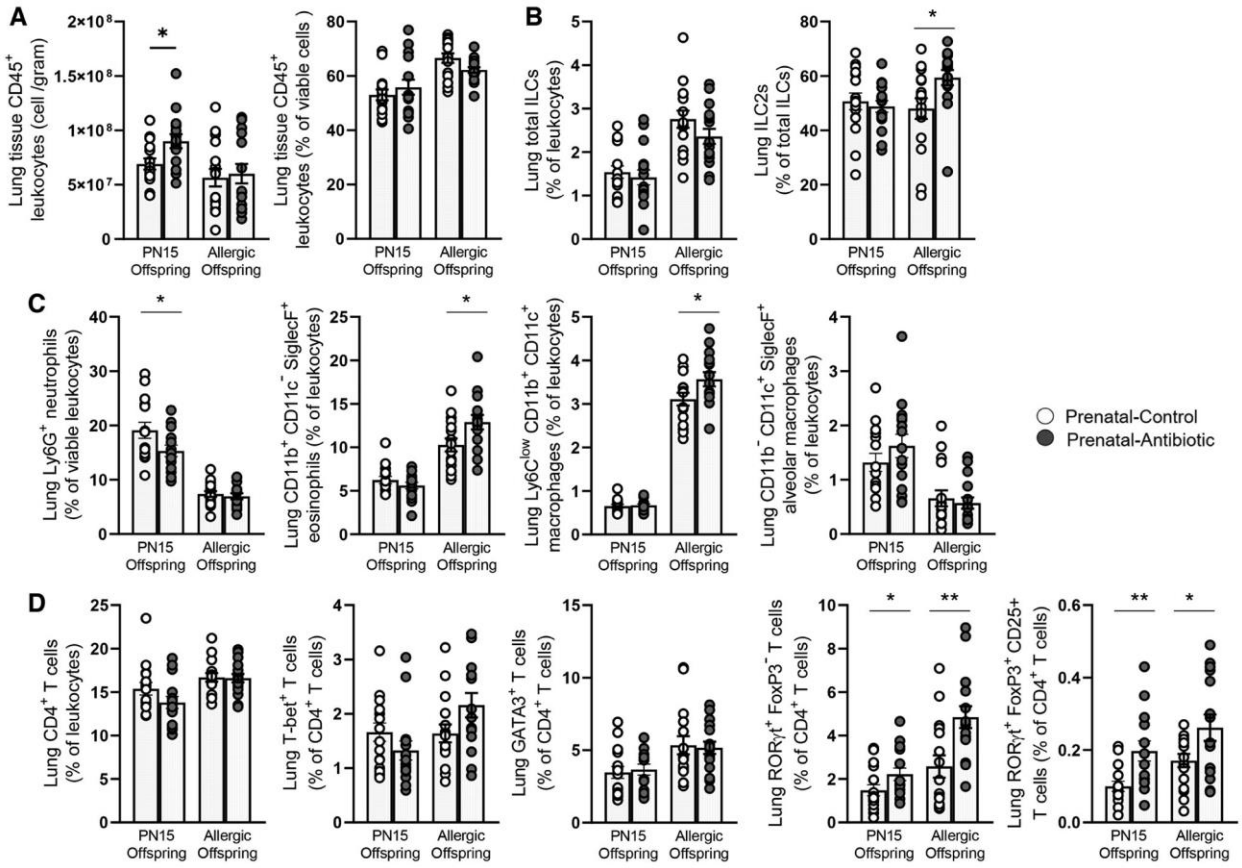

Figure 19. Intestinal dysbiosis in early life is associated with changes to lung immune cells PN15 and increased asthma severity.

A Lung leukocyte counts and percentages. **B** Percentages of total ILCs and ILC2s **C** Percentages of neutrophils, eosinophils, CD11c$^+$ macrophages and SiglecF$^+$ alveolar macrophages. **D** Percentages of CD4$^+$ T cells and T-bet$^+$, GATA3$^+$, RORγt$^+$ FoxP3$^-$, and RORγt$^+$ FoxP3$^+$ CD25$^+$ subpopulations**.** Means ± SEM are shown and n>8. Significance is represented by *P < .05, **P < .01, ***P < .001. Student's t-test or Mann-Whitney test was performed [90].

In conclusion, maternal antibiotic treatment during pregnancy was associated with gut dysbiosis and reduction in fecal SCFA concentrations in both mothers and their offspring in early life. This was associated with inflammation in the SI-LP (increased inflammatory ILC3 populations, increased IgA and lipocalin-2 concentrations), a compromised gut barrier (FITC-dextran assay) and dissemination of LPS to the serum. Finally, we observed increased Th17 cells in both blood and lung and hypothesize that this cell type may have contributed to the increased asthma severity observed in Prenatal-Antibiotic offspring. This indicates that Th17 cell populations present in the neonatal lung are an interesting candidate for future studies on asthma susceptibility.

4. Discussion

We successfully established a mouse model in which treatment of pregnant mice with antibiotics resulted in increased asthma severity in the offspring. Assessment of the gut microbiota revealed a transfer of antibiotic-induced-dysbiosis from mothers to offspring, with significantly increased gram-negative bacterial genera such as *Bacteriodes* and *Escherichia*. Since gut dysbiosis in early life is linked to both maldevelopment of the immune system [96] and increased susceptibility to allergic asthma [47] we also assessed offspring immune system development along the gut-lung-axis. Gut dysbiosis in early life promoted gut inflammation, indicated by increased fecal IgA and lipocalin-2 concentrations, and was also associated with epithelial barrier disruption and LPS dissemination to the circulation. In the blood, immunophenotyping revealed an increase in the RORγt T helper cell (Th17) population which was also observed in the lung in early life and after allergy induction, indicating a potential role for this cell type in asthma pathogenesis that merits further investigation. We propose that the disruption of the intestinal barrier in early life is an early programming event contributing to major alterations along the gut-lung axis, cumulating in significant overexpression of lung tissue RORγt T cells and increased asthma severity in the offspring.

4.1. Model establishment

4.1.1. Maternal treatment

Previous to this work, the existing mouse models studying antibiotic use during pregnancy employed perinatal treatment of both mothers and offspring with antibiotics [16,47]. The model established during my work is novel, due to the use of single-dose of an oral antibiotic only during pregnancy, allowing us to dissect how maternal gut dysbiosis contributes to increased asthma risk in the offspring. During model establishment, several factors were considered, including: 1) Antibiotic selection, 2) Dosage, timing and treatment duration, and 3) Administration method.

1) Antibiotic selection: The antibiotic vancomycin was selected for this study due to its low oral bioavailability and poor intestinal absorbance, which allows maximal impact on the maternal gut microbiome while simultaneously ensuring lower fetal exposure. Although vancomycin is not commonly used during pregnancy, it does share a similar antimicrobial spectrum with the many beta-lactam groups (penicillin and cephalosporins), which are a first-line therapy during pregnancy in treating infections. Penicillin or

cephalosporin were not chosen, however, due to the possible systemic impact on the fetus from the passage of these absorbable antibiotics across the placenta [97].

2) Dosage, timing and treatment duration: To determine the appropriate vancomycin dosage, we tested 3 different concentrations (10, 20 and 40 mg/kg) corresponding to low, middle and high human dosages. As it is reported that antibiotic administration in early pregnancy can interfere with implantation and increase abortion rate [98], antibiotic treatment was started at G8 after implantation was finished. However, even with these precautions a dosage related correlation with abortion was still observed. To mimic prescription of multiple antibiotic courses during pregnancy, mice were treated with vancomycin for 10 days.
3) Administration method: Several considerations were given to the route of antibiotic delivery. Though antibiotics are often given in the drinking water [16,47], this method was not chosen because it is unlikely that the minimum effective concentration of the antibiotic would be reached due to the consumption of small doses in the water over the course of the day. Additionally with this method, it is not possible to determine the amount of antibiotics consumed by each individual mouse due to the ethical requirement of housing multiple mice together. Antibiotic delivery by oral gavage was also rejected, due to the high amount of stress associated with this procedure. For antibiotic treatment of our pregnant mice, we developed a stress-free method to deliver appropriate concentrations to individual animals by adapting a method used for antibiotic treatment in children. To aid medication delivery, vancomycin was mixed with a small volume of syrup (Ora-Sweet) and orally delivered via micropipette.

In summary, our antibiotic treatment method offers many advantages including: 1) Ease of antibiotic delivery 2) Ensured administration of an exact, human-comparable dose, 3) Meeting the minimum inhibitory concentration of the medication 4) Use of an animal friendly and stress-free method, 5) And an environmentally friendly method that reduces the amount of antibiotic used, thus avoiding waste.

4.1.2. Offspring allergic asthma phenotype

We initially tested three different concentrations of vancomycin (10, 20 and 40 mg/kg) in pregnant mice to assess their effect on asthma development in the offspring. Offspring asthma severity in the low vancomycin (10 mg/kg) group was comparable to the control, whereas maternal treatment with the 20 and 40 mg/kg concentrations during pregnancy resulted in increased asthma severity in the offspring. The 40 mg/kg vancomycin concentration was not chosen for future studies, however, due to an observation of increased abortion rate [91]. For this reason, the 20mg/kg vancomycin was chosen and through several model replications, we can confidently say that this maternal treatment is associated with increased lung inflammation and airway reactivity. To improve asthma assessment for our experimental asthma model, I successfully implemented a unique tool for quantification of lung inflammation that is now routinely used in the Conrad lab. This technique, developed by the Önder lab (Comprehensive Pneumology Center, Hemholtz, Munich) [99] uses the newCAST software and a Meander Sampling Protocol to randomly choose 100 locations thought out the whole lung and quantitively screen for inflammation. This protocol eliminates subjectivity issues that could occur during pathology score assessment and delivers an accurate, unbiased quantification of both inflammatory cell influx and goblet cell mucous production.

Considering serum measurements in the allergic offspring, several interesting observations were made regarding both antibody and cytokine concentrations. Although during the establishment of our model we did not initially observe differences in serum antibody concentrations (total IgG1, OVA specific IgG1 and OVA specific IgE), the use of a more sensitive assay and measurement equipment eventually revealed replicable increases in serum antibody concentrations in offspring from antibiotic treated mothers. In addition to this, though some mouse models report that increased BAL or lung cytokine concentrations are associated with an increased asthma phenotype [100,101], our model conversely revealed that prenatal-antibiotic exposed offspring had lower BAL cytokine concentrations compared to allergic offspring from control mothers. For example, in the 20 mg/kg group, we observed lower IL-4, IL-5, MCP-1, MIP-1a, MIP-1b and RANTES concentrations, measured 72 hours after the first OVA challenge (initiation of the experimental asthma phenotype)[91]. We have also observed this phenomenon in a different asthma risk model in our lab [102]. As a possible explanation for this, BAL cells from murine asthma models are usually stimulated with PMA-ionomycin or allergen and then cytokine production is measured in the supernatant [100,103,104]. In our assessment,

however, we measured the BAL cytokines directly 72 hours after the first asthma challenge. As these cytokines are produced during initiation of allergic lung inflammation, and are presumably consumed during the inflammatory process, we propose that a more severe asthma phenotype might have led to higher cytokine “consumption,” resulting in lower remaining cytokine concentrations. Supporting this hypothesis, measurement of BAL cytokines in allergic offspring 24 hours after the initiation of allergic airway inflammation showed that there were no observable differences in cytokine concentrations at this early time point.

4.2. The effect of antibiotic treatment during pregnancy on the maternal system and offspring development

4.2.1. Microbiota transfer from mother to offspring and its impact on fecal SCFA levels

The maternal gut microbiome is a key contributor to the colonization of the infant gut [50]. Our analysis of the maternal and offspring gut microbiota used both quantitative qPCR (providing bacterial counts) and 16S rRNA amplicon sequencing (providing genus and species level relative abundance) to show the transfer of antibiotic-induced gut microbial dysbiosis from mothers to their progeny. This finding is in line with human studies reporting the vertical transmission of gut microbiota from mother to child [105–107]. In our mouse model, at the end of vancomycin treatment mothers showed a depletion of 30 different bacterial clades, mostly gram-positive due to the action of the antibiotic vancomycin. Although this was already reported by others using perinatal models of antibiotic treatment [16,48,108], our publication was the first to report this alteration in mice treated only during pregnancy and is the most comprehensive microbiota assessment to date with respect to both bacterial concentration and relative abundance at the genus level [90].

Despite the depletion of many gram-positive bacterial strains, the total bacterial load in the mothers and offspring from the antibiotic treated group was significantly higher than the control. We hypothesize that the open niches and excess nutrient availability that arose from the elimination of gram-positive bacteria allowed gram-negative bacteria to flourish, which is a phenomenon consistent with human studies [109]. Among the most enriched gram-negative bacteria were *Parabacteroides* in the mothers, and *Escherichia and Sutterella* in the offspring. Gram-negative bacteria contain the endotoxin LPS in the cell wall [110] which we suspect plays an important role in the mechanism of our model

due to transport across the inflamed epithelium of the intestine and dissemination to the circulation [111].

Considering metabolite production, the most depleted bacterial strains in prenatal-antibiotic mothers and their offspring were SCFA producers such as *Clostridiales* and *Lachnospiraceae.* SCFAs (acetate, propionate, butyrate, valerate and isovalerate) are saturated, aliphatic acids that are mainly produced by anaerobic commensal bacteria through fermentation of saccharides and indigestible dietary fibers in the intestine [72]. SCFAs are well-known immune modulators, and it has been shown that low fecal SCFA concentrations in first year of life are correlated with increased susceptibility to allergic diseases [112]. It has also been shown that infant supplementation with SCFAs can protect from atopic disease development in several different ways [113], including: ILC2 suppression [71], limiting eosinophil trafficking and survival [101], attenuating DC activation and chemotaxis [16], inhibiting mast cell degranulation [114] and enhancing myeloid-derived suppressor cell (MDSC) and Treg expansion [115]. In addition to this, SCFAs importantly have the ability to promote epithelial barrier homeostasis and repair[116].

Members of the phylum *Firmicutes* ferment dietary fibers by hydrolyzing polysaccharides to produce SCFAs [117], and since maternal vancomycin treatment depleted many clades within this phylum, a reduction in fecal SCFA concentrations was expected. Indeed, prenatal treatment with vancomycin was associated with reduced fecal concentrations of acetate, propionate and butyrate in both mothers during pregnancy and lactation, as well as in their offspring from early life to adulthood. Considering the influence of SCFAs during early life, murine studies demonstrate that SCFA supplementation during pregnancy [118] or during infancy [16,113] protects against offspring allergic airway inflammation. For this reason, we propose that maternal supplementation with SCFAs during an antibiotic influenced pregnancy may be a future possibility to rescue the severe asthma phenotype observed in our model.

4.2.2. The effect of maternal antibiotic treatment on breast milk.

Breast milk is an important factor that shapes not only the infant's microbiota, but also contributes to immunity in early life. It provides essential nutrients as well as immunological components (leukocytes and their stem cells [119], cytokines [120] and immunoglobulins that direct the development of immunological tolerance [121]. Until now, however, the impact of prenatal antibiotic use on maternal milk has not been well studied, thus we used our model to assess how antibiotic treatment during pregnancy influences

immunological components such as SCFAs, cytokines and immunoglobulins at PN15. Interestingly, though we saw no differences in the SCFAs acetate, propionate and butyrate, or the cytokines IL-1a, eotaxin, G-CSF, RANTES, KC and TNFa, we did observe significant increases in breast milk IgA concentrations in antibiotic treated mothers.

The intestinal lymphatic organs are the main source of IgA producing plasma cells [122], and through the entero-mammary link, plasma cells travel during late pregnancy and early lactation to the mammary glands to produce milk IgA [123]. Though milk IgA contributes significantly to gut microbial homeostasis [123,124] and is known to restrain bacterial and viral intestinal infections in infants [123], its role in regulating allergic diseases remains vague [125]. A human study has demonstrated that patients with severe asthma had increased IgA+ memory B cells in the blood [126], and intestinal IgA analysis in asthmatic children revealed that the genera *Escherichia, Bacteroides and Parabacteroides* were significantly less bound to IgA (IgA free), whereas members of the phylum *Firmicutes* such as *Lachnospiraceae* and *Clostridium* were more IgA bound [127]. As the relative abundance of these bacterial clades were altered in my study, and increased IgA concentrations were observed in the maternal feces, blood and breast milk, as well as in the offspring serum [90], IgA-bacteria binding studies will likely be of great relevance for future studies.

4.2.3. Impact of dysbiosis in early life on the development of innate and adaptive gut lymphocytes

The gut microbiota is essential for mucosal health and immune system development in early life. Notably in our model, immunophenotyping of the SI-LP revealed that when offspring had a dysbiotic gut microbiome (due to maternal antibiotic exposure) that ILC3 subtypes were significantly altered compared to offspring from control mothers. ILC3s maintain gut homeostasis by supporting the epithelial barrier, endorsing secondary lymphoid organ development and fighting infections [128,129]. The role of these cells in the intestinal mucosa is highly dependent on bidirectional communication with the microbiota [130,131], and the ILC3s consist of two main subgroups, the NCR+ ILC3s which are (CCR6-T-bet+) and the NCR- ILC3s which are CCR6+T-bet. NCR+ ILC3s patrol the intestinal lamina propria producing mainly IL-22 [132,133], fortifying the gut epithelial barrier, enhancing mucus production and supporting gut colonization with commensal bacteria[130,133–136]. NCR- ILC3s on the other hand produce IL-17 and can reside in the intestinal lymph structures such as the Peyer's patches and cryptopatches, aggravating intestinal inflammation by promoting class switch of B cells into IgA producing plasma

cells [137,138] and recruiting neutrophils to the gut [135,136]. In our model, the disturbed gut microbiota composition led to imbalance between these ILC3 subgroups in the offspring, showing a decrease in anti-inflammatory NCR+ and an increase in inflammatory NCR- ILC3 percentages, which we hypothesize contributed to intestinal inflammation in early life.

ILC3s interact with the gut microbiota via receptors that recognize both bacterial components (TLRs) and bacterially produced metabolites (SCFAs) [139]. Considering SCFAs, ILC3s sense these molecules through different G protein-coupled receptors such as Gpr109a and free fatty acid receptor (Ffar2), which modulate gut inflammation by enhancing IL-22 production by NCR+ ILC3s [140] and simultaneously suppressing IL-17 production by NCR- ILC3s [141], hence supporting gut homeostasis. We speculate that the reduced SCFA concentrations observed in the feces of Prenatal-Antibiotic exposed offspring in our model contributed to this ILC3 disbalance, thus disrupting the establishment of gut homeostasis in early life.

4.2.4. Microbial dysbiosis in early life is associated with gut inflammation and barrier disruption.

The gut is the largest mucosal immune surface in the body, and ILC3s are abundant in the mucosal layers to help maintain gut integrity [142,143]. Recent evidence suggests that dysregulation of ILC3 subtypes can lead to intestinal immune system activation, gut inflammation and the subsequent disruption of gut homeostasis [139]. Indeed, further investigation in our model revealed gut inflammation in offspring that were prenatally exposed to antibiotics, evidenced by an increased, and sustained influx of leukocytes into the SI-LP, accompanied by an increase in fecal IgA concentration, which is also linked to intestinal inflammation [144–147]. Early life gut inflammation was confirmed in our model through increased lipocalin-2 concentrations in the feces of the offspring in early life. Lipocalin-2 is an anti-microbial peptide that is produced to restrain gut dysbiosis [148–151].

Gut inflammation disturbs epithelial barrier integrity and leads to gut leakiness by damaging tight junctions [152], and previous research has linked intestinal dysbiosis and inflammation with dissemination of bacterial components to the circulation [153,154]. In our model we used two methods to confirm disruption of the gut barrier; a FITC-dextran permeability assay, which demonstrated increased FITC deposition in the circulation, as well as serum LPS measurement, which showed significantly increased concentrations of LPS

in the circulation of prenatal-antibiotic exposed offspring in early life, compared to controls.

4.2.5. LPS dissemination to the circulation impacts the immune system along the gut lung axis.

LPS is a component of the gram-negative bacterial cell wall that has a profound impact on the immune system through interaction with TLR4 present on many immune cell types [155]. It has been found that LPS can stimulate eosinophil mobilization from the bone marrow via the integrin CD11b [156], and in our model, we hypothesize that the observed increase in cell surface expression of CD11b and SiglecF circulating eosinophils may be related to the presence of LPS [157–159]. As CD11b expression on eosinophils is essential for cell adhesion and degranulation, this is an interesting future target to examine regarding LPS, eosinophils and the gut-lung axis.

Another important effect mediated by LPS is stimulation of naïve CD4+ T cell differentiation to RORγt+ Th cells or Th17 cells [155,160]. In conjunction with increased LPS concentrations in the Prenatal-Antibiotic offspring blood we also observed an expansion in the Th17 population that began in early life and remained until adulthood. Th17 cells, through the production of IL-17 an IL-21, instruct B cells to produce an antigen-specific IgA response [161] which helps to restrain the gut microbiota [162]. Additionally, these cells increase eosinophil activation and inflammatory mediator production [163–165], which may play an important role in the programming of tissues such as the lung in early life. Examination of the lung tissue in our model demonstrated that Prenatal-Antibiotic exposed offspring, which had a more severe asthma phenotype than Prenatal-Control offspring, exhibited increased percentages of lung Th17 cells both in early life and after asthma induction. In the context of asthma, many studies suggest that Th17 cells are involved in asthma development. Increased Th17 cells in the lungs were linked with corticosteroid resistant asthma [166,167], and IL-17 was found to increase airway reactivity through the induction of airway remodeling processes [168]. Recent studies have found that RORγt expressing T cells are important for Th2 cell differentiation and the development of allergic asthma [169,170]. The results of our research contribute to this information, indicating that Th17 cells likely play a larger role in asthma development than previously imagined, especially in early life.

5. Conclusion

Asthma is a condition that has lifelong impacts on the individual's quality of life, and until now, there is no cure for this complex disease. Our best available method in fighting asthma lies in understanding the factors that contribute to disease susceptibility and the underlying mechanisms of pathogenesis. Considering factors contributing to asthma risk, epidemiological studies correlate taking antibiotics during pregnancy with increased asthma severity in children [171]. During my doctoral project I confirmed this association by designing a proof-of-concept mouse model and additionally identified a possible mechanism contributing to this phenomenon.

Antibiotic use during pregnancy in our mouse model was associated with maternal to offspring transfer of gut dysbiosis, evidenced by enrichment of gram-negative bacteria and depletion of SCFA-producing bacteria in the offspring from early life until adulthood which was accompanied with decreased fecal SCFA concentrations. Offspring gut dysbiosis in early life was associated with major immunological changes along the gut-lung-axis including dysregulated gut ILC3 cells, intestinal inflammation and barrier disruption that lead to dissemination of bacterial components such as LPS to the blood stream and increased Th17 cells in the blood and the lung. I hypothesize that the LPS observed in the circulation stimulated and increased percentage of Th17 cells in the blood that migrated to the lung where they subsequently contributed to the increased asthma severity observed in this model. This research provides ample evidence for continued investigation of Th17 cells in asthma. Ultimately, this work highlights the importance of a healthy microbiota in early life for immune system development and homeostasis along the gut-lung-axis and emphasizes the importance of rationalizing antibiotic prescriptions during pregnancy.

Reference list

1. Ferrante G, La Grutta S. The Burden of Pediatric Asthma. Front Pediatr [Internet]. 2018 Jun 22;6. Available from: https://www.frontiersin.org/article/10.3389/fped.2018.00186/full

2. Komlósi ZI, van de Veen W, Kovács N, Szűcs G, Sokolowska M, O'Mahony L, Akdis M, Akdis CA. Cellular and molecular mechanisms of allergic asthma. Mol Aspects Med [Internet]. 2022 Jun 1 [cited 2023 Oct 1];85:100995. Available from: https://linkinghub.elsevier.com/retrieve/pii/S0098299721000558

3. Momtazmanesh S, Moghaddam SS, Ghamari SH, Rad EM, Rezaei N, Shobeiri P, Aali A, Abbasi-Kangevari M, Abbasi-Kangevari Z, Abdelmasseh M, Abdoun M, Abdulah DM, Md Abdullah AY, Abedi A, Abolhassani H, Abrehdari-Tafreshi Z, Achappa B, Adane DEA, Adane TD, Addo IY, Adnan M, Adnani QES, Ahmad S, Ahmadi A, Ahmadi K, Ahmed A, Ahmed A, Rashid TA, Al Hamad H, Alahdab F, Alemayehu A, Alif SM, Aljunid SM, Almustanyir S, Altirkawi KA, Alvis-Guzman N, Dehkordi JA, Amir-Behghadami M, Ancuceanu R, Andrei CL, Andrei T, Antony CM, Anyasodor AE, Arabloo J, Arulappan J, Ashraf T, Athari SS, Attia EF, Ayele MT, Azadnajafabad S, Babu AS, Bagherieh S, Baltatu OC, Banach M, Bardhan M, Barone-Adesi F, Barrow A, Basu S, Bayileyegn NS, Bensenor IM, Bhardwaj N, Bhardwaj P, Bhat AN, Bhattacharyya K, Bouaoud S, Braithwaite D, Brauer M, Butt MH, Butt ZA, Calina D, Cámera LA, Chanie GS, Charalampous P, Chattu VK, Chimed-Ochir O, Chu DT, Cohen AJ, Cruz-Martins N, Dadras O, Darwesh AM, Das S, Debela SA, Delgado-Ortiz L, Dereje D, Dianatinasab M, Diao N, Diaz D, Digesa LE, Dirirsa G, Doku PN, Dongarwar D, Douiri A, Dsouza HL, Eini E, Ekholuenetale M, Ekundayo TC, Elagali AEM, Elhadi M, Enyew DB, Erkhembayar R, Etaee F, Fagbamigbe AF, Faro A, Fatehizadeh A, Fekadu G, Filip I, Fischer F, Foroutan M, Franklin RC, Gaal PA, Gaihre S, Gaipov A, Gebrehiwot M, Gerema U, Getachew ME, Getachew T, Ghafourifard M, Ghanbari R, Ghashghaee A, Gholami A, Gil AU, Golechha M, Goleij P, Golinelli D, Guadie HA, Gupta B, Gupta S, Gupta VB, Gupta VK, Hadei M, Halwani R, Hanif A, Hargono A, Harorani M, Hartono RK, Hasani H, Hashi A, Hay SI, Heidari M, Hellemons ME, Herteliu C, Holla R, Horita N, Hoseini M, Hosseinzadeh M, Huang J, Hussain S, Hwang BF, Iavicoli I, Ibitoye SE, Ibrahim S, Ilesanmi OS, Ilic IM, Ilic MD, Immurana M, Ismail NE, Merin J L, Jakovljevic M, Jamshidi E, Janodia MD, Javaheri T, Jayapal SK, Jayaram S, Jha RP, Johnson O, Joo T, Joseph N, Jozwiak JJ, Kraghuabr V, Kaambwa B, Kabir Z, Kalankesh LR, Kalhor R, Kandel H, Karanth SD, Karaye IM, Kassa BG, Kassie GM, Keikavoosi-Arani L, Keykhaei M, Khajuria H, Khan IA, Khan MAB, Khan YH, Khreis H, Kim MS, Kisa A, Kisa S, Knibbs LD, Kolkhir P, Komaki S, Kompani F, Koohestani HR, Koolivand A, Korzh O, Koyanagi A, Krishan K, Krohn KJ, Kumar N, Kumar N, Kurmi OP, Kuttikkattu A, Vecchia C La, Lám J, Lan Q, Lasrado S, Latief K, Lauriola P, Lee SW, Lee YH, Legesse SM, Lenzi J, Li MC, Lin RT, Liu G, Liu W, Lo CH, Lorenzovici L, Lu Y, Mahalingam S, Mahmoudi E, Mahotra NB, Malekpour MR, Malik AA, Mallhi TH, Malta DC, Mansouri B, Mathews E, Maulud SQ, Mechili EA, Nasab EM, Menezes RG, Mengistu DA, Mentis AFA, Meshkat M, Mestrovic T, De Sá ACMGN, Mirrakhimov EM, Misganaw A, Mithra P, Moghadasi J, Mohammadi E, Mohammadi M, Mohammadshahi M, Mohammed S, Mohan S, Moka N, Monasta L, Moni MA, Moniruzzaman M, Montazeri F, Moradi M, Mostafavi E, Mpundu-Kaambwa C, Murillo-Zamora E, Murray CJL, Nair TS, Nangia V, Swamy SN, Narayana AI, Natto ZS, Nayak BP, Negash WW, Nena E, Kandel SN, Niazi RK, De Sá ATN, Nowroozi A, Nzoputam CI, Nzoputam OJ, Oancea B, Obaidur RM, Odukoya OO, Okati-

Aliabad H, Okekunle AP, Okonji OC, Olagunju AT, Bali AO, Ostojic SM, Mahesh PA, Padron-Monedero A, Padubidri JR, Fallahy MTP, Palicz T, Pana A, Park EK, Patel J, Paudel R, Paudel U, Pedersini P, Pereira M, Pereira RB, Petcu IR, Pirestani M, Postma MJ, Prashant A, Rabiee M, Radfar A, Rafiei S, Rahim F, Ur Rahman MH, Rahman M, Rahman MA, Rahmani AM, Rahmani S, Rahmanian V, Rajput P, Rana J, Rao CR, Rao SJ, Rashedi S, Rashidi MM, Ratan ZA, Rawaf DL, Rawaf S, Rawal L, Rawassizadeh R, Razeghinia MS, Redwan EMM, Rezaei M, Rezaei N, Rezaei N, Rezaeian M, Rodrigues M, Rodriguez JAB, Roever L, Rojas-Rueda D, Rudd KE, Saad AMA, Sabour S, Saddik B, Sadeghi E, Sadeghi M, Saeed U, Sahebazzamani M, Sahebkar A, Sahoo H, Sajid MR, Sakhamuri S, Salehi S, Samy AM, Santric-Milicevic MM, Jose BPS, Sathian B, Satpathy M, Saya GK, Senthilkumaran S, Seylani A, Shahabi S, Shaikh MA, Shanawaz M, Shannawaz M, Sheikhi RA, Shekhar S, Sibhat MM, Simpson CR, Singh JA, Singh P, Singh S, Skryabin VY, Skryabina AA, Soltani-Zangbar MS, Song S, Soyiri IN, Steiropoulos P, Stockfelt L, Sun J, Takahashi K, Talaat IM, Tan KK, Tat NY, Tat VY, Taye BT, Thangaraju P, Thapar R, Thienemann F, Tiyuri A, Tran MTN, Tripathy JP, Car LT, Tusa BS, Ullah I, Ullah S, Vacante M, Valdez PR, Valizadeh R, Van Boven JFM, Vasankari TJ, Vaziri S, Violante FS, Vo B, Wang N, Wei MY, Westerman R, Wickramasinghe ND, Xu S, Xu X, Yadav L, Yismaw Y, Yon DK, Yonemoto N, Yu C, Yu Y, Yunusa I, Zahir M, Zangiabadian M, Zareshahrabadi Z, Zarrintan A, Zastrozhin MS, Zegeye ZB, Zhang Y, Naghavi M, Larijani B, Farzadfar F. Global burden of chronic respiratory diseases and risk factors, 1990–2019: an update from the Global Burden of Disease Study 2019. EClinicalMedicine [Internet]. 2023 May 1 [cited 2024 Jun 6];59:101936. Available from: http://www.thelancet.com/article/S258953702300113X/fulltext

4. Lambrecht BN, Hammad H. The immunology of asthma. Nat Immunol [Internet]. 2015 Jan 18 [cited 2023 Aug 25];16(1):45–56. Available from: https://www.nature.com/articles/ni.3049

5. Li Y, Lan F, Yang Y, Xu Y, Chen Y, Qin X, Lv Z, Wang W, Ying S, Zhang L. The absence of IL-9 reduces allergic airway inflammation by reducing ILC2, Th2 and mast cells in murine model of asthma. BMC Pulm Med [Internet]. 2022 Dec 6;22(1):180. Available from: https://bmcpulmmed.biomedcentral.com/articles/10.1186/s12890-022-01976-2

6. Khor YH, Teoh AKY, Lam SM, Mo DCQ, Weston S, Reid DW, Walters EH. Increased vascular permeability precedes cellular inflammation as asthma control deteriorates. Clinical & Experimental Allergy [Internet]. 2009 Nov 21;39(11):1659–67. Available from: https://onlinelibrary.wiley.com/doi/10.1111/j.1365-2222.2009.03349.x

7. Thomsen SF. Genetics of asthma: an introduction for the clinician. Eur Clin Respir J [Internet]. 2015 Jan 1 [cited 2024 Feb 2];2(1):24643. Available from: https://www.tandfonline.com/doi/full/10.3402/ecrj.v2.24643

8. Lynch NR, Hagel I, Perez M, Di Prisco MC, Lopez R, Alvarez N. Effect of anthelmintic treatment on the allergic reactivity of children in a tropical slum. J Allergy Clin Immunol [Internet]. 1993 [cited 2023 Oct 15];92(3):404–11. Available from: https://pubmed.ncbi.nlm.nih.gov/8360391/

9. Wang CC, Nolan TJ, Schad GA, Abraham D. Infection of mice with the helminth Strongyloides stercoralis suppresses pulmonary allergic responses to ovalbumin.

Clin Exp Allergy [Internet]. 2001 [cited 2023 Oct 15];31(3):495–503. Available from: https://pubmed.ncbi.nlm.nih.gov/11260163/

10. Strieker S, Weinmann T, Gerlich J, von Mutius E, Nowak D, Radon K, Wengenroth L. Farm living and allergic rhinitis from childhood to young adulthood: Prospective results of the GABRIEL study. J Allergy Clin Immunol [Internet]. 2022 Nov 1 [cited 2023 Oct 15];150(5):1209-1215.e2. Available from: https://pubmed.ncbi.nlm.nih.gov/35779667/
11. Steiman CA, Evans MD, Lee KE, Lasarev MR, Gangnon RE, Olson BF, Barnes KL, Bendixsen CG, Seroogy CM, Gern JE. Patterns of farm exposure are associated with reduced incidence of atopic dermatitis in early life. Journal of Allergy and Clinical Immunology [Internet]. 2020 Dec 1 [cited 2023 Jan 24];146(6):1379-1386.e6. Available from: http://www.jacionline.org/article/S0091674920309544/fulltext
12. Stein MM, Hrusch CL, Gozdz J, Igartua C, Pivniouk V, Murray SE, Ledford JG, Marques dos Santos M, Anderson RL, Metwali N, Neilson JW, Maier RM, Gilbert JA, Holbreich M, Thorne PS, Martinez FD, von Mutius E, Vercelli D, Ober C, Sperling AI. Innate Immunity and Asthma Risk in Amish and Hutterite Farm Children. New England Journal of Medicine [Internet]. 2016 Aug 4 [cited 2024 Jun 6];375(5):411–21. Available from: http://www.nejm.org/doi/10.1056/NEJMoa1508749
13. Conrad ML, Ferstl R, Teich R, Brand S, Blümer N, Yildirim AO, Patrascan CC, Hanuszkiewicz A, Akira S, Wagner H, Holst O, von Mutius E, Pfefferle PI, Kirschning CJ, Garn H, Renz H. Maternal TLR signaling is required for prenatal asthma protection by the nonpathogenic microbe Acinetobacter lwoffii F78. J Exp Med [Internet]. 2009 Dec 21 [cited 2023 Jan 24];206(13):2869–77. Available from: http://www.ncbi.nlm.nih.gov/pubmed/19995952
14. Metzler S, Frei R, Schmaußer-Hechfellner E, von Mutius E, Pekkanen J, Karvonen AM, Kirjavainen P V., Dalphin J, Divaret-Chauveau A, Riedler J, Lauener R, Roduit C. Association between antibiotic treatment during pregnancy and infancy and the development of allergic diseases. Pediatric Allergy and Immunology [Internet]. 2019 Jun 5 [cited 2023 Aug 23];30(4):423–33. Available from: https://onlinelibrary.wiley.com/doi/10.1111/pai.13039
15. Turi KN, Gebretsadik T, Ding T, Abreo A, Stone C, Hartert T V, Wu P. Dose, Timing, and Spectrum of Prenatal Antibiotic Exposure and Risk of Childhood Asthma. Clinical Infectious Diseases [Internet]. 2021 Feb 1 [cited 2023 Oct 3];72(3):455–62. Available from: https://academic.oup.com/cid/article/72/3/455/5717237
16. Cait A, Hughes MR, Antignano F, Cait J, Dimitriu PA, Maas KR, Reynolds LA, Hacker L, Mohr J, Finlay BB, Zaph C, McNagny KM, Mohn WW. Microbiome-driven allergic lung inflammation is ameliorated by short-chain fatty acids. Mucosal Immunol [Internet]. 2018 May;11(3):785–95. Available from: https://linkinghub.elsevier.com/retrieve/pii/S1933021922005529
17. Wills-Karp M, Santeliz J, Karp CL. The germless theory of allergic disease: Revisiting the hygiene hypothesis [Internet]. Vol. 1, Nature Reviews Immunology. ilm: Nature Publishing Group; 2001 [cited 2023 Aug 31]. p. 69–75. Available from: https://www.nature.com/articles/nri35095579
18. Darabi B, Rahmati S, Hafeziahmadi MR, Badfar G, Azami M. The association between caesarean section and childhood asthma: An updated systematic review and meta-analysis. Allergy, Asthma and Clinical Immunology [Internet]. 2019 Oct 29

[cited 2023 Oct 15];15(1):1–13. Available from: https://aacijournal.biomedcentral.com/articles/10.1186/s13223-019-0367-9

19. Stokholm J, Thorsen J, Blaser MJ, Rasmussen MA, Hjelmsø M, Shah S, Christensen ED, Chawes BL, Bønnelykke K, Brix S, Mortensen MS, Brejnrod A, Vestergaard G, Trivedi U, Sørensen SJ, Bisgaard H. Delivery mode and gut microbial changes correlate with an increased risk of childhood asthma. Sci Transl Med [Internet]. 2020 Nov 11 [cited 2023 Oct 15];12(569). Available from: https://www.science.org/doi/10.1126/scitranslmed.aax9929
20. Frontela-Saseta C, González-Bermúdez CA, García-Marcos L. Diet: A Specific Part of the Western Lifestyle Pack in the Asthma Epidemic. J Clin Med [Internet]. 2020 Jul 1 [cited 2023 Oct 15];9(7):2063. Available from: https://www.mdpi.com/2077-0383/9/7/2063
21. Barker DJP, Osmond C. Infant mortality, childhood nutrition, and ischaemic heart disease in England and Wales. Lancet [Internet]. 1986 May 10 [cited 2023 Oct 15];1(8489):1077–81. Available from: https://pubmed.ncbi.nlm.nih.gov/2871345/
22. Barker DJP. Fetal origins of coronary heart disease. BMJ [Internet]. 1995 Jul 15 [cited 2023 Aug 27];311(6998):171. Available from: https://www.bmj.com/lookup/doi/10.1136/bmj.311.6998.171
23. Strachan DP. Hayfever, hygeine, and household size. Br Med J [Internet]. 1989 [cited 2023 Jan 24];299(November):1259–60. Available from: https://www.ncbi.nlm.nih.gov/pmc/articles/PMC1838109/pdf/bmj00259-0027.pdf
24. Bach JF. The Effect of Infections on Susceptibility to Autoimmune and Allergic Diseases. New England Journal of Medicine [Internet]. 2002 Sep 19 [cited 2023 Oct 1];347(12):911–20. Available from: http://www.nejm.org/doi/abs/10.1056/NEJMra020100
25. Romagnani S. Immunologic influences on allergy and the TH1/TH2 balance. Journal of Allergy and Clinical Immunology [Internet]. 2004 Mar [cited 2023 Aug 31];113(3):395–400. Available from: https://linkinghub.elsevier.com/retrieve/pii/S0091674903026873
26. Yazdanbakhsh M, Kremsner PG, Van Ree R. Allergy, parasites, and the hygiene hypothesis. Science [Internet]. 2002 Apr 19 [cited 2023 Oct 1];296(5567):490–4. Available from: https://pubmed.ncbi.nlm.nih.gov/11964470/
27. Mandy M, Nyirenda M. Developmental Origins of Health and Disease: the relevance to developing nations. Int Health [Internet]. 2018 Mar 1 [cited 2023 Aug 23];10(2):66–70. Available from: https://academic.oup.com/inthealth/article/10/2/66/4924744
28. Sarkar A, Yoo JY, Valeria Ozorio Dutra S, Morgan KH, Groer M. The Association between Early-Life Gut Microbiota and Long-Term Health and Diseases. J Clin Med [Internet]. 2021 Jan 25 [cited 2023 Aug 25];10(3):459. Available from: http://www.ncbi.nlm.nih.gov/pubmed/33504109
29. Hoffman DJ, Powell TL, Barrett ES, Hardy DB. Developmental origins of metabolic diseases. Physiol Rev [Internet]. 2021 Jul 1 [cited 2023 Sep 8];101(3):739–95. Available from: http://www.ncbi.nlm.nih.gov/pubmed/33270534
30. Hutchings MI, Truman AW, Wilkinson B. Antibiotics: past, present and future. Curr Opin Microbiol [Internet]. 2019 Oct 1 [cited 2023 Sep 11];51:72–80. Available from: https://pubmed.ncbi.nlm.nih.gov/31733401/

31. Browne AJ, Chipeta MG, Haines-Woodhouse G, Kumaran EPA, Hamadani BHK, Zaraa S, Henry NJ, Deshpande A, Reiner RC, Day NPJ, Lopez AD, Dunachie S, Moore CE, Stergachis A, Hay SI, Dolecek C. Global antibiotic consumption and usage in humans, 2000–18: a spatial modelling study. Lancet Planet Health [Internet]. 2021 Dec 1 [cited 2023 Oct 1];5(12):e893–904. Available from: http://www.thelancet.com/article/S2542519621002801/fulltext

32. Richardson AN, Pollak EA, Williams D, Smith MA. Intrauterine Infection. In: Comprehensive Toxicology [Internet]. Elsevier; 2010 [cited 2023 Sep 12]. p. 239–58. Available from: https://linkinghub.elsevier.com/retrieve/pii/B9780080468846015232

33. Källén B, Finnström O, Nygren KG, Otterblad Olausson P. Maternal drug use during pregnancy and asthma risk among children. Pediatr Allergy Immunol [Internet]. 2013 Feb;24(1):28–32. Available from: http://www.ncbi.nlm.nih.gov/pubmed/23331527

34. Brandon Bookstaver P, Bland CM, Griffin B, Stover KR, Eiland LS, McLaughlin M. A Review of Antibiotic Use in Pregnancy. Pharmacotherapy [Internet]. 2015 Nov 1 [cited 2023 Feb 7];35(11):1052–62. Available from: https://pubmed.ncbi.nlm.nih.gov/26598097/

35. McKeever TM, Lewis SA, Smith C, Hubbard R. The importance of prenatal exposures on the development of allergic disease: a birth cohort study using the West Midlands General Practice Database. Am J Respir Crit Care Med [Internet]. 2002 Sep 15 [cited 2023 Sep 11];166(6):827–32. Available from: https://pubmed.ncbi.nlm.nih.gov/12231492/

36. Benn CS, Thorsen P, Jensen JS, Kjaer BB, Bisgaard H, Andersen M, Rostgaard K, Björkstén B, Melbye M. Maternal vaginal microflora during pregnancy and the risk of asthma hospitalization and use of antiasthma medication in early childhood. J Allergy Clin Immunol [Internet]. 2002 Jul;110(1):72–7. Available from: http://www.ncbi.nlm.nih.gov/pubmed/12110824

37. Stensballe LG, Simonsen J, Jensen SM, Bønnelykke K, Bisgaard H. Use of antibiotics during pregnancy increases the risk of asthma in early childhood. Journal of Pediatrics [Internet]. 2013;162(4):832-838.e3. Available from: http://dx.doi.org/10.1016/j.jpeds.2012.09.049

38. Örtqvist AK, Lundholm C, Kieler H, Ludvigsson JF, Fall T, Ye W, Almqvist C. Antibiotics in fetal and early life and subsequent childhood asthma: nationwide population based study with sibling analysis. BMJ [Internet]. 2014 Nov 28 [cited 2023 Jan 23];349(nov28 3):g6979. Available from: http://www.ncbi.nlm.nih.gov/pubmed/25432937

39. Metsälä J, Lundqvist A, Virta LJ, Kaila M, Gissler M, Virtanen SM. Prenatal and post-natal exposure to antibiotics and risk of asthma in childhood. Clinical & Experimental Allergy [Internet]. 2015 Jan 26;45(1):137–45. Available from: https://onlinelibrary.wiley.com/doi/10.1111/cea.12356

40. Lapin B, Piorkowski J, Ownby D, Freels S, Chavez N, Hernandez E, Wagner-Cassanova C, Pelzel D, Vergara C, Persky V. Relationship between prenatal antibiotic use and asthma in at-risk children. Annals of Allergy, Asthma & Immunology [Internet]. 2015 Mar;114(3):203–7. Available from: https://linkinghub.elsevier.com/retrieve/pii/S1081120614008552

41. Mulder B, Pouwels KB, Schuiling-Veninga CCM, Bos HJ, de Vries TW, Jick SS, Hak E. Antibiotic use during pregnancy and asthma in preschool children: the influence of confounding. Clin Exp Allergy [Internet]. 2016 Sep 1 [cited 2023 Oct 3];46(9):1214–26. Available from: https://pubmed.ncbi.nlm.nih.gov/27159872/

42. Zhang Z, Zhang W, Guo J, Gu Q, Zhu X, Zhou X. Activation and Functional Specialization of Regulatory T Cells Lead to the Generation of Foxp3 Instability. The Journal of Immunology [Internet]. 2017 Apr 1;198(7):2612–25. Available from: https://journals.aai.org/jimmunol/article/198/7/2612/109509/Activation-and-Functional-Specialization-of

43. Kashanian M, Mohtashami SS, Bemanian MH, Moosavi SAJ, Moradi Lakeh M. Evaluation of the associations between childhood asthma and prenatal and perinatal factors. Int J Gynaecol Obstet [Internet]. 2017 Jun 1 [cited 2023 Oct 3];137(3):290–4. Available from: https://pubmed.ncbi.nlm.nih.gov/28273340/

44. Örtqvist AK, Lundholm C, Fang F, Fall T, Almqvist C. Parental antibiotics and childhood asthma—a population-based study. J Allergy Clin Immunol Pract [Internet]. 2017 Sep 1 [cited 2024 Jun 6];5(5):1451-1454.e4. Available from: https://linkinghub.elsevier.com/retrieve/pii/S2213219817301782

45. Stokholm J, Sevelsted A, Bønnelykke K, Bisgaard H. Maternal propensity for infections and risk of childhood asthma: a registry-based cohort study. Lancet Respir Med [Internet]. 2014 Aug [cited 2023 Sep 12];2(8):631–7. Available from: https://linkinghub.elsevier.com/retrieve/pii/S2213260014701523

46. Yoshida S, Ide K, Takeuchi M, Kawakami K. Prenatal and early-life antibiotic use and risk of childhood asthma: A retrospective cohort study. Pediatric Allergy and Immunology [Internet]. 2018 Aug 22 [cited 2023 Oct 3];29(5):490–5. Available from: https://onlinelibrary.wiley.com/doi/10.1111/pai.12902

47. Russell SL, Gold MJ, Hartmann M, Willing BP, Thorson L, Wlodarska M, Gill N, Blanchet M, Mohn WW, McNagny KM, Finlay BB. Early life antibiotic-driven changes in microbiota enhance susceptibility to allergic asthma. EMBO Rep [Internet]. 2012 May 16 [cited 2023 Sep 12];13(5):440–7. Available from: https://www.embopress.org/doi/10.1038/embor.2012.32

48. Russell SL, Gold MJ, Willing BP, Thorson L, McNagny KM, Finlay BB. Perinatal antibiotic treatment affects murine microbiota, immune responses and allergic asthma. Gut Microbes [Internet]. 2013 Mar [cited 2023 Sep 29];4(2):158–64. Available from: https://www.tandfonline.com/doi/abs/10.4161/gmic.23567

49. Salminen S. Influence of mode of delivery on gut microbiota composition in seven year old children. Gut [Internet]. 2004 Sep 1 [cited 2023 Jan 23];53(9):1388–9. Available from: https://gut.bmj.com/lookup/doi/10.1136/gut.2004.041640

50. Mueller NT, Bakacs E, Combellick J, Grigoryan Z, Dominguez-Bello MG. The infant microbiome development: mom matters. Trends Mol Med [Internet]. 2015 Feb 1 [cited 2023 Oct 23];21(2):109–17. Available from: https://pubmed.ncbi.nlm.nih.gov/25578246/

51. Dominguez-Bello MG, Costello EK, Contreras M, Magris M, Hidalgo G, Fierer N, Knight R. Delivery mode shapes the acquisition and structure of the initial microbiota across multiple body habitats in newborns. Proc Natl Acad Sci U S A [Internet]. 2010 Jun 29 [cited 2023 Jan 22];107(26):11971–5. Available from: https://www.pnas.org/doi/abs/10.1073/pnas.1002601107

52. Derrien M, Alvarez AS, de Vos WM. The Gut Microbiota in the First Decade of Life. Trends Microbiol [Internet]. 2019 Dec 1 [cited 2024 Jun 8];27(12):997–1010. Available from: https://linkinghub.elsevier.com/retrieve/pii/S0966842X19302148

53. Fouhy F, Watkins C, Hill CJ, O'Shea CA, Nagle B, Dempsey EM, O'Toole PW, Ross RP, Ryan CA, Stanton C. Perinatal factors affect the gut microbiota up to four years after birth. Nat Commun [Internet]. 2019 Apr 3;10(1):1517. Available from: https://www.nature.com/articles/s41467-019-09252-4

54. Ball TM, Castro-Rodriguez JA, Griffith KA, Holberg CJ, Martinez FD, Wright AL. Siblings, day-care attendance, and the risk of asthma and wheezing during childhood. N Engl J Med [Internet]. 2000 Aug 24 [cited 2023 Oct 16];343(8):538–43. Available from: https://pubmed.ncbi.nlm.nih.gov/10954761/

55. Amir A, Erez-Granat O, Braun T, Sosnovski K, Hadar R, BenShoshan M, Heiman S, Abbas-Egbariya H, Glick Saar E, Efroni G, Haberman Y. Gut microbiome development in early childhood is affected by day care attendance. NPJ Biofilms Microbiomes [Internet]. 2022 Jan 11 [cited 2023 Sep 26];8(1):2. Available from: http://www.ncbi.nlm.nih.gov/pubmed/35017536

56. Reyman M, van Houten MA, Watson RL, Chu MLJN, Arp K, de Waal WJ, Schiering I, Plötz FB, Willems RJL, van Schaik W, Sanders EAM, Bogaert D. Effects of early-life antibiotics on the developing infant gut microbiome and resistome: a randomized trial. Nature Communications 2022 13:1 [Internet]. 2022 Feb 16 [cited 2023 Sep 26];13(1):1–12. Available from: https://www.nature.com/articles/s41467-022-28525-z

57. Almeida A, Mitchell AL, Boland M, Forster SC, Gloor GB, Tarkowska A, Lawley TD, Finn RD. A new genomic blueprint of the human gut microbiota. Nature [Internet]. 2019 Apr 25;568(7753):499–504. Available from: http://www.ncbi.nlm.nih.gov/pubmed/30745586

58. Valdes AM, Walter J, Segal E, Spector TD. Role of the gut microbiota in nutrition and health. BMJ [Internet]. 2018 Jun 13;k2179. Available from: https://www.bmj.com/lookup/doi/10.1136/bmj.k2179

59. Kalbermatter C, Fernandez Trigo N, Christensen S, Ganal-Vonarburg SC. Maternal Microbiota, Early Life Colonization and Breast Milk Drive Immune Development in the Newborn. Front Immunol [Internet]. 2021 May 13 [cited 2022 Oct 10];12:683022. Available from: http://www.ncbi.nlm.nih.gov/pubmed/34054875

60. Ivanov II, Atarashi K, Manel N, Brodie EL, Shima T, Karaoz U, Wei D, Goldfarb KC, Santee CA, Lynch S V., Tanoue T, Imaoka A, Itoh K, Takeda K, Umesaki Y, Honda K, Littman DR. Induction of Intestinal Th17 Cells by Segmented Filamentous Bacteria. Cell [Internet]. 2009 Oct [cited 2023 Jan 24];139(3):485–98. Available from: https://linkinghub.elsevier.com/retrieve/pii/S0092867409012483

61. Li YN, Huang F, Cheng HJ, Li SY, Liu L, Wang LY. Intestine-derived Clostridium leptum induces murine tolerogenic dendritic cells and regulatory T cells in vitro. Hum Immunol [Internet]. 2014 Dec 1 [cited 2023 Aug 26];75(12):1232–8. Available from: http://www.ncbi.nlm.nih.gov/pubmed/25300998

62. Nagano Y, Itoh K, Honda K. The induction of Treg cells by gut-indigenous Clostridium. Curr Opin Immunol [Internet]. 2012 Aug 1 [cited 2023 Aug 26];24(4):392–7. Available from: https://linkinghub.elsevier.com/retrieve/pii/S0952791512000787

63. Budden KF, Gellatly SL, Wood DLA, Cooper MA, Morrison M, Hugenholtz P, Hansbro PM. Emerging pathogenic links between microbiota and the gut–lung axis.

Nature Reviews Microbiology 2016 15:1 [Internet]. 2016 Oct 3 [cited 2022 Oct 7];15(1):55–63. Available from: https://www.nature.com/articles/nrmicro.2016.142

64. Abdi K, Singh NJ, Matzinger P. Lipopolysaccharide-Activated Dendritic Cells: "Exhausted" or Alert and Waiting? The Journal of Immunology [Internet]. 2012 Jun 15 [cited 2023 Oct 3];188(12):5981–9. Available from: https://journals.aai.org/jimmunol/article/188/12/5981/85963/Lipopolysaccharide-Activated-Dendritic-Cells

65. Chaiwut R, Kasinrerk W. Very low concentration of lipopolysaccharide can induce the production of various cytokines and chemokines in human primary monocytes. BMC Res Notes [Internet]. 2022 Dec 10 [cited 2023 Oct 3];15(1):42. Available from: https://bmcresnotes.biomedcentral.com/articles/10.1186/s13104-022-05941-4

66. Krieg AM, Yi AK, Matson S, Waldschmidt TJ, Bishop GA, Teasdale R, Koretzky GA, Klinman DM. CpG motifs in bacterial DNA trigger direct B-cell activation. Nature [Internet]. 1995 Apr 6 [cited 2023 Sep 27];374(6522):546–9. Available from: https://pubmed.ncbi.nlm.nih.gov/7700380/

67. Liu H, Ji Y, Ma X, He A, Zhao W, Zhang P, Gu L, Lei B, Zhang Y, Wang Y, Zhang W, Wang J. Effects of CpG oligodeoxynucleotides on the differentiation of Treg/Th17 cells. Mol Immunol [Internet]. 2021 Apr 1 [cited 2023 Sep 27];132:199–208. Available from: https://pubmed.ncbi.nlm.nih.gov/33454107/

68. Feng W, Liu J, Cheng H, Zhang D, Tan Y, Peng C. Dietary compounds in modulation of gut microbiota-derived metabolites. Front Nutr [Internet]. 2022 Jul 19 [cited 2024 Apr 22];9:939571. Available from: https://www.frontiersin.org/articles/10.3389/fnut.2022.939571/full

69. Furusawa Y, Obata Y, Fukuda S, Endo TA, Nakato G, Takahashi D, Nakanishi Y, Uetake C, Kato K, Kato T, Takahashi M, Fukuda NN, Murakami S, Miyauchi E, Hino S, Atarashi K, Onawa S, Fujimura Y, Lockett T, Clarke JM, Topping DL, Tomita M, Hori S, Ohara O, Morita T, Koseki H, Kikuchi J, Honda K, Hase K, Ohno H. Commensal microbe-derived butyrate induces the differentiation of colonic regulatory T cells. Nature [Internet]. 2013 Dec 19;504(7480):446–50. Available from: https://www.nature.com/articles/nature12721

70. Sepahi A, Liu Q, Friesen L, Kim CH. Dietary fiber metabolites regulate innate lymphoid cell responses. Mucosal Immunol [Internet]. 2021 Mar 1 [cited 2023 Jan 24];14(2):317–30. Available from: https://linkinghub.elsevier.com/retrieve/pii/S1933021922001337

71. Lewis G, Wang B, Shafiei Jahani P, Hurrell BP, Banie H, Aleman Muench GR, Maazi H, Helou DG, Howard E, Galle-Treger L, Lo R, Santosh S, Baltus A, Bongers G, San-Mateo L, Gilliland FD, Rehan VK, Soroosh P, Akbari O. Dietary Fiber-Induced Microbial Short Chain Fatty Acids Suppress ILC2-Dependent Airway Inflammation. Front Immunol [Internet]. 2019 Sep 18 [cited 2023 Nov 2];10. Available from: https://pubmed.ncbi.nlm.nih.gov/31620118/

72. Sturm EM, Knuplez E, Marsche G. Role of Short Chain Fatty Acids and Apolipoproteins in the Regulation of Eosinophilia-Associated Diseases. Int J Mol Sci [Internet]. 2021 Apr 22 [cited 2024 Mar 2];22(9):4377. Available from: http://www.ncbi.nlm.nih.gov/pubmed/33922158

73. Arpaia N, Campbell C, Fan X, Dikiy S, van der Veeken J, deRoos P, Liu H, Cross JR, Pfeffer K, Coffer PJ, Rudensky AY. Metabolites produced by commensal bacteria promote peripheral regulatory T-cell generation. Nature [Internet]. 2013 Dec

13 [cited 2023 Sep 27];504(7480):451–5. Available from: https://www.nature.com/articles/nature12726

74. Thio CLP, Chi PY, Lai ACY, Chang YJ. Regulation of type 2 innate lymphoid cell-dependent airway hyperreactivity by butyrate. J Allergy Clin Immunol [Internet]. 2018 Dec;142(6):1867-1883.e12. Available from: http://www.ncbi.nlm.nih.gov/pubmed/29522844

75. Belkaid Y, Hand TW. Role of the Microbiota in Immunity and Inflammation. Cell [Internet]. 2014 Mar 27 [cited 2023 Nov 19];157(1):121–41. Available from: https://linkinghub.elsevier.com/retrieve/pii/S0092867414003456

76. Zou F, Qiu Y, Huang Y, Zou H, Cheng X, Niu Q, Luo A, Sun J. Effects of short-chain fatty acids in inhibiting HDAC and activating p38 MAPK are critical for promoting B10 cell generation and function. Cell Death & Disease 2021 12:6 [Internet]. 2021 Jun 7 [cited 2023 Sep 27];12(6):1–17. Available from: https://www.nature.com/articles/s41419-021-03880-9

77. Buttó LF, Haller D. Dysbiosis in intestinal inflammation: Cause or consequence. International Journal of Medical Microbiology [Internet]. 2016 Aug 1 [cited 2023 Sep 27];306(5):302–9. Available from: https://linkinghub.elsevier.com/retrieve/pii/S1438422116300157

78. Borbet TC, Pawline MB, Li J, Ho ML, Yin YS, Zhang X, Novikova E, Jackson K, Mullins BJ, Ruiz VE, Hines MJ, Zhang XS, Müller A, Koralov SB, Blaser MJ. Disruption of the early-life microbiota alters Peyer's patch development and germinal center formation in gastrointestinal-associated lymphoid tissue. iScience [Internet]. 2023 Jun [cited 2023 Sep 27];26(6):106810. Available from: https://doi.org/10.1016/j.isci.

79. Jiménez-Saiz R, Anipindi VC, Galipeau H, Ellenbogen Y, Chaudhary R, Koenig JF, Gordon ME, Walker TD, Mandur TS, Abed S, Humbles A, Chu DK, Erjefält J, Ask K, Verdú EF, Jordana M. Microbial Regulation of Enteric Eosinophils and Its Impact on Tissue Remodeling and Th2 Immunity. Front Immunol [Internet]. 2020 Feb 13 [cited 2023 Jan 23];11:155. Available from: https://www.frontiersin.org/article/10.3389/fimmu.2020.00155/full

80. Renz H, Brandtzaeg P, Hornef M. The impact of perinatal immune development on mucosal homeostasis and chronic inflammation [Internet]. Vol. 12, Nature Reviews Immunology. Nat Rev Immunol; 2012 [cited 2023 Sep 27]. p. 9–23. Available from: https://pubmed.ncbi.nlm.nih.gov/22158411/

81. Enaud R, Prevel R, Ciarlo E, Beaufils F, Wieërs G, Guery B, Delhaes L. The Gut-Lung Axis in Health and Respiratory Diseases: A Place for Inter-Organ and Inter-Kingdom Crosstalks. Front Cell Infect Microbiol [Internet]. 2020 Feb 19 [cited 2023 Oct 20];10:9. Available from: https://www.frontiersin.org/article/10.3389/fcimb.2020.00009/full

82. Stokholm J, Blaser MJ, Thorsen J, Rasmussen MA, Waage J, Vinding RK, Schoos AMM, Kunøe A, Fink NR, Chawes BL, Bønnelykke K, Brejnrod AD, Mortensen MS, Al-Soud WA, Sørensen SJ, Bisgaard H. Maturation of the gut microbiome and risk of asthma in childhood. Nat Commun [Internet]. 2018 Jan 10 [cited 2023 Oct 4];9(1):141. Available from: https://www.nature.com/articles/s41467-017-02573-2

83. Ver Heul A, Planer J, Kau AL. The Human Microbiota and Asthma. Clin Rev Allergy Immunol [Internet]. 2019 Dec 13 [cited 2023 Jan 24];57(3):350–63. Available from: https://link.springer.com/article/10.1007/s12016-018-8719-7

84. Zwittink RD, Renes IB, van Lingen RA, van Zoeren-Grobben D, Konstanti P, Norbruis OF, Martin R, Groot Jebbink LJM, Knol J, Belzer C. Association between duration of intravenous antibiotic administration and early-life microbiota development in late-preterm infants. European Journal of Clinical Microbiology & Infectious Diseases [Internet]. 2018 Mar 24 [cited 2023 Oct 4];37(3):475–83. Available from: http://link.springer.com/10.1007/s10096-018-3193-y

85. Dierikx TH, Visser DH, Benninga MA, van Kaam AHLC, de Boer NKH, de Vries R, van Limbergen J, de Meij TGJ. The influence of prenatal and intrapartum antibiotics on intestinal microbiota colonisation in infants: A systematic review. Journal of Infection [Internet]. 2020 Aug 1 [cited 2023 Oct 16];81(2):190–204. Available from: https://linkinghub.elsevier.com/retrieve/pii/S0163445320302747

86. Heimesaat MM, Nogai A, Bereswill S, Plickert R, Fischer A, Loddenkemper C, Steinhoff U, Tchaptchet S, Thiel E, Freudenberg MA, Gobel UB, Uharek L. MyD88/TLR9 mediated immunopathology and gut microbiota dynamics in a novel murine model of intestinal graft-versus-host disease. Gut [Internet]. 2010 Aug 1;59(8):1079–87. Available from: https://gut.bmj.com/lookup/doi/10.1136/gut.2009.197434

87. Schloss PD, Westcott SL, Ryabin T, Hall JR, Hartmann M, Hollister EB, Lesniewski RA, Oakley BB, Parks DH, Robinson CJ, Sahl JW, Stres B, Thallinger GG, Van Horn DJ, Weber CF. Introducing mothur: Open-source, platform-independent, community-supported software for describing and comparing microbial communities. Appl Environ Microbiol [Internet]. 2009 Dec [cited 2022 Oct 7];75(23):7537–41. Available from: https://journals.asm.org/doi/10.1128/AEM.01541-09

88. Gómez-Gallego C, Ilo T, Ulla-Marjut J, Salminen S, Periago MJ, Ros G, Frias R. A method to collect high volumes of milk from mice. Anales de Veterinaria de Murcia [Internet]. 2013;29(2013):55–61. Available from: http://revistas.um.es/analesvet/article/view/208991

89. Gronke K, Kofoed-Nielsen M, Diefenbach A. Isolation and flow cytometry analysis of innate lymphoid cells from the intestinal lamina propria. Methods in Molecular Biology [Internet]. 2017 [cited 2022 Oct 7];1559:255–65. Available from: https://link.springer.com/protocol/10.1007/978-1-4939-6786-5_17

90. Alhasan MM, Hölsken O, Duerr C, Helfrich S, Branzk N, Philipp A, Leitz D, Duerr J, Almousa Y, Barrientos G, Mohn WW, Gamradt S, Conrad ML. Antibiotic use during pregnancy is linked to offspring gut microbial dysbiosis, barrier disruption, and altered immunity along the gut–lung axis. Eur J Immunol [Internet]. 2023 Jul 10 [cited 2023 Jul 19];0:2350394. Available from: https://onlinelibrary.wiley.com/doi/10.1002/eji.202350394

91. Alhasan MM, Cait AM, Heimesaat MM, Blaut M, Klopfleisch R, Wedel A, Conlon TM, Yildirim AÖ, Sodemann EB, Mohn WW, Bereswill S, Conrad ML. Antibiotic use during pregnancy increases offspring asthma severity in a dose-dependent manner. Allergy [Internet]. 2020 Aug 11 [cited 2022 Oct 7];75(8):1979–90. Available from: https://onlinelibrary.wiley.com/doi/full/10.1111/all.14234

92. Campbell RM, Fell BF. Gastro-intestinal hypertrophy in the lactating rat and its relation to food intake. J Physiol [Internet]. 1964 May;171(1):90–7. Available from: https://physoc.onlinelibrary.wiley.com/doi/10.1113/jphysiol.1964.sp007363

93. Hammond KA. Adaptation of the maternal intestine during lactation. J Mammary Gland Biol Neoplasia [Internet]. 1997 [cited 2023 Aug 4];2(3):243–52. Available from: https://link.springer.com/article/10.1023/A:1026332304435

94. Liu Y, Yuan X, Li L, Lin L, Zuo X, Cong Y, Li Y. Increased Ileal Immunoglobulin A Production and Immunoglobulin A-Coated Bacteria in Diarrhea-Predominant Irritable Bowel Syndrome. Clin Transl Gastroenterol [Internet]. 2020 Mar 1 [cited 2024 Apr 22];11(3):e00146. Available from: https://journals.lww.com/10.14309/ctg.0000000000000146

95. Kayama H, Takeda K. Regulation of intestinal homeostasis by innate and adaptive immunity. Int Immunol [Internet]. 2012 Nov 1 [cited 2024 Apr 22];24(11):673–80. Available from: https://dx.doi.org/10.1093/intimm/dxs094

96. Parkin K, Christophersen CT, Verhasselt V, Cooper MN, Martino D. Risk Factors for Gut Dysbiosis in Early Life. Microorganisms [Internet]. 2021 Sep 30 [cited 2023 Dec 3];9(10):2066. Available from: https://www.mdpi.com/2076-2607/9/10/2066

97. Viel-Theriault I, Fell DB, Grynspan D, Redpath S, Thampi N. The transplacental passage of commonly used intrapartum antibiotics and its impact on the newborn management: A narrative review. Early Hum Dev [Internet]. 2019 Aug 1 [cited 2023 Dec 6];135:6–10. Available from: https://linkinghub.elsevier.com/retrieve/pii/S0378378219300799

98. Muanda FT, Sheehy O, Bérard A. Use of antibiotics during pregnancy and risk of spontaneous abortion. CMAJ [Internet]. 2017 May 1 [cited 2023 Dec 3];189(17):E625–33. Available from: http://www.ncbi.nlm.nih.gov/pubmed/28461374

99. Conlon TM, John-Schuster G, Heide D, Pfister D, Lehmann M, Hu Y, Ertüz Z, Lopez MA, Ansari M, Strunz M, Mayr C, Angelidis I, Ciminieri C, Costa R, Kohlhepp MS, Guillot A, Günes G, Jeridi A, Funk MC, Beroshvili G, Prokosch S, Hetzer J, Verleden SE, Alsafadi H, Lindner M, Burgstaller G, Becker L, Irmler M, Dudek M, Janzen J, Goffin E, Gosens R, Knolle P, Pirotte B, Stoeger T, Beckers J, Wagner D, Singh I, Theis FJ, de Angelis MH, O'Connor T, Tacke F, Boutros M, Dejardin E, Eickelberg O, Schiller HB, Königshoff M, Heikenwalder M, Yildirim AÖ. Inhibition of LTβR signalling activates WNT-induced regeneration in lung. Nature [Internet]. 2020 Dec 3 [cited 2024 Apr 22];588(7836):151–6. Available from: https://www.nature.com/articles/s41586-020-2882-8

100. Richgels PK, Yamani A, Chougnet CA, Lewkowich IP. Maternal house dust mite exposure during pregnancy enhances severity of house dust mite–induced asthma in murine offspring. Journal of Allergy and Clinical Immunology [Internet]. 2017 Nov;140(5):1404-1415.e9. Available from: https://linkinghub.elsevier.com/retrieve/pii/S0091674917302208

101. Theiler A, Bärnthaler T, Platzer W, Richtig G, Peinhaupt M, Rittchen S, Kargl J, Ulven T, Marsh LM, Marsche G, Schuligoi R, Sturm EM, Heinemann A. Butyrate ameliorates allergic airway inflammation by limiting eosinophil trafficking and survival. J Allergy Clin Immunol [Internet]. 2019 Sep 1 [cited 2024 Apr 22];144(3):764–76. Available from: https://pubmed.ncbi.nlm.nih.gov/31082458/

102. Sodemann E. Ist mütterliches, allergisches Asthma bronchiale ein Risikofaktor für die Nachkommen an allergischem Asthma bronchiale zu erkranken? [Internet]. 2021 [cited 2024 Apr 21]. Available from: https://refubium.fu-berlin.de/handle/fub188/30098

103. Brightling CE, Symon FA, Birring SS, Bradding P, Pavord ID, Wardlaw AJ. TH2 cytokine expression in bronchoalveolar lavage fluid T lymphocytes and bronchial submucosa is a feature of asthma and eosinophilic bronchitis. Journal of Allergy

and Clinical Immunology [Internet]. 2002 Dec 1 [cited 2024 Apr 22];110(6):899–905. Available from: http://www.jacionline.org/article/S0091674902014732/fulltext

104. Halim TYF, Krauss RH, Sun AC, Takei F. Lung natural helper cells are a critical source of Th2 cell-type cytokines in protease allergen-induced airway inflammation. Immunity [Internet]. 2012 Mar 23 [cited 2024 Apr 22];36(3):451–63. Available from: http://www.ncbi.nlm.nih.gov/pubmed/22425247

105. Milani C, Mancabelli L, Lugli GA, Duranti S, Turroni F, Ferrario C, Mangifesta M, Viappiani A, Ferretti P, Gorfer V, Tett A, Segata N, van Sinderen D, Ventura M. Exploring vertical transmission of bifidobacteria from mother to child. Appl Environ Microbiol [Internet]. 2015 [cited 2024 Mar 6];81(20):7078–87. Available from: https://journals.asm.org/doi/10.1128/AEM.02037-15

106. Asnicar F, Manara S, Zolfo M, Truong DT, Scholz M, Armanini F, Ferretti P, Gorfer V, Pedrotti A, Tett A, Segata N. Studying Vertical Microbiome Transmission from Mothers to Infants by Strain-Level Metagenomic Profiling. mSystems [Internet]. 2017 Feb 28 [cited 2024 Mar 6];2(1). Available from: https://journals.asm.org/doi/10.1128/mSystems.00164-16

107. Li W, Tapiainen T, Brinkac L, Lorenzi HA, Moncera K, Tejesvi M V., Salo J, Nelson KE. Vertical Transmission of Gut Microbiome and Antimicrobial Resistance Genes in Infants Exposed to Antibiotics at Birth. J Infect Dis [Internet]. 2021 Oct 13 [cited 2024 Mar 6];224(7):1236–46. Available from: https://dx.doi.org/10.1093/infdis/jiaa155

108. Yang X, Feng H, Zhan X, Zhang C, Cui R, Zhong L, Ying S, Chen Z. Early-life vancomycin treatment promotes airway inflammation and impairs microbiome homeostasis. Aging [Internet]. 2019 Apr 15 [cited 2023 Oct 29];11(7):2071–81. Available from: https://pubmed.ncbi.nlm.nih.gov/30981206/

109. Panda S, El Khader I, Casellas F, López Vivancos J, García Cors M, Santiago A, Cuenca S, Guarner F, Manichanh C. Short-Term Effect of Antibiotics on Human Gut Microbiota. PLoS One [Internet]. 2014 Apr 18 [cited 2024 Mar 6];9(4):e95476. Available from: https://journals.plos.org/plosone/article?id=10.1371/journal.pone.0095476

110. Maldonado RF, Sá-Correia I, Valvano MA. Lipopolysaccharide modification in Gram-negative bacteria during chronic infection. Whitfield C, editor. FEMS Microbiol Rev [Internet]. 2016 Jul 1 [cited 2023 Oct 23];40(4):480–93. Available from: https://academic.oup.com/femsre/article-lookup/doi/10.1093/femsre/fuw007

111. Ghosh SS, Wang J, Yannie PJ, Ghosh S. Intestinal Barrier Dysfunction, LPS Translocation, and Disease Development. J Endocr Soc [Internet]. 2020 Feb 2 [cited 2023 Oct 23];4(2). Available from: /pmc/articles/PMC7033038/

112. Cheng HY, Chan JCY, Yap GC, Huang CH, Kioh DYQ, Tham EH, Loo EXL, Shek LPC, Karnani N, Goh A, Van Bever HPS, Teoh OH, Chan YH, Lay C, Knol J, Yap F, Tan KH, Chong YS, Godfrey KM, Chan ECY, Lee BW, Ta LDH. Evaluation of Stool Short Chain Fatty Acids Profiles in the First Year of Life With Childhood Atopy-Related Outcomes. Frontiers in allergy [Internet]. 2022 Apr 6 [cited 2023 Nov 1];3. Available from: https://pubmed.ncbi.nlm.nih.gov/35769572/

113. Roduit C, Frei R, Ferstl R, Loeliger S, Westermann P, Rhyner C, Schiavi E, Barcik W, Rodriguez-Perez N, Wawrzyniak M, Chassard C, Lacroix C, Schmausser-Hechfellner E, Depner M, von Mutius E, Braun-Fahrländer C, Karvonen AM, Kirjavainen P V., Pekkanen J, Dalphin JC, Riedler J, Akdis C, Lauener R, O'Mahony L,

Hyvärinen A, Remes S, Roponen M, Chauveau A, Dalphin ML, Kaulek V, Ege M, Genuneit J, Illi S, Kabesch M, Schaub B, Pfefferle P, Doekes G. High levels of butyrate and propionate in early life are associated with protection against atopy. Allergy [Internet]. 2019 Apr 1 [cited 2024 Apr 22];74(4):799–809. Available from: https://pubmed.ncbi.nlm.nih.gov/30390309/

114. Folkerts J, Redegeld F, Folkerts G, Blokhuis B, van den Berg MPM, de Bruijn MJW, van IJcken WFJ, Junt T, Tam SY, Galli SJ, Hendriks RW, Stadhouders R, Maurer M. Butyrate inhibits human mast cell activation via epigenetic regulation of FcεRI-mediated signaling. Allergy [Internet]. 2020 Aug 1 [cited 2023 Nov 2];75(8):1962–74. Available from: https://pubmed.ncbi.nlm.nih.gov/32112426/

115. Huang MT, Chiu CJ, Tsai CY, Lee YR, Liu WL, Chuang HL, Huang MT. Short-chain fatty acids ameliorate allergic airway inflammation via sequential induction of PMN-MDSCs and Treg cells. The journal of allergy and clinical immunology Global [Internet]. 2023 Nov [cited 2023 Nov 5];2(4):100163. Available from: https://pubmed.ncbi.nlm.nih.gov/37781663/

116. Bilotta AJ, Ma C, Huang X, Yang W, Chen L, Yao S, Cong Y. Microbiota metabolites SCFA promote intestinal epithelial repair and wound healing through promoting epithelial cell production of milk fat globule-EGF factor 8. The Journal of Immunology [Internet]. 2018 May 1 [cited 2024 Mar 13];200(1_Supplement):53.17-53.17. Available from: https://journals.aai.org/jimmunol/article/200/1_Supplement/53.17/60929/Microbiota-metabolites-SCFA-promote-intestinal

117. Fusco W, Lorenzo MB, Cintoni M, Porcari S, Rinninella E, Kaitsas F, Lener E, Mele MC, Gasbarrini A, Collado MC, Cammarota G, Ianiro G. Short-Chain Fatty-Acid-Producing Bacteria: Key Components of the Human Gut Microbiota. Nutrients [Internet]. 2023 May 6 [cited 2024 Apr 22];15(9):2211. Available from: http://www.ncbi.nlm.nih.gov/pubmed/37432351

118. Gray LEK, O'Hely M, Ranganathan S, Sly PD, Vuillermin P. The Maternal Diet, Gut Bacteria, and Bacterial Metabolites during Pregnancy Influence Offspring Asthma. Front Immunol [Internet]. 2017 Mar 31 [cited 2024 Apr 22];8(MAR):365. Available from: http://journal.frontiersin.org/article/10.3389/fimmu.2017.00365/full

119. Witkowska-Zimny M, Kaminska-El-Hassan E. Cells of human breast milk. Cell Mol Biol Lett [Internet]. 2017 Dec 13 [cited 2024 Apr 22];22(1):11. Available from: http://cmbl.biomedcentral.com/articles/10.1186/s11658-017-0042-4

120. Holmlund U, Amoudruz P, Johansson MA, Haileselassie Y, Ongoiba A, Kayentao K, Traoré B, Doumbo S, Schollin J, Doumbo O, Montgomery SM, Sverremark-Ekström E. Maternal country of origin, breast milk characteristics and potential influences on immunity in offspring. Clin Exp Immunol [Internet]. 2010 Dec [cited 2023 Nov 7];162(3):500–9. Available from: https://pubmed.ncbi.nlm.nih.gov/20942805/

121. Rajani PS, Seppo AE, Järvinen KM. Immunologically Active Components in Human Milk and Development of Atopic Disease, With Emphasis on Food Allergy, in the Pediatric Population. Front Pediatr [Internet]. 2018 Aug 7 [cited 2023 Nov 7];6:392153. Available from: https://www.frontiersin.org/article/10.3389/fped.2018.00218/full

122. Keppler SJ, Goess MC, Heinze JM. The Wanderings of Gut-Derived IgA Plasma Cells: Impact on Systemic Immune Responses. Front Immunol [Internet]. 2021 Apr 15;12. Available from: https://www.frontiersin.org/articles/10.3389/fimmu.2021.670290/full

123. Donald K, Petersen C, Turvey SE, Finlay BB, Azad MB. Secretory IgA: Linking microbes, maternal health, and infant health through human milk. Cell Host Microbe [Internet]. 2022 May 11 [cited 2024 Jan 6];30(5):650–9. Available from: https://linkinghub.elsevier.com/retrieve/pii/S1931312822000919

124. Augustine T, Kumar M, Al Khodor S, van Panhuys N. Microbial Dysbiosis Tunes the Immune Response Towards Allergic Disease Outcomes. Clinical Reviews in Allergy & Immunology 2022 65:1 [Internet]. 2022 Jun 1 [cited 2023 Nov 19];65(1):43–71. Available from: https://link.springer.com/article/10.1007/s12016-022-08939-9

125. Scheurer S, Junker AC, He C, Schülke S, Toda M. The Role of IgA in the Manifestation and Prevention of Allergic Immune Responses. Curr Allergy Asthma Rep [Internet]. 2023 Oct 1 [cited 2024 Jan 7];23(10):589–600. Available from: https://link.springer.com/article/10.1007/s11882-023-01105-x

126. Habener A, Grychtol R, Gaedcke S, DeLuca D, Dittrich AM, Happle C, Abdo M, Watz H, Pedersen F, König IR, Thiele D, Kopp MV, von Mutius E, Bahmer T, Rabe KF, Meyer-Bahlburg A, Hansen G, Fuchs O, Roesler B, Welchering N, Kohistani-Greif N, Kurz J, Landgraf-Rauf K, Laubhahn K, Maison N, Liebl C, Schaub B, Ege M, Illi S, Hose A, Zeitlmann E, Berbig M, Marzi C, Schauberger C, Zissler U, Schmidt-Weber C, Ricklefs I, Diekmann G, Liboschik L, Voigt G, Sultansei L, Weckmann M, Nissen G, Kirsten AM, Waschki B, Herzmann C, Biller H, Gaede KI, Bovermann X, Steinmetz A, Husstedt BL, Nitsche C, Veith V, Szewczyk M, Brinkmann F, Malik A, Schwerk N, Dopfer C, Price M, Jirmo AC, Liu B, Calveron MR, Weber S, Foth S, Skevaki C, Renz H, Meyer M, Schildberg T, Rietschel E, van Koningsbruggen-Rietschel S, Alcazar M. IgA+ memory B-cells are significantly increased in patients with asthma and small airway dysfunction. Eur Respir J [Internet]. 2022 Nov 1 [cited 2024 Jan 7];60(5). Available from: https://pubmed.ncbi.nlm.nih.gov/35595320/

127. Dzidic M, Abrahamsson TR, Artacho A, Björkstén B, Collado MC, Mira A, Jenmalm MC. Aberrant IgA responses to the gut microbiota during infancy precede asthma and allergy development. Journal of Allergy and Clinical Immunology [Internet]. 2017 Mar 1 [cited 2024 Jan 7];139(3):1017-1025.e14. Available from: https://linkinghub.elsevier.com/retrieve/pii/S0091674916307862

128. Niu X, Daniel S, Kumar D, Ding EY, Savani RC, Koh AY, Mirpuri J. Transient neonatal antibiotic exposure increases susceptibility to late-onset sepsis driven by microbiota-dependent suppression of type 3 innate lymphoid cells. Sci Rep [Internet]. 2020 Jul 31 [cited 2024 Apr 6];10(1):12974. Available from: https://www.nature.com/articles/s41598-020-69797-z

129. Li M, Wang Z, Jiang W, Lu Y, Zhang J. The role of group 3 innate lymphoid cell in intestinal disease. Front Immunol [Internet]. 2023 Apr 14 [cited 2024 Apr 6];14:1171826. Available from: https://www.frontiersin.org/articles/10.3389/fimmu.2023.1171826/full

130. Melo-Gonzalez F, Hepworth MR. Functional and phenotypic heterogeneity of group 3 innate lymphoid cells. Immunology [Internet]. 2017 Mar 3 [cited 2024 Jan 19];150(3):265–75. Available from: https://onlinelibrary.wiley.com/doi/10.1111/imm.12697

131. Kotas ME, Locksley RM. Why Innate Lymphoid Cells? Immunity [Internet]. 2018 Jun 19 [cited 2023 Oct 29];48(6):1081–90. Available from: https://linkinghub.elsevier.com/retrieve/pii/S1074761318302577

132. Vonarbourg C, Mortha A, Bui VL, Hernandez PP, Kiss EA, Hoyler T, Flach M, Bengsch B, Thimme R, Hölscher C, Hönig M, Pannicke U, Schwarz K, Ware CF, Finke D, Diefenbach A. Regulated expression of nuclear receptor RORγt confers distinct functional fates to NK cell receptor-expressing RORγt+ innate lymphocytes. Immunity [Internet]. 2010 Nov 24 [cited 2024 Feb 12];33(5):736–51. Available from: http://www.cell.com/article/S1074761310004036/fulltext

133. Klose CSN, Kiss EA, Schwierzeck V, Ebert K, Hoyler T, d'Hargues Y, Göppert N, Croxford AL, Waisman A, Tanriver Y, Diefenbach A. A T-bet gradient controls the fate and function of CCR6−RORγt+ innate lymphoid cells. Nature [Internet]. 2013 Feb 16;494(7436):261–5. Available from: https://www.nature.com/articles/nature11813

134. Powell N, Walker AW, Stolarczyk E, Canavan JB, Gökmen MR, Marks E, Jackson I, Hashim A, Curtis MA, Jenner RG, Howard JK, Parkhill J, MacDonald TT, Lord GM. The Transcription Factor T-bet Regulates Intestinal Inflammation Mediated by Interleukin-7 Receptor+ Innate Lymphoid Cells. Immunity [Internet]. 2012 Oct 19 [cited 2024 Feb 12];37(4):674–84. Available from: http://www.cell.com/article/S1074761312004219/fulltext

135. Zeng B, Shi S, Ashworth G, Dong C, Liu J, Xing F. ILC3 function as a double-edged sword in inflammatory bowel diseases. Cell Death & Disease 2019 10:4 [Internet]. 2019 Apr 8 [cited 2022 Oct 7];10(4):1–12. Available from: https://www.nature.com/articles/s41419-019-1540-2

136. Zhang Y, Feng X, Chen J, Liu J, Wu J, Tan H, Mi Z, Rong P. Controversial role of ILC3s in intestinal diseases: A novelty perspective on immunotherapy. Front Immunol [Internet]. 2023 Mar 28 [cited 2024 Jan 20];14:1134636. Available from: https://www.frontiersin.org/articles/10.3389/fimmu.2023.1134636/full

137. Tsuji M, Suzuki K, Kitamura H, Maruya M, Kinoshita K, Ivanov II, Itoh K, Littman DR, Fagarasan S. Requirement for Lymphoid Tissue-Inducer Cells in Isolated Follicle Formation and T Cell-Independent Immunoglobulin A Generation in the Gut. Immunity [Internet]. 2008 Aug 15 [cited 2024 Feb 13];29(2):261–71. Available from: https://linkinghub.elsevier.com/retrieve/pii/S1074761308003038

138. Kruglov AA, Grivennikov SI, Kuprash D V., Winsauer C, Prepens S, Seleznik GM, Eberl G, Littman DR, Heikenwalder M, Tumanov A V., Nedospasov SA. Nonredundant function of soluble ltα3 produced by innate lymphoid cells in intestinal homeostasis. Science (1979) [Internet]. 2013 Dec 6 [cited 2024 Feb 13];342(6163):1243–6. Available from: https://www.science.org/doi/10.1126/science.1243364

139. Drommi F, Calabrò A, Vento G, Pezzino G, Cavaliere R, Omero F, Muscolino P, Granata B, D'Anna F, Silvestris N, De Pasquale C, Ferlazzo G, Campana S. Crosstalk between ILC3s and Microbiota: Implications for Colon Cancer Development and Treatment with Immune Check Point Inhibitors. Cancers (Basel) [Internet]. 2023 May 24 [cited 2024 Apr 11];15(11):2893. Available from: https://www.mdpi.com/2072-6694/15/11/2893

140. Yang W, Yu T, Huang X, Bilotta AJ, Xu L, Lu Y, Sun J, Pan F, Zhou J, Zhang W, Yao S, Maynard CL, Singh N, Dann SM, Liu Z, Cong Y. Intestinal microbiota-derived short-chain fatty acids regulation of immune cell IL-22 production and gut immunity. Nature Communications 2020 11:1 [Internet]. 2020 Sep 8 [cited 2024 Apr 7];11(1):1–18. Available from: https://www.nature.com/articles/s41467-020-18262-6

141. Bhatt B, Zeng P, Zhu H, Sivaprakasam S, Li S, Xiao H, Dong L, Shiao P, Kolhe R, Patel N, Li H, Levy-Bercowski D, Ganapathy V, Singh N. Gpr109a Limits Microbiota-Induced IL-23 Production To Constrain ILC3-Mediated Colonic Inflammation. The Journal of Immunology [Internet]. 2018 Apr 15 [cited 2024 Apr 12];200(8):2905–14. Available from: https://dx.doi.org/10.4049/jimmunol.1701625

142. WERSHIL B, FURUTA G. 4. Gastrointestinal mucosal immunity. Journal of Allergy and Clinical Immunology [Internet]. 2008 Feb 1 [cited 2024 Apr 14];121(2):S380–3. Available from: https://linkinghub.elsevier.com/retrieve/pii/S0091674907019732

143. Chassaing B, Kumar M, Baker MT, Singh V, Vijay-Kumar M. Mammalian gut immunity. Biomed J [Internet]. 2014 Sep 1 [cited 2024 Apr 14];37(5):246–58. Available from: http://www.ncbi.nlm.nih.gov/pubmed/25163502

144. Scribano ML, Prantera C. Antibiotics and Inflammatory Bowel Diseases. Digestive Diseases [Internet]. 2013 Nov 1 [cited 2023 Oct 31];31(3–4):379–84. Available from: https://dx.doi.org/10.1159/000354704

145. Ungaro R, Bernstein CN, Gearry R, Hviid A, Kolho KL, Kronman MP, Shaw S, Van Kruiningen H, Colombel JF, Atreja A. Antibiotics Associated With Increased Risk of New-Onset Crohn's Disease But Not Ulcerative Colitis: A Meta-Analysis. American Journal of Gastroenterology [Internet]. 2014 Nov 13 [cited 2023 Oct 31];109(11):1728–38. Available from: https://journals.lww.com/00000434-201411000-00009

146. Lin R, Chen H, Shu W, Sun M, Fang L, Shi Y, Pang Z, Wu W, Liu Z. Clinical significance of soluble immunoglobulins A and G and their coated bacteria in feces of patients with inflammatory bowel disease. J Transl Med [Internet]. 2018 Dec 17 [cited 2023 Aug 4];16(1):359. Available from: https://translational-medicine.biomedcentral.com/articles/10.1186/s12967-018-1723-0

147. Hviid A, Svanström H, Frisch M. Antibiotic use and inflammatory bowel diseases in childhood. Gut [Internet]. 2011 Jan 1 [cited 2023 Oct 31];60(1):49–54. Available from: http://www.ncbi.nlm.nih.gov/pubmed/20966024

148. Chassaing B, Srinivasan G, Delgado MA, Young AN, Gewirtz AT, Vijay-Kumar M. Fecal Lipocalin 2, a Sensitive and Broadly Dynamic Non-Invasive Biomarker for Intestinal Inflammation. PLoS One [Internet]. 2012 Sep 5 [cited 2024 Jan 24];7(9):e44328. Available from: https://journals.plos.org/plosone/article?id=10.1371/journal.pone.0044328

149. Singh V, Yeoh BS, Chassaing B, Zhang B, Saha P, Xiao X, Awasthi D, Shashidharamurthy R, Dikshit M, Gewirtz A, Vijay-Kumar M. Microbiota-Inducible Innate Immune Siderophore Binding Protein Lipocalin 2 Is Critical for Intestinal Homeostasis. CMGH [Internet]. 2016 Jul 1 [cited 2024 Apr 14];2(4):482-498.e6. Available from: http://www.cmghjournal.org/article/S2352345X1630011X/fulltext

150. Zollner A, Schmiderer A, Reider SJ, Oberhuber G, Pfister A, Texler B, Watschinger C, Koch R, Effenberger M, Raine T, Tilg H, Moschen AR. Faecal Biomarkers in Inflammatory Bowel Diseases: Calprotectin Versus Lipocalin-2—a Comparative Study. J Crohns Colitis [Internet]. 2021 Jan 13 [cited 2024 Jan 24];15(1):43–54. Available from: https://dx.doi.org/10.1093/ecco-jcc/jjaa124

151. Yadav M, Kapoor A, Verma A, Ambatipudi K. Functional Significance of Different Milk Constituents in Modulating the Gut Microbiome and Infant Health. J Agric Food Chem [Internet]. 2022 Apr 6 [cited 2023 Nov 5];70(13):3929–47. Available from: https://pubmed.ncbi.nlm.nih.gov/35324181/

152. Lechuga S, Braga-Neto MB, Naydenov NG, Rieder F, Ivanov AI. Understanding disruption of the gut barrier during inflammation: Should we abandon traditional epithelial cell lines and switch to intestinal organoids? Front Immunol [Internet]. 2023 Feb 16 [cited 2024 Jan 23];14:1108289. Available from: https://www.frontiersin.org/articles/10.3389/fimmu.2023.1108289/full

153. Salguero M, Al-Obaide M, Singh R, Siepmann T, Vasylyeva T. Dysbiosis of Gram-negative gut microbiota and the associated serum lipopolysaccharide exacerbates inflammation in type 2 diabetic patients with chronic kidney disease. Exp Ther Med [Internet]. 2019 Aug 26 [cited 2024 Apr 14];18(5). Available from: https://pubmed.ncbi.nlm.nih.gov/31602221/

154. Phillippi DT, Daniel S, Pusadkar V, Youngblood VL, Nguyen KN, Azad RK, McFarlin BK, Lund AK. Inhaled diesel exhaust particles result in microbiome-related systemic inflammation and altered cardiovascular disease biomarkers in C57Bl/6 male mice. Part Fibre Toxicol [Internet]. 2022 Dec 1 [cited 2024 Apr 14];19(1):1–29. Available from: https://particleandfibretoxicology.biomedcentral.com/articles/10.1186/s12989-022-00452-3

155. Park JH, Jeong SY, Choi AJ, Kim SJ. Lipopolysaccharide directly stimulates Th17 differentiation in vitro modulating phosphorylation of RelB and NF-κB1. Immunol Lett [Internet]. 2015 May 1 [cited 2024 Apr 16];165(1):10–9. Available from: https://pubmed.ncbi.nlm.nih.gov/25794633/

156. Larangeira AP, Silva AR, Gomes RN, Penido C, Henriques MGMO, Castro-Faria-Neto HC, Bozza PT. Mechanisms of allergen- and LPS-induced bone marrow eosinophil mobilization and eosinophil accumulation into the pleural cavity: a role for CD11b/CD18 complex. Inflamm Res [Internet]. 2001 [cited 2024 Mar 2];50(6):309–16. Available from: https://pubmed.ncbi.nlm.nih.gov/11475332/

157. Horie S, Kita H. CD11b/CD18 (Mac-1) is required for degranulation of human eosinophils induced by human recombinant granulocyte-macrophage colony-stimulating factor and platelet-activating factor. The Journal of Immunology [Internet]. 1994 Jun 1 [cited 2024 Mar 2];152(11):5457–67. Available from: https://dx.doi.org/10.4049/jimmunol.152.11.5457

158. Walker C, Rihs S, Braun RK, Betz S, Bruijnzeel PL. Increased expression of CD11b and functional changes in eosinophils after migration across endothelial cell monolayers. The Journal of Immunology [Internet]. 1993 May 1 [cited 2024 Mar 2];150(9):4061–71. Available from: https://dx.doi.org/10.4049/jimmunol.150.9.4061

159. Zhou X, Gao XP, Fan J, Liu Q, Anwar KN, Frey RS, Malik AB. LPS activation of Toll-like receptor 4 signals CD11b/CD18 expression in neutrophils. American Journal of Physiology-Lung Cellular and Molecular Physiology [Internet]. 2005 Apr;288(4):L655–62. Available from: https://www.physiology.org/doi/10.1152/ajplung.00327.2004

160. Ohnmacht C, Park JH, Cording S, Wing JB, Atarashi K, Obata Y, Gaboriau-Routhiau V, Marques R, Dulauroy S, Fedoseeva M, Busslinger M, Cerf-Bensussan N, Boneca IG, Voehringer D, Hase K, Honda K, Sakaguchi S, Eberl G. The microbiota regulates type 2 immunity through RORγt+ T cells. Science (1979) [Internet]. 2015 Aug 28 [cited 2024 Apr 19];349(6251):989–93. Available from: https://www.science.org/doi/10.1126/science.aac4263

161. Hirota K, Turner JE, Villa M, Duarte JH, Demengeot J, Steinmetz OM, Stockinger B. Plasticity of Th17 cells in Peyer's patches is responsible for the induction of T

cell-dependent IgA responses. Nat Immunol [Internet]. 2013 Apr [cited 2024 Feb 19];14(4):372–9. Available from: https://pubmed.ncbi.nlm.nih.gov/23475182/

162. Saravia J, Chapman NM, Chi H. Helper T cell differentiation. Cellular & Molecular Immunology 2019 16:7 [Internet]. 2019 Mar 12 [cited 2024 Feb 19];16(7):634–43. Available from: https://www.nature.com/articles/s41423-019-0220-6

163. Cheung PFY, Wong CK, Lam CWK. Molecular Mechanisms of Cytokine and Chemokine Release from Eosinophils Activated by IL-17A, IL-17F, and IL-23: Implication for Th17 Lymphocytes-Mediated Allergic Inflammation. The Journal of Immunology [Internet]. 2008 Apr 15 [cited 2024 Apr 18];180(8):5625–35. Available from: https://dx.doi.org/10.4049/jimmunol.180.8.5625

164. Dias PM, Banerjee G. The Role of Th17/IL-17 on Eosinophilic Inflammation. J Autoimmun. 2013 Feb 1;40(1):9–20.

165. Al-Muhsen S, Letuve S, Vazquez-Tello A, Pureza MA, Al-Jahdali H, Bahammam AS, Hamid Q, Halwani R. Th17 cytokines induce pro-fibrotic cytokines release from human eosinophils. Respir Res [Internet]. 2013 Mar 13 [cited 2024 Apr 18];14(1):1–11. Available from: https://respiratory-research.biomedcentral.com/articles/10.1186/1465-9921-14-34

166. Nakae S, Komiyama Y, Nambu A, Sudo K, Iwase M, Homma I, Sekikawa K, Asano M, Iwakura Y. Antigen-specific T cell sensitization is impaired in IL-17-deficient mice, causing suppression of allergic cellular and humoral responses. Immunity [Internet]. 2002 Sep 1 [cited 2024 Feb 22];17(3):375–87. Available from: http://www.ncbi.nlm.nih.gov/pubmed/12354389

167. McKinley L, Alcorn JF, Peterson A, DuPont RB, Kapadia S, Logar A, Henry A, Irvin CG, Piganelli JD, Ray A, Kolls JK. TH17 Cells Mediate Steroid-Resistant Airway Inflammation and Airway Hyperresponsiveness in Mice. The Journal of Immunology [Internet]. 2008 Sep 15 [cited 2024 Feb 22];181(6):4089–97. Available from: https://dx.doi.org/10.4049/jimmunol.181.6.4089

168. Margelidon-Cozzolino V, Tsicopoulos A, Chenivesse C, de Nadai P. Role of Th17 Cytokines in Airway Remodeling in Asthma and Therapy Perspectives. Frontiers in Allergy [Internet]. 2022 Feb 2 [cited 2024 Feb 22];3:806391. Available from: https://www.frontiersin.org/articles/10.3389/falgy.2022.806391/full

169. Na H, Lim H, Choi G, Kim BK, Kim SH, Chang YS, Nurieva R, Dong C, Chang SH, Chung Y. Concomitant suppression of TH2 and TH17 cell responses in allergic asthma by targeting retinoic acid receptor–related orphan receptor γt. Journal of Allergy and Clinical Immunology [Internet]. 2018 Jun 1 [cited 2022 Oct 7];141(6):2061-2073.e5. Available from: http://www.jacionline.org/article/S0091674917314811/fulltext

170. Bhaumik S, Mickael ME, Moran M, Spell M, Basu R. RORγt Promotes Foxp3 Expression by Antagonizing the Effector Program in Colonic Regulatory T Cells. The Journal of Immunology [Internet]. 2021 Oct 15 [cited 2024 Apr 20];207(8):2027–38. Available from: /pmc/articles/PMC8490938/

171. Cait A, Wedel A, Arntz JL, Duinkerken J, Datye S, Cait J, Alhasan MM, Conrad ML. Prenatal antibiotic exposure, asthma, and the atopic march: A systematic review and meta-analysis. Allergy [Internet]. 2022 Nov 27;77(11):3233–48. Available from: https://onlinelibrary.wiley.com/doi/10.1111/all.15404

Statutory Declaration

Eidesstattliche Versicherung

„Ich, Moumen Alhasan, versichere an Eides statt durch meine eigenhändige Unterschrift, dass ich die vorgelegte Dissertation mit dem Thema: " Pränatale Antibiotikaeinnahme erhöht den allergischen Asthmaschweregrad bei Mäusenachkommen: Nachweis eines kausalen Zusammenhangs und Ermittlung potenzieller Mechanismen“ „Antibiotic use during pregnancy increases allergic asthma severity in murine offspring: Establishing a causal association and identifying potential mechanisms“ selbstständig und ohne nicht offengelegte Hilfe Dritter verfasst und keine anderen als die angegebenen Quellen und Hilfsmittel genutzt habe.

Alle Stellen, die wörtlich oder dem Sinne nach auf Publikationen oder Vorträgen anderer Autoren/innen beruhen, sind als solche in korrekter Zitierung kenntlich gemacht. Die Abschnitte zu Methodik (insbesondere praktische Arbeiten, Laborbestimmungen, statistische Aufarbeitung) und Resultaten (insbesondere Abbildungen, Graphiken und Tabellen) werden von mir verantwortet.

Ich versichere ferner, dass ich die in Zusammenarbeit mit anderen Personen generierten Daten, Datenauswertungen und Schlussfolgerungen korrekt gekennzeichnet und meinen eigenen Beitrag sowie die Beiträge anderer Personen korrekt kenntlich gemacht habe (siehe Anteilserklärung). Texte oder Textteile, die gemeinsam mit anderen erstellt oder verwendet wurden, habe ich korrekt kenntlich gemacht.

Meine Anteile an etwaigen Publikationen zu dieser Dissertation entsprechen denen, die in der untenstehenden gemeinsamen Erklärung mit dem/der Erstbetreuer/in, angegeben sind. Für sämtliche im Rahmen der Dissertation entstandenen Publikationen wurden die Richtlinien des ICMJE (International Committee of Medical Journal Editors; www.icmje.og) zur Autorenschaft eingehalten. Ich erkläre ferner, dass ich mich zur Einhaltung der Satzung der Charité – Universitätsmedizin Berlin zur Sicherung Guter Wissenschaftlicher Praxis verpflichte.

Weiterhin versichere ich, dass ich diese Dissertation weder in gleicher noch in ähnlicher Form bereits an einer anderen Fakultät eingereicht habe.

Die Bedeutung dieser eidesstattlichen Versicherung und die strafrechtlichen Folgen einer unwahren eidesstattlichen Versicherung (§§156, 161 des Strafgesetzbuches) sind mir bekannt und bewusst.“

Berlin den, 12.07.2024

Declaration of your own contribution to the publications

Moumen Alhasan hatte folgenden Anteil an den folgenden Publikationen:

Publikation 1: [Moumen M. Alhasan, Alissa M. Cait, Markus M. Heimesaat, Michael Blaut, Robert Klopfleisch, Alexander Wedel, Thomas M. Conlon, Ali Ö. Yildirim, Elisa B. Sodemann, William W. Mohn, Stefan Bereswill, Melanie L. Conrad], [Antibiotic use dur-ing pregnancy increases offspring asthma severity in a dose-dependent manner], [Allergy], [2020]

Moumen Alhasan´s Anteil war: Studiendesign, Etablierung des Modells, Arbeit an der Tierhaltungsanlage und Sammeln von biometrischen Daten (Abbildung 1A, B, C, D, E), Probenentnahme und -aufbereitung. Messung von Antikörpern mittels ELISA (Abbildung 2A), Entzündungs-Quantifizierung (Abbildung 2B), Vorbereitung von Zytospins und Durchführung der differenzierten Zellzählung (Abbildung 2D), BAL-Zytokinemessung mittels Luminex (Tabelle 1) und Verfassen des Manuskripts.

Publication 2: [Alhasan MM, Hölsken O, Duerr C, Helfrich S, Branzk N, Philipp A, Leitz D, Duerr J, Almousa Y, Barrientos G, Mohn WW, Gamradt S, Conrad ML], [Antibiotic use during pregnancy is linked to offspring gut microbial dysbiosis, barrier disruption, and altered immunity along the gut-lung axis], [European Journal of Immunology], [2023]

Moumen Alhasan´s Anteil war: Studiendesign, Arbeit an der Tierhaltungsanlage, und Sammeln von biometrischen Daten (Abbildung 1). Probensammlung und -aufbereitung, Sammeln von biometrischen Daten, Milch-Zytokinemessung mittels Luminex (Abbildung 2), Mikrobiom, SCFAs und Durchflusszytometrie-Datenanalyse (Abbildung 2-6 und ergänzende Abbildungen 1,3,4,5). Asthma-Phänotyp-Analyse (ELISA, Atemwegs-Hyperreaktivitätstest Zytospins und Durchführung der differenzierten Zellzählung (ergänzende Abbildung 2) und Verfassen des Manuskripts

Printed copies of the publications

Received: 31 May 2019 | Revised: 7 December 2019 | Accepted: 23 December 2019

DOI: 10.1111/all.14234

ORIGINAL ARTICLE

Asthma and Lower Airway Disease

Allergy EAACI WILEY

Antibiotic use during pregnancy increases offspring asthma severity in a dose-dependent manner

Moumen M. Alhasan[1,2] | Alissa M. Cait[3] | Markus M. Heimesaat[1] | Michael Blaut[4] | Robert Klopfleisch[5] | Alexander Wedel[6] | Thomas M. Conlon[7] | Ali Ö. Yildirim[7] | Elisa B. Sodemann[1] | William W. Mohn[3] | Stefan Bereswill[1] | Melanie L. Conrad[1,2]

[1]Institute of Microbiology, Infectious Diseases and Immunology, Charité–Universitätsmedizin Berlin, Corporate Member of Freie Universität Berlin, Humboldt-Universität zu Berlin, Berlin Institute of Health, Berlin, Germany

[2]Division of Psychosomatic Medicine, Department of Internal Medicine, Charité-Universitätsmedizin Berlin, Corporate Member of Freie Universität Berlin, Humboldt-Universität zu Berlin, Berlin Institute of Health, Berlin, Germany

[3]Department of Microbiology and Immunology, Life Sciences Institute, University of British Columbia, Vancouver, BC, Canada

[4]Department of Gastrointestinal Microbiology, German Institute of Human Nutrition Potsdam-Rehbruecke, Nuthetal, Germany

[5]Department of Veterinary Medicine, Freie Universität Berlin, Berlin, Germany

[6]Department of Educational Psychology, Institute of Education, Technische Universität Berlin, Berlin, Germany

[7]Comprehensive Pneumology Center (CPC), Institute of Lung Biology and Disease, Helmholtz Zentrum München, Member of the German Center for Lung Research (DZL), Neuherberg, Germany

Correspondence
Melanie L. Conrad, Charité–Universitätsmedizin Berlin, Institute of Microbiology, Infectious Diseases and Immunology, Hindenburgmotherm 30, Berlin 12203, Germany.
Email: conradml@gmail.com

Funding information
Deutsche Forschungsgemeinschaft, Grant/Award Number: CO 1058/3-1; Konrad-Adenauer-Stiftung

Abstract

Background: The use of antibiotics during pregnancy is associated with increased allergic asthma risk in the offspring, and given that approximately 25% of pregnant women are prescribed antibiotics, it is important to understand the mechanisms contributing to this phenomenon. Currently, there are no studies that directly test this association experimentally. Our objective was to develop a mouse model in which antibiotic treatment during pregnancy results in increased offspring asthma susceptibility.

Methods: Pregnant mice were treated daily from gestation day 8-17 with an oral solution of the antibiotic vancomycin, and three concentrations were tested. At weaning, offspring were subjected to an adjuvant-free experimental asthma protocol using ovalbumin as an allergen. The composition of the gut microbiome was determined in mothers and offspring with samples collected from five different time points; short-chain fatty acids were also analyzed in allergic offspring.

Results: We found that maternal antibiotic treatment during pregnancy was associated with increased offspring asthma severity in a dose-dependent manner. Furthermore, maternal vancomycin treatment during pregnancy caused marked changes in the gut microbiome composition in both mothers and pups at several different time points. The increased asthma severity and intestinal microbiome changes in pups were also associated with significantly decreased cecal short-chain fatty acid concentrations.

Conclusion: Consistent with the "Developmental Origins Hypothesis," our results confirm that exposure to antibiotics during pregnancy shapes the neonatal intestinal environment and increases offspring allergic lung inflammation.

KEYWORDS
antibiotics, asthma, microbiome, pregnancy, short-chain fatty acid

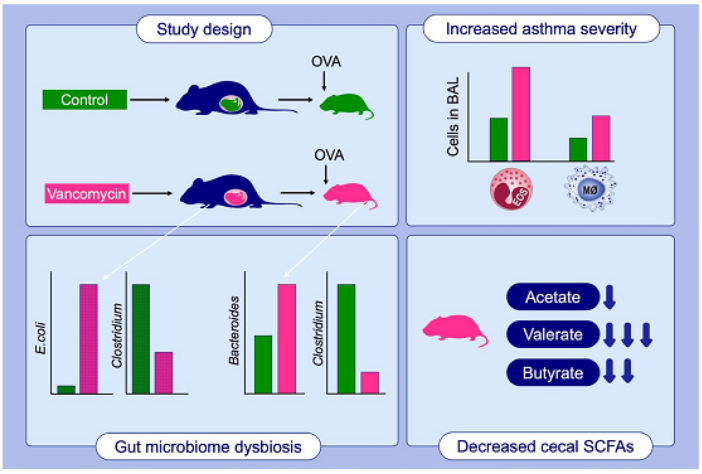

GRAPHICAL ABSTRACT
We found that maternal antibiotic treatment during pregnancy was associated with increased offspring asthma severity in a dose dependent manner. Maternal vancomycin treatment during pregnancy caused marked changes in the gut microbiome composition in both mothers and pups at several different time points. The increased asthma severity and intestinal microbiome changes in pups were also associated with significantly decreased cecal short chain fatty acid concentrations.
Abbreviations: BAL, bronchoalveolar lavage; OVA, ovalbumin; SCFAs, short chain fatty acids.

1 | INTRODUCTION

Allergic asthma constitutes a morbidity of increasing prevalence and is the leading cause of chronic disease in children. During asthma exacerbation, inflammation of the respiratory epithelia manifests as airway hyperreactivity and breathing difficulties that can substantially reduce quality of life. Though it is not completely clear how atopy initially arises, it is commonly accepted that allergic asthma results from a failure to generate protective immunologic tolerance against particular aeroallergens. Pursuing this further, several lines of evidence suggest that the ability to generate tolerance is developed during the fetal and neonatal life stages.[1] The "Developmental Origins Hypothesis" proposes that environmental influences during these critical time points can alter disease susceptibility in early life.[2]

There is considerable evidence that the use of antibiotics during pregnancy contributes to increased asthma susceptibility in children.[3-6] During birth, the maternal vaginal, perineal, and fecal microbiome seed the initial intestinal colonization of the newborn.[7,8] Consequently, antibiotics taken during pregnancy have been shown to alter both the maternal and neonatal microbiomes in humans,[9] rats,[10] and mice.[11] The early life microbiome is crucial for the proper development of immune system functions, whereas microbial dysbiosis in early life is associated with altered neonatal immunity [11] and is thought to bias the maturing neonatal immune system toward a hypersensitive state.[2,12] Considering allergic airway diseases, studies demonstrate that germ-free mice displayed increased asthma severity compared to mice with a conventional commensal microbiome.[13] It was also shown that rescue of the severe asthma phenotype in germ-free mice was only possible by supplementation with commensal microbes during early life, but not in adulthood.[14] The neonatal microbiome is therefore critical for establishing immunity and mucosal tolerance.

In addition to contributing to immune system development in early life, intestinal microbes also facilitate the digestion of dietary fiber, resulting in the production of short-chain fatty acids (SCFAs). Acetate, propionate, and butyrate are the major metabolic by-products of bacterial fiber fermentation, and these SCFAs are associated with asthma susceptibility. Longitudinal human studies revealed that

increased levels of fecal butyrate and propionate in the first year of life were significantly associated with protection from asthma at 6 years of age,[15] whereas decreased fecal acetate concentrations at 3 months of age were associated with asthma diagnosis at 3 years of age.[16] Studies in mice showed that increased fecal SCFAs were associated with protection against airway inflammation,[17] whereas decreased SCFA concentrations were associated with more severe allergic airway diseases.[18] Direct supplementation of adult mice with SCFAs[17,19,20] also effectively protected from airway inflammation.

Antibiotics account for 80% of prescriptions given during pregnancy.[21] Given the strong association between maternal antibiotic use and offspring asthma susceptibility, it is increasingly important to understand the mechanisms behind this phenomenon. There are, however, no experimental in vivo models available to date that examine the effect of antibiotics given only during pregnancy on offspring asthma. In the present study, we therefore established a mouse model in which maternal exposure to vancomycin resulted in increased asthma severity in the offspring.

2 | METHODS

2.1 | Animals

Twelve-week-old female BALB/c mice were obtained from Janvier Labs (Le Genest-Saint-Isle). Mice were kept under specific pathogen-free conditions and housed five animals per cage in a 12/12 hours light/dark cycle. Food and water were available ad libitum. All animal experiments were approved by local authorities (Landesamt für Gesundheit und Soziales; LAGeSo; registration number: G0158/18) and were performed in accordance with German and international guidelines.

2.2 | Experimental design

The presence of a vaginal plug after male and female co-habitation was denoted as gestation day (G)0. From G8 to G17, pregnant mice received a daily oral dose of the antibiotic vancomycin (Sigma-Aldrich) corresponding to 10, 20 or 40 mg/kg body weight. Vancomycin was specifically chosen because it is poorly absorbable, limiting the possibility that the antibiotic will directly affect the developing fetus, and allowing investigation of the downstream effects of maternal vancomycin use during pregnancy. Pregnant mice were given the antibiotic mixture (25 µL of vancomycin +15 µL Ora-Sweet syrup; Paddock Laboratories) through drops from a pipet; control animals were sham treated with water + syrup (Figure 1A, B). To reduce human error, we used a calibrated micropipette to administer this volume orally to each individual mouse. To ensure that the entirety of the volume was consumed, we visually confirmed after drug administration that each mouse had finished swallowing (5-10 seconds) before returning the animal to the cage (Figure 1C). Female offspring were weaned at 21 days of age, and experimental asthma was induced by subcutaneous sensitization using 10 µg ovalbumin (OVA VI—Sigma) in 200 µL PBS, once per week for 3 weeks. The asthma phenotype was induced by exposing the offspring for 20 minutes daily to a 1% OVA aerosol (OVA V—Sigma) for 3 days (Figure 1A, B). Twenty-four hours after the last OVA challenge, the asthma phenotype was assessed.[22]

2.3 | Molecular analysis of maternal and offspring fecal microbiomes

2.3.1 | 16S rRNA qPCR

Fresh fecal pellets were immediately frozen and stored at −80°C. Maternal fecal samples were collected 14 days before mating, at G17, and at weaning. Offspring feces were collected at weaning (21 days of age) and after allergic asthma exacerbation (7 weeks of age). Fecal DNA was extracted and then quantified using Quant-iT PicoGreen reagent (Invitrogen) as described in.[23] qPCR was chosen to obtain a broad survey of the bacterial groups present, as well as to determine how maternal vancomycin treatment influenced the quantity of bacteria present in mothers and offspring. Briefly, numbers of 16S rRNA gene copies per ng DNA were quantified in each sample using species-, genera- or group-specific primers (TIB MOLBIOL) assessed by qRT-PCR. Primer sequences can be found in Table S1.[24] Total bacteria load was assessed, as well as the following bacterial groups: Gammaproteobacteria/Enterobacteriaceae (Enterobacteriaceae), *Bacteroides/Prevotella/Porphyromonas* (Bacteroidetes), Mouse Intestinal *Bacteroides*, *Clostridium leptum*, *Clostridium coccoides/Eubacterium rectale*, *Enterococcus*, *Lactobacillus*, and *Bifidobacterium*.

2.3.2 | 16S rRNA sequencing

DNA was extracted using the PowerSoil for KingFisher kit (MO Bio) following manufacturer's instructions. 16S rRNA V4 gene fragments were amplified using bar-coded primers as described in [25] with the following primer regions (5′-3′): fwd: GTGCCAGCMGCCGCGGTAA, rev: GGACTACHVGGGTWTCTAAT. Pooled PCR amplicons were diluted to 20 ng/mL and sequenced using MiSeq 2000 bi-directional Illumina sequencing and Cluster Kit v4 (Macrogen). Library preparation was done using TruSeq DNA Sample Prep v2 Kit (Illumina) with 100 ng of DNA per sample. The library was quantified and quality-checked using Qubit (Thermo Fisher Scientific). DNA extraction, amplification, and sequencing were performed by Microbiome Insights Inc. Sequence data were trimmed, quality-filtered, and clustered at 97% identity into operational taxonomic units (OTUs) using a modified MOTHUR standard operating procedure.[26] An average of 31 554 quality-filtered reads were generated per sample, and there was a total of 8631 OTUs. The OTUs were taxonomically annotated using the SILVA database.[27] Global community structure comparisons were made in an R environment using Phyloseq.[28]

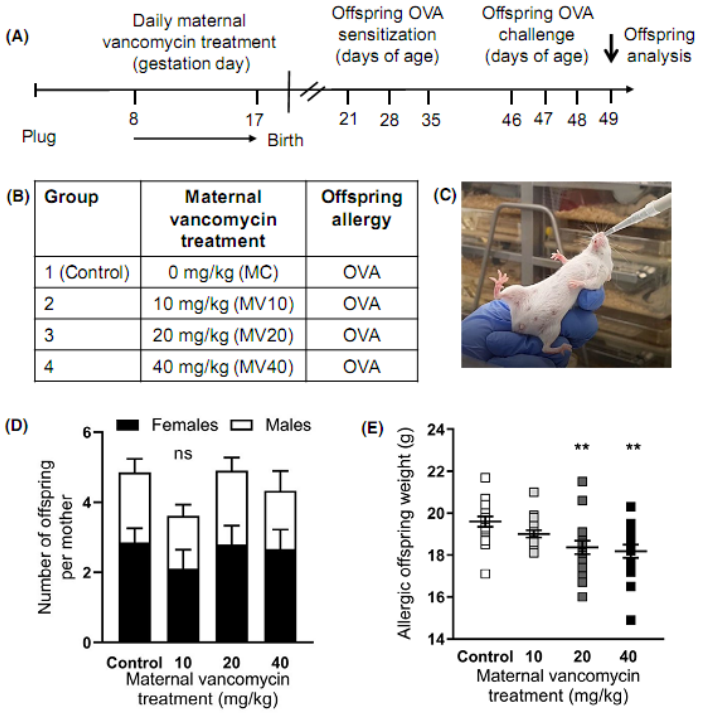

(B) Group	Maternal vancomycin treatment	Offspring allergy
1 (Control)	0 mg/kg (MC)	OVA
2	10 mg/kg (MV10)	OVA
3	20 mg/kg (MV20)	OVA
4	40 mg/kg (MV40)	OVA

FIGURE 1 The effect of antibiotic use during pregnancy on asthma development in the offspring—Mouse model description and pregnancy effects. A, Pregnant mothers were treated daily from G8-G17 with an oral dose of 10, 20 or 40 mg/kg vancomycin plus Ora-Sweet syrup. Control mothers were treated orally with water and Ora-Sweet. At weaning, all offspring were subjected to an experimental asthma protocol with a subcutaneous sensitization to ovalbumin (OVA) at 21, 28, and 35 days of age, and asthma provocation by a 20 min daily aerosol challenge at 46, 47, and 48 days of age. B, Overview of the treatment for each group. C, Oral administration of vancomycin plus Ora-Sweet. The mouse is scruffed and presented the antibiotic via pipet, allowing the animal to voluntarily consume the drug-Ora-Sweet mixture. Untrained mice immediately learn this procedure and consume the entire mixture within 5-10 s of presentation. D, Litter size—Total offspring (entire bar), females (black bar) and males (white bar) born to mothers in each group. E, Weight of 7-wk-old allergic offspring that were prenatally exposed to maternal control or vancomycin during pregnancy. Data information: Means ± SEM are shown, control (n = 18), prenatal 10 mg/kg (n = 19), prenatal 20 mg/kg (n = 18), prenatal 40 mg/kg (n = 16). Results represent two independently performed experiments. Significance is represented by $^{**}P < .01$, one-way ANOVA with Dunnett's multiple comparisons test (10, 20, and 40 compared against control)

2.4 | Blood collection and antibody measurements

Blood samples were taken from the orbital sinus of terminally anaesthetized mice and serum was stored at −80°C. Total IgG, OVA-specific IgE and OVA-specific IgG1 were measured in the serum of OVA allergic offspring by an enzyme-linked immunosorbent assay (ELISA) (BD Bioscience).

2.5 | Bronchoalveolar lavage, cytospins, and bronchoalveolar lavage cytokine measurements

Using a tracheal cannula on euthanized offspring, Bronchoalveolar lavage (BAL) was performed once using 1 mL of 1× Complete Protease Inhibitor Cocktail (Roche). BAL supernatant was stored at −80°C, total leukocytes were counted with a Neubauer chamber, and cytospin preparations were made and stained with Diff-Quick (Merz & Dade). Two hundred cells were counted per cytospin by a researcher blinded to the sample names. For BAL cytokine measurements, IL-1α, IL-1β, IL2, IL-3, IL-4, IL-5, IL-6, IL-9, IL-10, IL-12 (p40), IL-12 (p70), IL-13, IL-17A, Eotaxin, G-CSF, GM-CSF, IFNγ, KC, MCP-1, MIP-1α, MIP-1 β, RANTES, and TNF were measured using a mouse 23-plex cytokine assay (Bio-Rad), according to manufacturer's instructions.

2.6 | Lung collection and histology

Immediately after BAL, lungs were fixed with 4% formalin. 4 μm periodic acid-Schiff (PAS)-stained lung sections were microscopically analyzed using the new Computer Assisted Stereological Toolbox

(newCAST; Visiopharm) as described in,[29] by readers blinded to the study groups. For inflammation and goblet cell measurements, the software randomly selected 100 frames across multiple lung sections (40× objective), superimposed by a line grid and points. Point intercepts on an eosinophil or goblet cell were considered as a point of inflammation (PI) or point of goblet cell (PG), respectively. Line interceptions with the bronchial epithelium were considered a line of a goblet cell (LG) or line of a nongoblet cell (LnG), respectively. Line intercepts with blood vessel walls were labeled as line blood vessel (LV). Volume of inflammation (Vol. Inf), number of goblet cells (Nu. G), and volume of goblet cells (Vol. G) were calculated as follows:

$$\text{Vol. Inf} = (\Sigma PI) \times 9.395/(\Sigma LG + \Sigma LV)$$

$$\text{Nu. G} = (\Sigma LG \times 100)/(\Sigma LG + \Sigma LnG)$$

$$\text{Vol. G} = (\Sigma PG \times 9.395)/(\Sigma LG + \Sigma LnG)$$

2.7 | Analysis of SCFA from allergic offspring cecum

Cecal acetate, propionate, butyrate, and valerate were measured with an HP 5890 series II gas chromatograph (Hewlett-Packard) equipped with an HP-20 M column and a flame ionization detector. Previously, flash-frozen cecal contents from allergic offspring were diluted and centrifuged, then the supernatant was mixed with 2-ethylbutyric acid as an internal standard, 0.36 M $HClO_4$ and 1 M NaOH. The mixture was lyophilized overnight, and the remnant was re-dissolved in a mixture of 400 μL of acetone and 5 M formic acid. After centrifugation, 1 mL of the supernatant was injected into the gas chromatograph.

2.8 | Statistical analysis

Samples were tested for normal distribution using a Shapiro-Wilk normality test. Parametric/nonparametric data were analyzed by one-way ANOVA/Kruskal-Wallis (with Dunnett's multiple comparison test) or Mann-Whitney U test in the case of two groups. Calculations were performed with GraphPad Prism 7 software. To confirm the robustness of the statistics with respect to outliers, we performed an outlier analysis for every model with Cook's distance using base R. In the presence of outliers, the initial analyses were repeated after extracting the respective values from the dataset. These results confirmed our initial analyses. Additionally, all models were estimated with robust ANOVA's using the WRS2 Package (version 0.10). Again, the analyses showed only small and expected differences to the initial analyses. Hence, we retained the initial results from the one-way ANOVA and Kruskal-Wallis tests. Pearson's correlation analysis and statistics were performed using the R package psych (version 1.8.12). Correlation figures were generated using ggplot2[30] and ColorBrewer (https://CRAN.R-project.org/package=RColorBrewer). Multiple comparisons were corrected using the Benjamini-Hochberg method.

3 | RESULTS

3.1 | Model description

To examine the effect of antibiotics taken during pregnancy on the development of offspring asthma, we established a mouse model in which daily treatment of mothers with the antibiotic compound vancomycin from gestation day G8 until G17 resulted in increased asthma severity in the offspring (Figure 1A). Mothers were treated with either 10, 20 or 40 mg vancomycin per kg body weight, corresponding to low, medium, and high vancomycin doses in humans, and as a prenatal control, mothers received sterile water (Figure 1B). Using a novel method adapted from,[31] we used a pipet to feed mice vancomycin mixed with Ora-Sweet, which is a medically approved syrup used to sweeten antibiotics for children.[32] In our experience, untrained, hand-held mice readily ate the entirety of the antibiotic mixture within a 10 second delivery time (Figure 1C). Offspring from all groups were subjected to an ovalbumin (OVA) allergic asthma protocol beginning at weaning (Figure 1A, B).

3.2 | Maternal treatment with a high antibiotic concentration increased miscarriages and reduced offspring weight

To assess the effect of maternal treatment with antibiotics on pregnancy outcome, we recorded litter sizes, miscarriage rates, offspring sex and adult offspring weight. Of the term pregnancies, the mean litter size was 4.5 pups and no differences were observed in litter size or pup sex between groups (Figure 1D). In mice with confirmed pregnancy (more than 3.5 grams of weight gained from G0-G13),[33] we observed increased miscarriages, that is, abortion of all pups, with increasing antibiotic concentration. Mothers treated with 20 mg/kg vancomycin had a 9% miscarriage rate, whereas in mice with 40 mg/kg the number rose to 30%. Control mothers and those exposed to 10 mg/kg vancomycin had no observed miscarriages. In addition to miscarriage, prenatal exposure to increasing antibiotic concentrations was also associated with decreased offspring weight in a dose-dependent manner. Seven-week-old allergic offspring from mothers treated with 20 mg/kg and 40 mg/kg vancomycin weighed significantly less than allergic offspring from control mothers (Figure 1E).

3.3 | Maternal antibiotic treatment during pregnancy increased offspring asthma severity in a dose-dependent manner

To determine how antibiotic use during pregnancy impacts offspring asthma severity, we induced experimental allergic asthma in offspring derived from control- and antibiotic-treated mothers. As expected, serum from all allergic offspring contained OVA-specific IgE and OVA-specific IgG1, though no differences were observed in these antibodies or total IgG concentrations

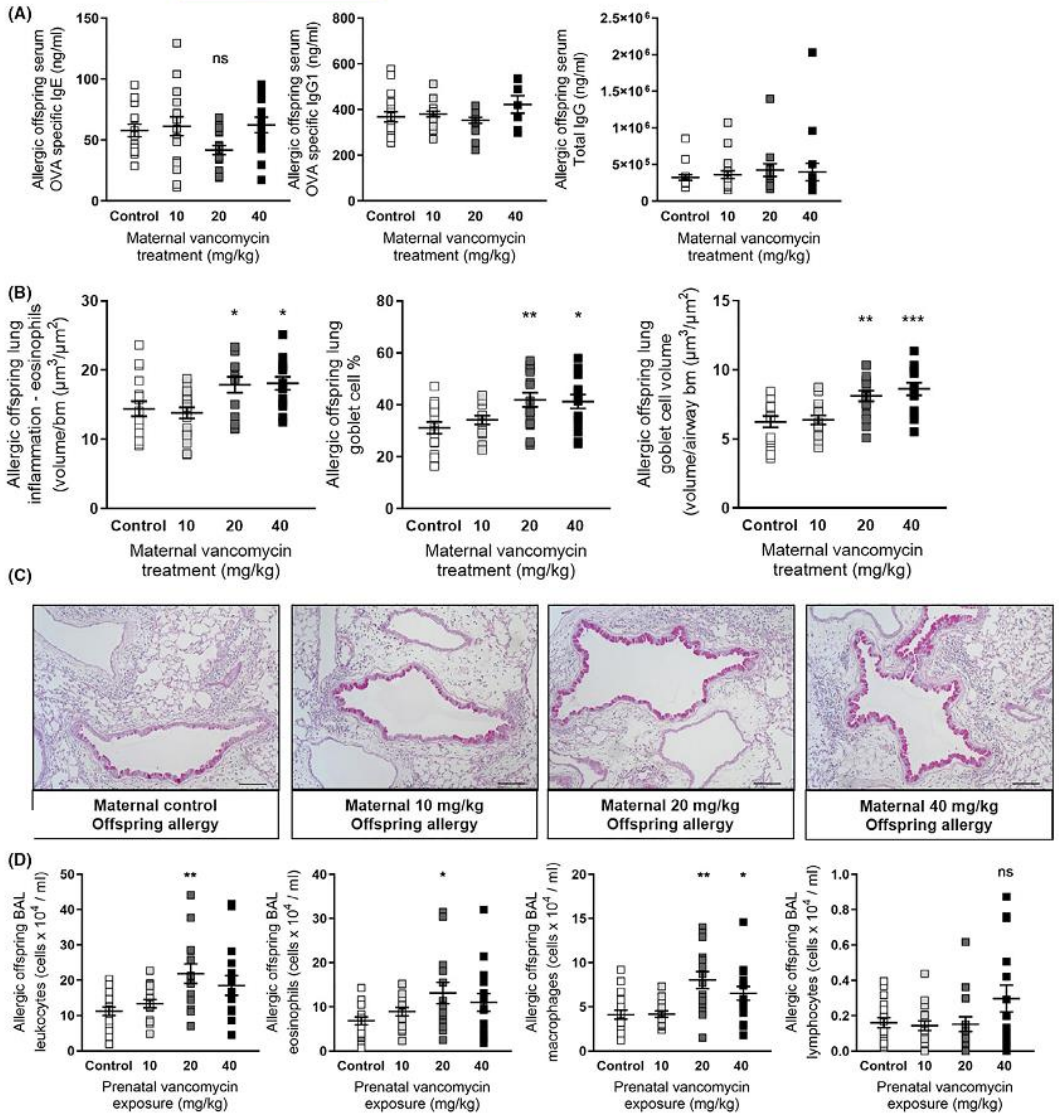

FIGURE 2 Maternal antibiotic treatment during pregnancy results in increased asthma severity in the offspring. A, Serum antibody titers from OVA allergic offspring: OVA-specific IgE, OVA-specific IgG1 and Total IgG. B, Allergic offspring lung histology quantification: eosinophilic inflammation, goblet cell percentage, goblet mucous volume. C, Allergic offspring lung histology images. Scale bar = 100 µm. D, Bronchoalveolar lavage (BAL) cell counts from allergic offspring: leukocytes, eosinophils, macrophages, and lymphocytes. Data information: Means ± SEM are shown, control (n = 18), prenatal 10 mg/kg (n = 19), prenatal 20 mg/kg (n = 18), prenatal 40 mg/kg (n = 16). Results represent two independently performed experiments. Significance is represented by *$P < .05$, **$P < .01$, ***$P < .001$, one-way ANOVA or Kruskal-Wallis test with Dunnett's multiple comparisons test (10, 20, and 40 compared against control)

between maternal control (MC) and maternal vancomycin (MV) allergic offspring groups (Figure 2A). Analysis of allergic offspring inflammation revealed increasing asthma severity in correspondence with increasing maternal vancomycin concentrations. Histopathological quantification of pulmonary inflammation and mucous production revealed that allergic offspring from

TABLE 1 Bronchoalveolar lavage from allergic offspring displays decreased cytokine concentrations with increasing prenatal antibiotic exposure

	Maternal control	Maternal 10 mg/kg	Maternal 20 mg/kg	Maternal 40 mg/kg
	n = 18	n = 18	n = 13	n = 16
Concentration (pg/mL)	Mean (SEM)	Mean (SEM)	Mean (SEM)	Mean (SEM)
IL-1α	7.2 (0.4)	8.5 (0.9)	9.0 (0.8)	9.0 (1.0)
IL-1β	48.0 (4.9)	36.1 (4.0)	**22.0 (5.3)****	**25.4 (5.6)***
IL-2	164.8 (18.1)	6.4 (0.4)	6.6 (0.4)	6.8 (0.7)
IL-4	165.4 (17.5)	142.9 (16.4)	**82.9 (16.9)***	145.0 (4.2)
IL-5	164.8 (18.1)	146.2 (11.4)	**103.2 (17.2)***	130.7 (13.4)
IL-6	9.7 (2.9)	10.3 (1.6)	9.7 (1.6)	8.2 (1.4)
IL-9	42.0 (6.0)	**20.9 (5.5)***	26.4 (7.8)	**9.7 (4.4)*****
IL-12p40	52.6 (4.2)	43.4 (2.8)	40.1 (3.8)	44.4 (4.2)
IL-12p70	12.4 (1.0)	11.1 (0.7)	**7.7 (0.8)****	**9.1 (1.3)***
IL-13	111.1 (13.4)	83.6 (9.3)	81.5 (12.1)	92.2 (9.6)
Eotaxin	161.6 (7.2)	141.0 (7.0)	135.6 (11.2)	**113.0 (16.9)****
G-CSF	8.4 (0.8)	7.9 (0.9)	**5.3 (0.9)***	**5.5 (0.9)***
GM-CSF	10.0 (0.6)	8.5 (0.3)	**6.5 (0.6)*****	**3.3 (6.5)*****
KC	213.2 (27.5)	230.8 (29.1)	240.7 (34.7)	207.3 (26.5)
MCP-1	28.9 (5.9)	16.2 (2.8)	**4.7 (3.0)*****	**6.1 (2.7)*****
MIP-1α	9.8 (0.9)	9.6 (0.6)	**5.1 (0.1)*****	7.7 (0.9)
MIP-1β	4.3 (0.4)	3.8 (0.2)	**2.4 (0.3)*****	**2.6 (0.2)*****
RANTES	6.5 (0.4)	5.8 (0.2)	**4.7 (0.3)****	**5.3 (0.4)***
TNFα	20.9 (1.3)	19.6 (1.0)	17.1 (1.9)	22.6 (4.7)

Note: Data information: Means ± SEM are shown, control (n = 18), prenatal 10 mg/kg (n = 19), prenatal 20 mg/kg (n = 18), prenatal 40 mg/kg (n = 16). Results represent two independently performed experiments. Significance is represented by *P < .05, **P < .01, ***P < .001 one-way ANOVA or Kruskal-Wallis test with Dunnett's multiple comparisons test (10, 20, and 40 compared against control).

mothers treated with 20 or 40 mg/kg vancomycin (henceforth referred to as MV20 and MV40 allergic offspring, respectively) displayed significantly increased airway and vessel eosinophilic inflammatory responses as well as increased goblet cell numbers and mucous volume when compared to allergic offspring from control mothers (Figure 2B, C).

In addition to tissue inflammation, total leukocyte influx into the bronchoalveolar lavage (BAL) fluid was significantly increased in MV20 and MV40 allergic offspring; this result was largely due to increased numbers of eosinophils and macrophages (Figure 2D). In the BAL, increased allergic lung inflammation correlated with significantly lower concentrations of 12 of the 23 measured BAL cytokines, namely IL-1β, IL-4, IL-5, IL-9 IL-10, IL-12p70, eotaxin, G-CSF, GM-CSF, MCP1, MIP-1α and RANTES (Table 1). Finally, correlation analysis showed that increasing vancomycin concentration during pregnancy correlated with significantly increased asthma severity in the offspring (Figure S1A-D). In summary, based on significant increases in lung inflammation, mucous production, and BAL cell infiltrates, as well as a correlated decrease in BAL cytokines in MV20 and MV40 allergic offspring, we thereby show that maternal antibiotic treatment during pregnancy was associated with increased severity of offspring allergic asthma.

3.4 | Antibiotic treatment during pregnancy altered the maternal and offspring intestinal microbiomes

To correlate increased MV offspring asthma severity with changes in gut microbial communities, we quantified the changing fecal microbiome composition of mothers and their offspring using qPCR. At G17, following antibiotic treatment, we observed a significant increase in total bacterial load in all mothers that were treated with vancomycin in comparison to control G17 mothers (Figure 3A). At weaning (23 days after the last antibiotic treatment), total bacterial loads of vancomycin-treated mothers returned to control levels; however, all MV offspring had significantly increased fecal bacterial numbers, both at weaning and as allergic adults. The increased bacterial load in MV mothers corresponded to greatly increased numbers (up to Log 4) of bacteria in the Enterobacteriaceae in all vancomycin-treated groups (Figure 3B). qPCR additionally revealed that microbes in the Bacteroidetes were also increased (Log 2) in G17 maternal feces in the MV10 and MV20 groups (Figure 3C). Again, members of this group returned to control levels in the mothers at weaning, whereas they remained elevated in offspring from all MV groups, both at weaning and as allergic adults (Figure 3C). Mouse

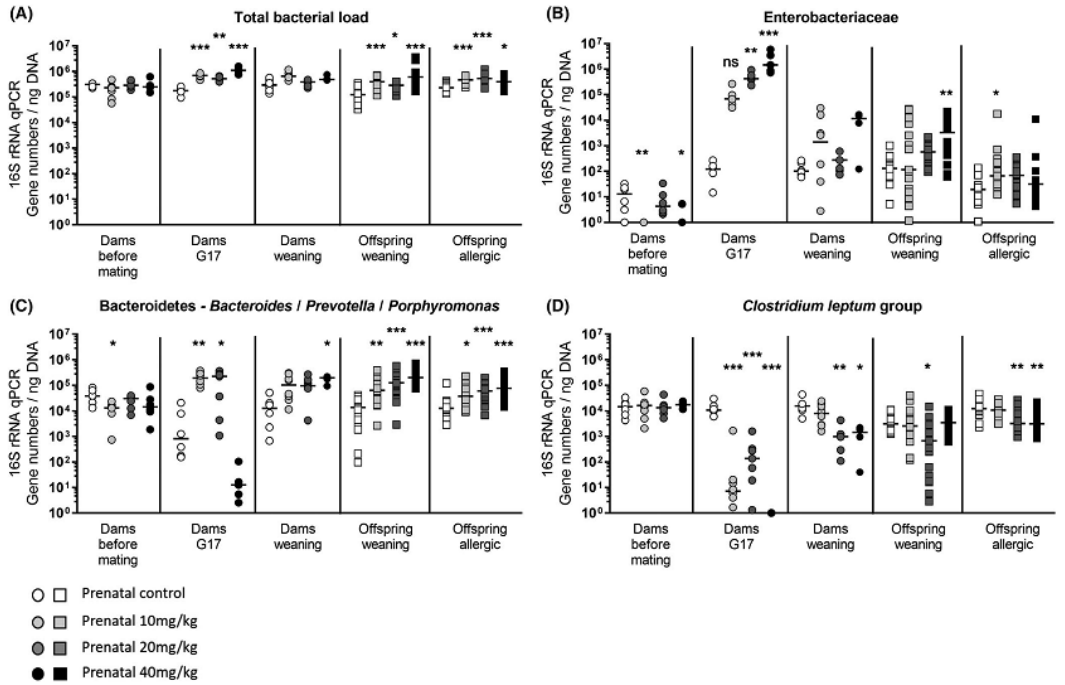

FIGURE 3 qPCR analysis of the fecal microbiome from mothers and offspring. Broad bacterial clades in the maternal and offspring fecal microbiome were quantified in all treatment groups using taxa-specific 16S rRNA qPCR. A, Total eubacterial load, B, γ-proteobacteria—Enterobacteriaceae, C, Bacteroidetes—*Bacteroides*, *Prevotella*, and *Porphyromonas*, D, *Clostridium leptum* group. Data information: Medians (black bars) are shown, *Maternal*: control (n = 6), 10 mg/kg, (n = 8), 20 mg/kg (n = 7), 40 mg/kg (n = 6). *Offspring*: from control mothers (n = 18), from 10 mg/kg vancomycin-treated mothers (n = 19), from 20 mg/kg vancomycin-treated mothers (n = 18), from 40 mg/kg vancomycin-treated mothers (n = 16). Results represent two independently performed experiments. Significance is represented by $^{*}P < .05$, $^{**}P < .01$, $^{***}P < .001$, one-way ANOVA or Kruskal-Wallis test with Dunnett's multiple comparisons test (10, 20, and 40 compared against control)

Intestinal *Bacteroides* (MIB) followed a similar pattern but with less pronounced differences between groups (Figure S2A).

Considering gram-positive bacteria, qPCR analysis revealed an expected decrease in the fecal *Clostridium leptum* group in all vancomycin-treated mothers at G17 (up to Log 4 decrease) (Figure 3D). A similar trend was observed in the *Clostridium coccoides/Eubacterium Rectale* group (Figure S2B). *Clostridium leptum* remained significantly decreased in both mothers and offspring at weaning and in the adult allergic offspring (Log1) (Figure 3D). Finally, *Lactobacillus* concentrations did not show any major differences between control and vancomycin-treated mothers or pups (Figure S2C).

To expand on the qPCR data, we chose the group with the greatest increase in asthma severity (MV20), to examine the maternal and offspring fecal microbiome by 16S amplicon sequencing. 16S amplicon analysis confirmed that members of the Enterobacteriaceae increased in relative abundance at G17 in MV20 maternal feces (Figure 4A). One of the most differentially abundant operational taxonomic units (OTUs) at G17 in MV20 maternal feces was identified as *Escherichia coli*, a member of the Enterobacteriaceae (Figure 4B). 16S amplicon analysis also allowed us to infer the contributions of particular taxa to the Bacteroidetes qPCR results. In MV20 mothers at G17, OTUs corresponding to unclassified Bacteroidetes had elevated relative abundances (Figure 4C), whereas in MV20 offspring at weaning and at adulthood, different OTUs belonging to the genus *Bacteroides* had increased relative abundances (Figure 4D). The genera, *Prevotella* and *Porphyromonas*, did not appear to contribute to the increase in Bacteroidetes, as the relative abundance of the former actually decreased in MV20 mothers and offspring at all time points measured after vancomycin treatment (Figure 4D); the latter did not make up a substantial proportion of sequencing reads (<0.001%).

16S amplicon analysis of *Clostridium* confirmed our observations in the MV20 groups, with the G17 time point, as well as mothers and offspring at weaning, having significantly lower relative abundances of OTUs classified as members of the order, Clostridiales. In summary, these data confirm that the increases in total fecal bacterial numbers in vancomycin-treated mothers at G17 and in their offspring at weaning and adulthood is likely due to a bloom of

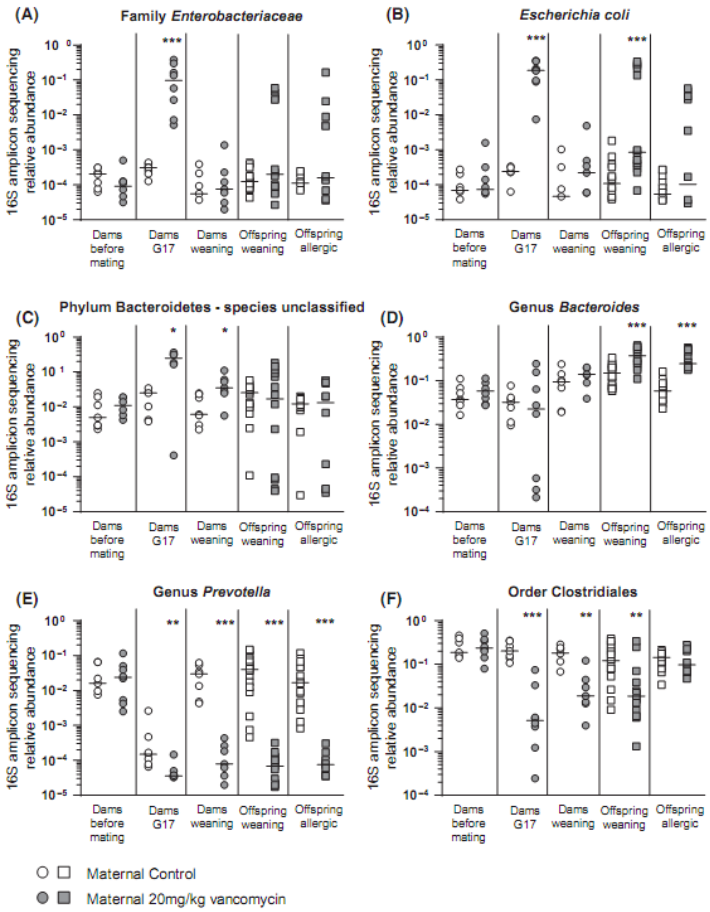

FIGURE 4 16S rRNA amplicon sequencing analysis of the fecal microbiome from MV20 mothers and offspring. Relative abundance of A, Enterobacteriaceae, B, *Escherichia coli*, C, an unclassified species of Bacteroidetes, D, *Bacteroides*, E, *Prevotella*, F, Clostridiales. Data information: Medians (black bars) are shown. *Maternal*: control (n = 6), 10 mg/kg, (n = 8), 20 mg/kg (n = 7), 40 mg/kg (n = 6). *Offspring*: from control mothers (n = 18), from 10 mg/kg vancomycin-treated mothers (n = 19), from 20 mg/kg vancomycin-treated mothers (n = 18), from 40 mg/kg vancomycin-treated mothers (n = 16). Results represent two independently performed experiments. Significance is represented by $^{*}P < .05$, $^{**}P < .01$, $^{***}P < .001$. A Mann-Whitney U test was performed (control vs 20 mg/kg)

gram-negative *E coli* as well as bacteria in the phylum Bacteroidetes. These increases were accompanied by comparable decreases in members from the order Clostridiales.

3.5 | SCFAs are significantly decreased in the cecum of MV allergic offspring

Due to the associations between the microbiome, SCFA production, and asthma susceptibility, we also measured SCFAs in the cecum of MC and MV allergic offspring. In both humans[16] and mice,[18] decreased levels of fecal SCFAs are associated with increased asthma susceptibility and severity. In agreement with these studies, we found that increased asthma severity in MV allergic offspring was associated with significant decreases in cecal SCFAs. Correlation analyses further indicated that increasing vancomycin dose during pregnancy (Figure S3A-D), as well as increasing total bacterial numbers at G17 (Figure S4A-D), were correlated with decreased SCFA concentrations in the offspring. As shown in Figure 5A and B, all MV allergic offspring had significantly decreased concentrations of cecal acetate and valerate, whereas cecal propionate was only decreased in the MV40 group (Figure 5C). Cecal butyrate was decreased in both the MV20 and MV40 allergic offspring groups (Figure 5D), of which MV20 displayed the most severe asthma phenotype. Decreased

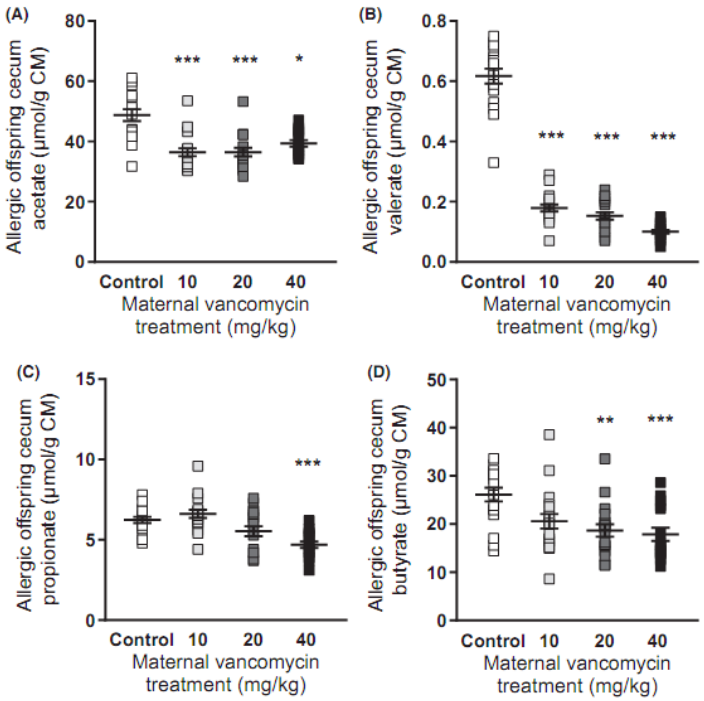

FIGURE 5 Short-chain fatty acids are decreased in the cecum of allergic offspring whose mothers were treated with vancomycin during pregnancy. Short-chain fatty acid concentrations in the cecum of allergic offspring. A, Acetate, B, valerate, C, propionate, D, butyrate. Data information: Means ± SEM are shown, control (n = 18), prenatal 10 mg/kg (n = 19), prenatal 20 mg/kg (n = 18), prenatal 40 mg/kg (n = 16). Results represent two independently performed experiments. Significance is represented by *P < .05, **P < .01, ***P < .001one-way ANOVA or Kruskal-Wallis test with Dunnett's multiple comparisons test (10, 20, and 40 compared against control)

cecal butyrate concentrations in these groups were also associated with significantly decreased *Clostridium leptum* gene numbers in the feces (Figure 3D).

4 | DISCUSSION

We have designed the first mouse model in which maternal treatment with antibiotics only during pregnancy resulted in increased asthma severity in the offspring. Our model is unique in that the offspring were not exposed directly to the antibiotic. Other groups have demonstrated that prenatal plus neonatal exposure to antibiotics resulted in increased offspring asthma severity; however, these models also treated the offspring with antibiotic from birth until allergy induction.[34,35] Russell et al (2013) tested the effect of vancomycin given only during pregnancy on offspring asthma development in mice, but found no difference between MV and MC allergic offspring.[36] We propose that the difference observed between studies reflects the mode of vancomycin delivery. Delivery of medication individually to mice with a pipet is an excellent alternative to delivering antibiotics by gavage or via water bottles. Gavage is very stressful for pregnant mice, while water bottle distribution of antibiotics is limited by the facts that (a) individual mouse dosage cannot be measured precisely and (b) antibiotic may not reach the minimum inhibitory concentration due to the small-dose, high-frequency manner of water bottle delivery.[37]

Maternal vancomycin treatment during pregnancy increased offspring asthma severity in a dose-dependent manner. This is in line with several human studies that show higher asthma risk in children whose mothers were prescribed antibiotics several times during pregnancy.[3] MV allergic offspring displayed significantly augmented inflammation in the lung tissue and BAL. Regarding BAL cytokine levels, which are often reported to increase with increasing asthma severity, we expected that animals with higher inflammation would also display increased type 2 cytokines. To our surprise, increased airway inflammation was associated with significantly lower concentrations of 12 of the 23 measured BAL cytokines. The type 2 cytokines IL-4 and IL-5 were among the cytokines decreased in the MV20 and MV40 allergic offspring; IL-13, however, did not show any difference between groups. Since the decreased allergic offspring BAL cytokine concentrations were correlated with increasing maternal vancomycin concentration, this strongly reduces the possibility of random error. Additionally, we have also observed this phenomenon using an unrelated prenatal risk model in our laboratory (unpublished information). At the moment, we unfortunately cannot offer a firm explanation as to *why* decreased cytokine levels were observed. This topic requires specifically designed future studies to examine this question in further detail.

Maternal vancomycin treatment during pregnancy was associated with microbial dysbiosis that was passed on to the offspring. Both taxa-specific 16S rRNA qPCR and universal bacterial primer

16S rRNA amplicon sequencing were used to analyze the intestinal microbiota of both mothers and offspring at several different time points. The two methods are complementary, with the former quantifying the density of targeted populations and the latter providing relative abundances of most bacterial taxa. At G17, maternal vancomycin treatment was associated with substantial (Log 4) increases in Enterobacteriaceae and unidentified Bacteroidetes. Given that vancomycin mainly targets gram-positive bacteria,[38] this bloom of bacteria is likely due to the availability of new intestinal ecological niches. Accordingly, at G17 we also observed log 4 decreases in maternal Clostridia. The maternal microbiota is thought to contribute directly to the neonatal microbiome composition due to transfer of bacteria during birth[7] and, in mice, through consumption of maternal feces by neonates in early life.[39] Our analysis of the fecal microbiota from the offspring supports this notion. Pups and adult allergic offspring from vancomycin-treated mothers had an increased bacterial load that was contributed to by Enterobacteriaceae as well as *Bacteroidetes*. Additionally, qPCR and amplicon sequencing confirmed that Clostridiales was also decreased in offspring at weaning.

In both humans [16] and mice,[18] changes to the microbiome are associated with decreased levels of fecal SCFAs and increased asthma susceptibility. Our study also demonstrated that MV allergic offspring had significantly decreased cecal SCFA concentrations compared to their MC allergic counterparts. Further analysis showed that both maternal vancomycin concentration and maternal total bacterial load at G17 were significantly associated with decreased SCFA concentrations in allergic offspring, with butyrate being the most strongly impacted. Studies have revealed the importance of this SCFA in allergic asthma, demonstrating that butyrate supplementation during asthma sensitization of adult mice resulted in protection against airway inflammation.[19] Additionally, mice treated with vancomycin since birth could be rescued from a severe asthma phenotype by supplementation with butyrate during vancomycin treatment.[40] Butyrate acts as an inflammatory regulator, and several studies have implicated butyrate in protection against asthma via FoxP3 induction on regulatory T cells and subsequent suppression of inflammatory Th9 cells in the allergic lung.[19]

4.1 | Conclusion

We have established the first mouse model in which maternal antibiotic treatment during pregnancy increases offspring asthma severity. Increased asthma severity was accompanied by maternal and offspring microbial dysbiosis, as well as decreases in offspring cecal acetate, butyrate, and valerate concentrations. Our model is ideal for mechanistic analysis of how antibiotics given during pregnancy can alter offspring immune system development and subsequent disease susceptibility. Future analyses will examine SCFA production in concert with fetal and neonatal development to better understand the effects of antibiotic use during pregnancy at critical developmental time points.

ACKNOWLEDGMENTS

We thank the staff at the animal research facility of the Charité—Universitätsmedizin Berlin for their amazing animal work. Additionally, we thank Maria Daniltchenko, Gernot Reifenberger, Bärbel Gruhl, Christine Hollauer and Maximilian Pankla for their excellent technical assistance. This work was supported through the Deutsche Forschungsgemeinschaft (DFG—grant CO 1058/3-1) as well as the Konrad Adenauer Stiftung.

CONFLICT OF INTEREST

The authors declare that they have no conflict of interest.

AUTHOR CONTRIBUTIONS

MA performed the mouse work. MA and ES analyzed the allergic offspring samples. MMH and SB performed qPCR microbiome analysis and co-edited paper. AC and WWM performed 16S rRNA amplicon analysis. MB performed the short-chain fatty acid analysis, RK TMC, and AOY analyzed lung histology. MLC and AC conceptualized the study and interpreted the data. AC performed correlation analyses. AW performed statistical outlier analysis and robust ANOVAs. MLC provided funding, performed mouse work, supervised all stages of the study and wrote the manuscript.

ORCID

Melanie L. Conrad https://orcid.org/0000-0002-8811-5536

REFERENCES

1. Peters JL, Boynton-Jarrett R, Sandel M. Prenatal environmental factors influencing IgE levels, atopy and early asthma. *Curr Opin Allergy Clin Immunol*. 2013;13(2):187-192.
2. Stiemsma LT, Michels KB. The role of the microbiome in the developmental origins of health and disease. *Pediatrics*. 2018;141(4):e20172437.
3. Loewen K, Monchka B, Mahmud SM, Jong G, Azad MB. Prenatal antibiotic exposure and childhood asthma: a population-based study. *Eur Respir J*. 2018;52(1):1702070.
4. Mulder B, Pouwels KB, Schuiling-Veninga CC, et al. Antibiotic use during pregnancy and asthma in preschool children: the influence of confounding. *Clin Exp Allergy*. 2016;46(9):1214-1226.
5. Wu P, Feldman AS, Rosas-Salazar C, et al. Relative importance and additive effects of maternal and infant risk factors on childhood asthma. *PLoS ONE*. 2016;11(3):e0151705.
6. Zhao D, Su H, Cheng J, et al. Prenatal antibiotic use and risk of childhood wheeze/asthma: a meta-analysis. *Pediatr Allergy Immunol*. 2015;26(8):756-764.
7. Mueller NT, Bakacs E, Combellick J, Grigoryan Z, Dominguez-Bello MG. The infant microbiome development: mom matters. *Trends Mol Med*. 2015;21(2):109-117.
8. Benn CS, Thorsen P, Jensen JS, et al. Maternal vaginal microflora during pregnancy and the risk of asthma hospitalization and use of antiasthma medication in early childhood. *J Allergy Clin Immunol*. 2002;110(1):72-77.
9. Meropol SB, Edwards A. Development of the infant intestinal microbiome: A bird's eye view of a complex process. *Birth Defects Res C Embryo Today*. 2015;105(4):228-239.
10. Fak F, Ahrne S, Molin G, Jeppsson B, Westrom B. Microbial manipulation of the rat mother changes bacterial colonization and alters properties of the gut in her offspring. *Am J Physiol Gastrointest Liver Physiol*. 2008;294(1):G148-154.

11. Nyangahu DD, Lennard KS, Brown BP, et al. Disruption of maternal gut microbiome during gestation alters offspring microbiome and immunity. *Microbiome*. 2018;6(1):124.
12. Noverr MC, Huffnagle GB. The 'microflora hypothesis' of allergic diseases. *Clin Exp Allergy*. 2005;35(12):1511-1520.
13. Herbst T, Sichelstiel A, Schar C, et al. Dysregulation of allergic airway inflammation in the absence of microbial colonization. *Am J Respir Crit Care Med*. 2011;184(2):198-205.
14. Olszak T, An D, Zeissig S, et al. Microbial exposure during early life has persistent effects on natural killer T cell function. *Science*. 2012;336(6080):489-493.
15. Roduit C, Frei R, Ferstl R, et al. High levels of butyrate and propionate in early life are associated with protection against atopy. *Allergy*. 2019;74(4):799-809.
16. Arrieta MC, Stiemsma LT, Dimitriu PA, et al. Early infancy microbial and metabolic alterations affect risk of childhood asthma. *Sci Transl Med*. 2015;7(307):307ra152.
17. Thorburn AN, McKenzie CI, Shen S, et al. Evidence that asthma is a developmental origin disease influenced by maternal diet and bacterial metabolites. *Nat Commun*. 2015;6:7320.
18. Trompette A, Gollwitzer ES, Yadava K, et al. Gut microbiome metabolism of dietary fiber influences allergic airway disease and hematopoiesis. *Nat Med*. 2014;20(2):159-166.
19. Vieira RS, Castoldi A, Basso PJ, Hiyane MI, Camara NOS, Almeida RR. Butyrate attenuates lung inflammation by negatively modulating Th9 cells. *Front Immunol*. 2019;10:67.
20. Thio CL, Chi PY, Lai AC, Chang YJ. Regulation of type 2 innate lymphoid cell-dependent airway hyperreactivity by butyrate. *J Allergy Clin Immunol*. 2018;142(6):1867-1883.e12.
21. Bookstaver PB, Bland CM, Griffin B, Stover KR, Eiland LS, McLaughlin M. A review of antibiotic use in pregnancy. *Pharmacotherapy*. 2015;35(11):1052-1062.
22. Conrad ML, Yildirim AO, Sonar SS, et al. Comparison of adjuvant and adjuvant-free murine experimental asthma models. *Clin Exp Allergy*. 2009;39(8):1246-1254.
23. Heimesaat MM, Bereswill S, Fischer A, et al. Gram-negative bacteria aggravate murine small intestinal Th1-type immunopathology following oral infection with Toxoplasma gondii. *J Immunol*. 2006;177(12):8785-8795.
24. Bereswill S, Escher U, Grunau A, et al. Pituitary adenylate cyclase-activating polypeptide—a neuropeptide as novel treatment option for subacute ileitis in mice harboring a human gut microbiome. *Front Immunol*. 2019;10:554.
25. Kozich JJ, Westcott SL, Baxter NT, Highlander SK, Schloss PD. Development of a dual-index sequencing strategy and curation pipeline for analyzing amplicon sequence data on the MiSeq Illumina sequencing platform. *Appl Environ Microbiol*. 2013;79(17):5112-5120.
26. Schloss PD, Westcott SL, Ryabin T, et al. Introducing mothur: open-source, platform-independent, community-supported software for describing and comparing microbial communities. *Appl Environ Microbiol*. 2009;75(23):7537-7541.
27. Pruesse E, Quast C, Knittel K, et al. SILVA: a comprehensive online resource for quality checked and aligned ribosomal RNA sequence data compatible with ARB. *Nucleic Acids Res*. 2007;35(21):7188-7196.
28. McMurdie PJ, Holmes S. phyloseq: an R package for reproducible interactive analysis and graphics of microbiome census data. *PLoS ONE*. 2013;8(4):e61217.
29. John-Schuster G, Hager K, Conlon TM, et al. Cigarette smoke-induced iBALT mediates macrophage activation in a B cell-dependent manner in COPD. *Am J Physiol Lung Cell Mol Physiol*. 2014;307(9):L692-706.
30. Wickham H. *ggplot2: Elegant graphics for data analysis*. New York, NY: Springer; 2009.
31. Kuster T, Zumkehr B, Hermann C, et al. Voluntary ingestion of antiparasitic drugs emulsified in honey represents an alternative to gavage in mice. *J Am Assoc Lab Anim Sci*. 2012;51(2):219-223.
32. Ensom MH, Decarie D, Lakhani A. Stability of vancomycin 25 mg/mL in ora-sweet and water in unit-dose cups and plastic bottles at 4 degrees C and 25 degrees C. *Can J Hosp Pharm*. 2010;63(5):366-372.
33. Heyne GW, Plisch EH, Melberg CG, Sandgren EP, Peter JA, Lipinski RJ. A simple and reliable method for early pregnancy detection in inbred mice. *J Am Assoc Lab Anim Sci*. 2015;54(4):368-371.
34. Russell SL, Gold MJ, Hartmann M, et al. Early life antibiotic-driven changes in microbiome enhance susceptibility to allergic asthma. *EMBO Rep*. 2012;13(5):440-447.
35. Yang X, Feng H, Zhan X, et al. Early-life vancomycin treatment promotes airway inflammation and impairs microbiome homeostasis. *Aging*. 2019;11(7):2071-2081.
36. Russell SL, Gold MJ, Willing BP, Thorson L, McNagny KM, Finlay BB. Perinatal antibiotic treatment affects murine microbiome, immune responses and allergic asthma. *Gut Microbes*. 2013;4(2):158-164.
37. Marx JO, Vudathala D, Murphy L, Rankin S, Hankenson FC. Antibiotic administration in the drinking water of mice. *J Am Assoc Lab Anim Sci*. 2014;53(3):301-306.
38. Reynolds PE. Structure, biochemistry and mechanism of action of glycopeptide antibiotics. *Eur J Clin Microbiol Infect Dis*. 1989;8(11):943-950.
39. Ebino KY. Studies on coprophagy in experimental animals. *Jikken Dobutsu*. 1993;42(1):1-9.
40. Cait A, Hughes MR, Antignano F, et al. Microbiome-driven allergic lung inflammation is ameliorated by short-chain fatty acids. *Mucosal Immunol*. 2018;11(3):785-795.

SUPPORTING INFORMATION

Additional supporting information may be found online in the Supporting Information section.

How to cite this article: Alhasan MM, Cait AM, Heimesaat MM, et al. Antibiotic use during pregnancy increases offspring asthma severity in a dose-dependent manner. *Allergy*. 2020;75:1979–1990. https://doi.org/10.1111/all.14234

Supporting Information

Supporting Information Figure S1

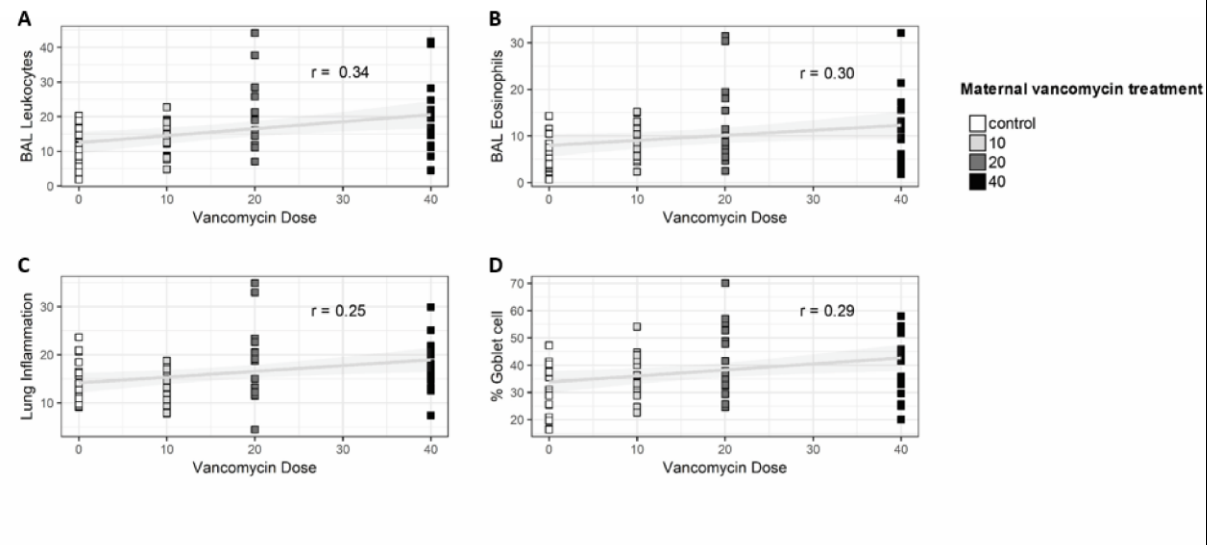

Supporting Information Figure S1: Increasing vancomycin dose during pregnancy correlates with increased asthma severity in allergic offspring.
Mothers were orally treated with 10, 20 or 40 mg/kg vancomycin + Ora-sweet syrup, or control (water + Ora-sweet syrup) from G8-17 and the offspring were subjected to an experimental asthma protocol. Increasing vancomycin dosage during pregnancy is correlated with increased: A) Leukocytes in allergic offspring BAL. B) Eosinophils in allergic offspring BAL. C) Offspring lung inflammation. D) Allergic offspring goblet cell percentage. Data information: Pearson's R correlation analysis with multiple comparisons corrected by the Benjamini-Hochberg method.

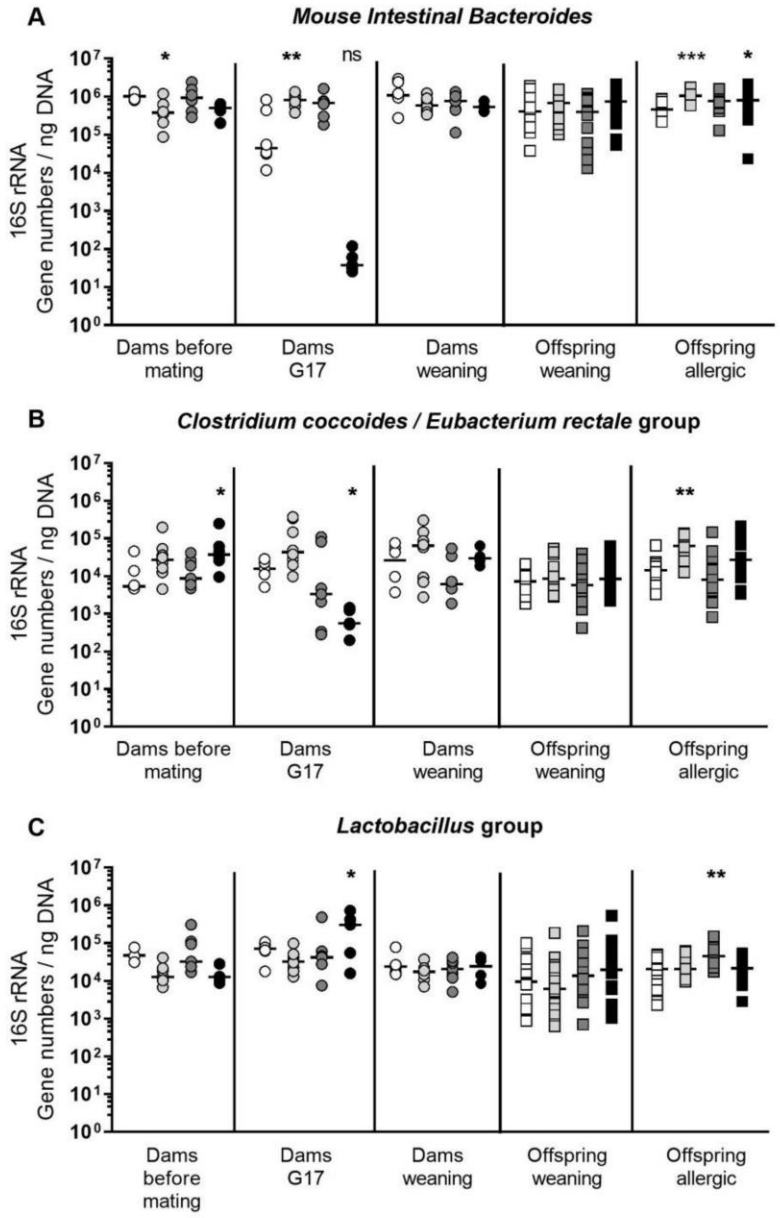

Supporting Information Figure S2: A kinetic of the fecal microbiome from mothers and pups.

Mothers were orally treated with 10, 20 or 40 mg/kg vancomycin + Ora-sweet syrup, or control (water + Ora-sweet syrup) from G8-17 and the offspring were subjected to an experimental asthma protocol at weaning. A comprehensive intestinal microbiome survey was performed to quantify the microbiome in individual fecal samples from mothers and offspring at several different time points: Maternal samples were collected before mating, at gestation day (G)17 and at weaning; offspring samples were collected at weaning and after allergy induction. The following bacterial groups are shown: A) *Mouse intestinal Bacteroides*. *B) Clostridium coccoides / Eubacterium rectale* group. D) *Lactobacillus* group. Data information: Medians (black bars) are shown, Maternal: control (n=6), 10 mg/kg, (n=8), 20 mg/kg (n=7), 40 mg/kg (n=6). Offspring: prenatal control (n=18), prenatal 10 mg/kg (n=19), prenatal 20 mg/kg (n=18), prenatal 40 mg/kg (n=16). Ssignificance is represented by *p<0.05, **p<0.01,

***p<0.001, one way ANOVA or Kruskal-Wallis test with Dunnett's multiple comparisons test (10, 20 and 40 compared against control).

Supporting Information Figure S3

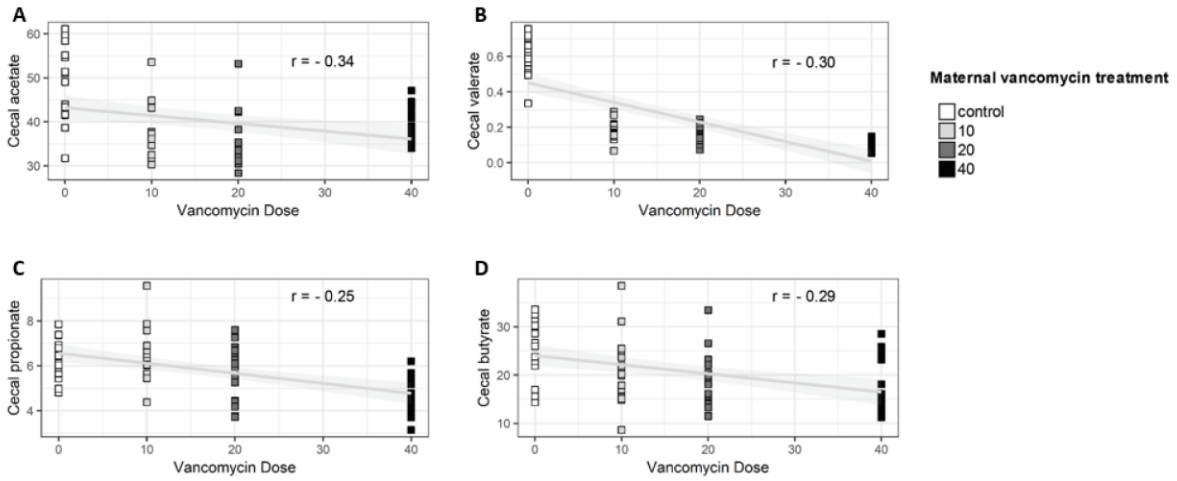

Supporting Information Figure S3: Increasing vancomycin dose during pregnancy correlates with decreased cecal SCFA levels in allergic offspring. Mothers were orally treated with 10, 20 or 40 mg/kg vancomycin + Ora-sweet syrup, or control (water + Ora-sweet syrup) from G8-17 and the offspring were subjected to an experimental asthma protocol. Increasing vancomycin dosage during pregnancy is correlated with increased: A) Allergic offspring cecal acetate, B) Allergic offspring cecal valerate, C) Allergic offspring cecal propionate, D) Allergic offspring cecal butyrate. Data information: Pearson's R correlation analysis with multiple comparisons corrected by the Benjamini-Hochberg method.

Supporting Information Figure S4

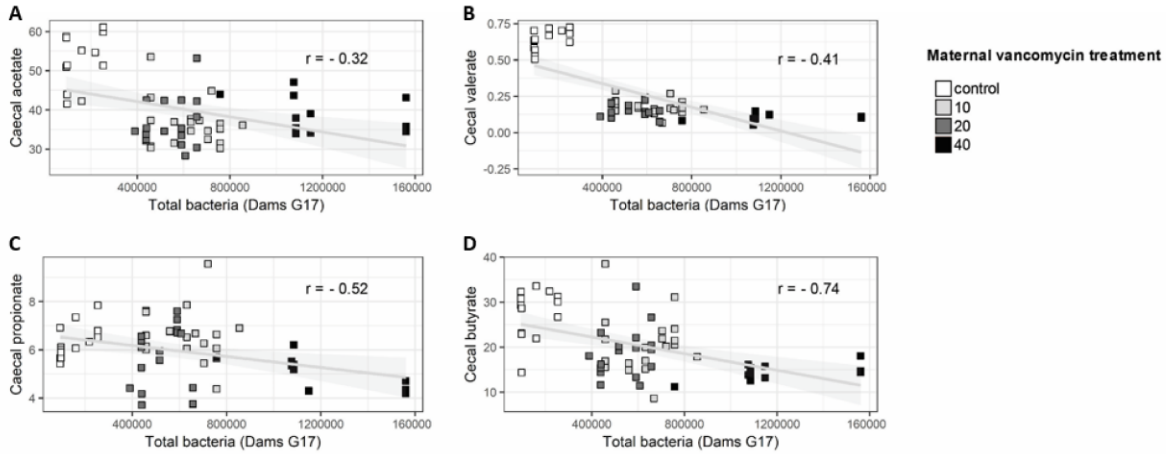

Supporting Information Figure S4: Increased total maternal fecal bacteria at G17 correlates with decreased cecal SCFA levels in the offspring.

Mothers were orally treated with 10, 20 or 40 mg/kg vancomycin + Ora-sweet syrup, or control (water + Ora-sweet syrup) from G8-17 and the offspring were subjected to an experimental asthma protocol. Increasing total bacteria in mothers at G17 is

correlated with increased: A) Allergic offspring cecal acetate, B) Allergic offspring cecal valerate, C) Allergic offspring cecal propionate, D) Allergic offspring cecal butyrate. Data information: Pearson's R correlation analysis with multiple comparisons corrected by the Benjamini-Hochberg method.

Supporting Information Table S1: Primer sequences for fecal microbiome analyses.

Target group	Amplicion size	Annealing (°C)	Sequence 5'-3'
Domain Bacteria (targets V3 region)	200	60	F: CGGYCCAGACTCCTACGGG R: TTACCGCGGCTGCTGGCAC
γ–Proteobacteria / Enterobacteriaceae	517	60	F: AAACTCAAATGAATTGACGG R: CTTTTGCAACCCACTCC
Bacteroides group, including *Prevotella, Porphyromonas*	418	59	F: GAAGGTCCCCCACATTG R: CAATCGGAGTTCTTCGTG
Mouse Intestinal Bacteroides	161	58	F: CCAGCAGCCGCGGTAATA R: CGCATTCCGCATACTTCTC
Enterococcus genus	337	55	F: ATCAGAGGGGGATAACACTT R: ACTCTCATCCTTGTTCTTCTC
Lactobacillus group including *Leuconostoc, Pediococcus, Aerococcus, Weissella*	341	58	F: CACCGCTACACATGGAG R: AGCAGTAGGGAATCTTCCA
Clostridium 16S rRNA cluster IV (*Clostridium leptum* subgroup)	239	50	F: GCACAAGCAGTGGAGT R: CTTCCTCCGTTTTGTCAA
Clostridium coccoides / Eubacterium rectale group	429	55	F: CGGTACCTGACTAAGAAGC R: AGTTT(C/T)ATTCTTGCGAACG
Bifidobacterium genus	243	58	F: TCGCGTC(C/T)GGTGTGAAAG R: CCACATCCAGC(A/G)TCCAC

Eur. J. Immunol. 2023;0:2350394 DOI: 10.1002/eji.202350394

European Journal of Immunology Clinical·Basic·Translational

Systems immunology

Basic

Research Article

Antibiotic use during pregnancy is linked to offspring gut microbial dysbiosis, barrier disruption, and altered immunity along the gut–lung axis

Moumen M. Alhasan[1], *Oliver Hölsken*[1,2,3,4], *Claudia Duerr*[1], *Sofia Helfrich*[1], *Nora Branzk*[1], *Alina Philipp*[1], *Dominik Leitz*[5], *Julia Duerr*[5], *Yahia Almousa*[6], *Gabriela Barrientos*[7], *William W. Mohn*[8], *Stefanie Gamradt*[9] *and Melanie L. Conrad*[1]

[1] Institute of Microbiology, Infectious Diseases and Immunology, Charité–Universitätsmedizin Berlin, Corporate Member of Freie Universität Berlin, Humboldt-Universität zu Berlin, Berlin Institute of Health, Berlin, Germany
[2] Charité–Universitätsmedizin Berlin, corporate member of Freie Universität Berlin and Humboldt Universität zu Berlin, Department of Anesthesiology and Intensive Care Medicine, Charité Campus Benjamin Franklin, Berlin, Germany
[3] German Rheuma Research Center Berlin (DRFZ), Mucosal and Developmental Immunology, Berlin, Germany
[4] Heidelberg Biosciences International Graduate School (HBIGS), Heidelberg University, Heidelberg, Germany
[5] Department of Pediatric Pulmonology, Immunology and Critical Care Medicine, Charité–Universitätsmedizin Berlin, Corporate Member of Freie Universität Berlin, Humboldt-Universität zu Berlin, Berlin Institute of Health, Berlin, Germany
[6] Laboratory of Molecular Tumor Pathology, Institute of Pathology, Charité–Universitätsmedizin Berlin, Corporate Member of Freie Universität Berlin, Humboldt-Universität Zu Berlin, and Berlin Institute of Health, Berlin, Germany
[7] Laboratorio de Medicina Experimental, Hospital Alemán. Consejo Nacional de Investigaciones Científicas y Técnicas (CONICET), Buenos Aires, Argentina
[8] Department of Microbiology and Immunology, Life Sciences Institute, University of British Columbia, Vancouver, British Columbia, Canada
[9] Department of Psychiatry and Psychotherapy, Campus Benjamin Franklin, Charité-Universitätsmedizin Berlin, Corporate Member of Freie Universität Berlin, Humboldt-Universität zu Berlin, Berlin Institute of Health, Berlin, Germany

Antibiotic use during pregnancy is associated with increased asthma risk in children. Since approximately 25% of women use antibiotics during pregnancy, it is important to identify the pathways involved in this phenomenon. We investigate how mother-to-offspring transfer of antibiotic-induced gut microbial dysbiosis influences immune system development along the gut–lung axis. Using a mouse model of maternal antibiotic exposure during pregnancy, we immunophenotyped offspring in early life and after asthma

Correspondence: Dr. Melanie L. Conrad
e-mail: conradml@gmail.com

induction. In early life, prenatal-antibiotic exposed offspring exhibited gut microbial dysbiosis, intestinal inflammation (increased fecal lipocalin-2 and IgA), and dysregulated intestinal ILC3 subtypes. Intestinal barrier dysfunction in the offspring was indicated by a FITC-dextran intestinal permeability assay and circulating lipopolysaccharide. This was accompanied by increased T-helper (Th)17 cell percentages in the offspring's blood and lungs in both early life and after allergy induction. Lung tissue additionally showed increased percentages of RORγt T-regulatory (Treg) cells at both time points. Our investigation of the gut–lung axis identifies early-life gut dysbiosis, intestinal inflammation, and barrier dysfunction as a possible developmental programming event promoting increased expression of RORγt in blood and lung $CD4^+$ T cells that may contribute to increased asthma risk.

Keywords: asthma · antibiotics · pregnancy · Th17 cell · gut–lung axis

Additional supporting information may be found online in the Supporting Information section at the end of the article.

Introduction

Antibiotic use during pregnancy and subsequent alterations to the maternal and offspring gut microbiomes, are associated with increased risk for the development of childhood asthma [1]. During infancy, the gut microbiota is established via a sequential process [2–4], and interactions between immune cells and intestine colonizing microbes are instrumental to educate the developing immune system [5, 6]. This early-life process of host–commensal interaction is critical for mucosal immunity and homeostasis, and subsequently, perturbations to the system can have long-term effects on immune function [7, 8]. Human studies have shown significant differences in the early-life gut microbiota composition between asthmatic and nonasthmatic children [2, 9], and germ-free mice have prominent immune system defects [10] and increased asthma severity compared to WT mice [11]. Collectively, these findings contribute to the Developmental Origins of Health and Disease Hypothesis, which identifies critical developmental "windows of opportunity" during the pre- and postnatal time periods in which programming of immune cell subsets can influence disease susceptibility later in life. Though epidemiological [12, 13] and proof-of-concept mouse models [14, 15] provide strong evidence for the association between antibiotic use during pregnancy, gut microbial dysbiosis, and increased offspring asthma susceptibility, the key players and pathways in this process are still yet to be elucidated. Since 25–40% of pregnant women use antibiotics [16, 17], it is increasingly important to understand these underlying mechanisms.

Considering the gut–lung axis, the intestinal microbiota is thought to have a far-reaching systemic influence that can also impact pulmonary immunity [18, 19]. Studies show that antibiotic-induced, gut bacterial dysbiosis transferred from the mother can induce intestinal inflammation and barrier dysfunction in murine progeny [20], allowing bacterial constituents such as lipopolysaccharide (LPS), access to the circulation [21]. There are several ways that the microbiota can influence intestinal inflammation, including dysregulation of short-chain fatty acid (SCFA) production, secretory immunoglobulin A (sIgA) concentrations, and innate lymphoid cell (ILC) function. Taken together, these candidate immune components can all also contribute to barrier dysfunction. SCFAs are anti-inflammatory metabolites produced by the microbiota during dietary fibre fermentation, and microbial dysbiosis results in decreased SCFA production due to the elimination of particular bacterial clades. Reduced concentrations of fecal acetate, propionate, and butyrate in early life are associated with barrier dysfunction [22] and increased asthma risk [2, 23]. Additionally, mouse models have shown that acetate can influence sIgA concentrations in the small intestine, which acts as a first line of defense at the mucosal surface by binding to commensal bacteria [24]. Dysregulation of sIgA binding specificity can disrupt barrier function [25] and was observed to precede asthma development in children [26].

In addition to soluble molecules, gut immune cells can also contribute to gut permeability in the inflamed intestine during microbial dysbiosis. Of particular interest in this regard are the ILCs, the innate counterparts of T cells that participate in the establishment of mucosal immunity [27]. Intestinal ILC populations in mice increase significantly 2–4 weeks after birth, corresponding to the rise in intestinal microbiota diversity that occurs during the weaning process [28]. In the case of the gut–lung axis, type 2 and 3 ILCs (ILC2 and ILC3) are of interest due to their respective roles in allergy and gut epithelial homeostasis [29]. Though ILCs are normally tissue resident, recent evidence shows that under inflammatory conditions, ILC2 subsets may migrate from the intestine to the lungs [28, 30]. In addition to this, ILC3s have been recently shown to "patrol" the intestinal barrier during times of inflammation, and cessation this movement was associated with intestinal barrier damage [31]. The mesenteric LNs provide a robust connection between the intestine and the circulation, and we propose that disruption of intestinal barrier function in early life may play a key role in susceptibility to allergic asthma [21, 22].

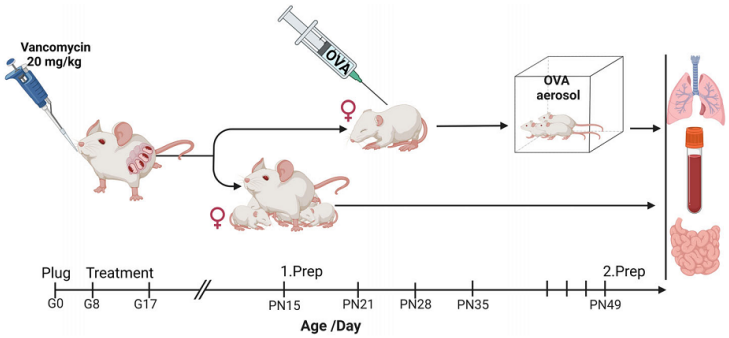

Figure 1. Experimental design. Pregnant mice were treated orally, daily from G8 to G17 with 20 mg/kg vancomycin plus Ora-Sweet syrup. Control mothers were treated orally with water and Ora-Sweet. At PN15, a group of pregnant mice and their pups were sacrificed for analysis of breast milk and offspring immune system development. At weaning (PN21), female offspring were subjected to an experimental asthma protocol consisting of subcutaneous sensitization with OVA at offspring age 21, 28, and 35, followed by asthma provocation with a 20-min daily OVA aerosol challenge at offspring age 46, 47, and 48. G = Gestation day, PN = Postnatal day, OVA = Ovalbumin.

Though there is much evidence that gut dysbiosis alters the developing mucosal immune system, there is still a paucity of information regarding how maternal antibiotic use during pregnancy influences offspring immunity and asthma susceptibility. To study this phenomenon, we recently developed a mouse model in which maternal treatment with the antibiotic vancomycin during pregnancy resulted in increased allergic asthma severity in the offspring [15]. The objective of this research is to use our newly developed mouse model to investigate how the transfer of antibiotic-induced maternal gut dysbiosis to the next generation influences gut permeability and immune system development in the progeny along the gut–lung axis. We hope to delineate important pathways that may be involved in the increased asthma susceptibility observed in our model. Further, we aim to assess the persistence of these immune changes by examining the influence of this early-life programming on susceptibility to allergic asthma in adult mice.

Results

Experimental design

We previously established a model in which treatment of pregnant mice with vancomycin resulted in increased asthma severity in the offspring [15]. For the present study, we treated pregnant mothers with vancomycin from gestation day (G)8-17, then conducted immunophenotyping of the offspring gut–lung axis both in early life (postnatal day-PN15) and after asthma induction PN49, shown in Fig. 1.

Vancomycin during pregnancy, offspring gut dysbiosis, and decreased fecal SCFA concentrations

To temporally assess changes in the maternal and offspring gut microbiota and SCFA concentrations after treatment with vancomycin during pregnancy, we collected fecal samples at the following time points: Maternal (before mating, at the end of antibiotic treatment at gestation day (G)17, and at weaning postnatal day (PN)21, offspring (at weaning at PN21, and after allergic asthma induction at PN49). The top 16 abundant clades identified by 16S rRNA sequencing showed that G17 pregnant mice had a marked gut dysbiosis on the last day of antibiotic treatment when compared with control pregnant animals. This was evidenced by a significantly increased abundance of the genera *Parabacteroides*, *Escherichia*, and *Sutterella*. G17 antibiotic-treated mothers also exhibited significantly decreased proportions in unclassified members of the families Lachnospiraceae and Rikenellaceae and the genera *Oscillospira, Odoribacter*, and *Prevotella*, shown in Fig. 2A and Supporting Information Table S1.

Analysis at weaning (PN21) confirmed the transgenerational transmission of gut bacterial dysbiosis, as the gut microbiota resembled each other in prenatal-control as well as prenatal-antibiotic mother-offspring groups. In antibiotic-treated mothers and offspring at PN21, we observed increased proportions of the genera *Akkermansia* and *Sutterella* compared to controls. The PN21 offspring also displayed increased proportions of *Bacteroides* and *Escherichia*. Proportions of Lachnospiraceae, *Oscillospira*, *Odoribacter*, and *Prevotella* decreased in mothers from G17 to PN21, and these decreases were also observed in their offspring. PN21 prenatal-antibiotic offspring also exhibited decreased proportions of Rikenellaceae and *Lactobacillus* (Fig. 2B and Supporting Information Table S1). Finally, prenatal-antibiotic adult allergic offspring exhibited gut dysbiosis until PN49. This was characterized by increased proportions of *Akkermansia*, *Bacteroides, Parabacteroides*, and *Sutterella*, and reduced *Odoribacter* and *Prevotella* compared to PN49 prenatal-control allergic offspring (Fig. 2C and Supporting Information Table S1). In addition to changes to the top 16 clades of the maternal and offspring gut microbiota, there were also several significant changes observed in less abundant bacterial groups including increased proportions of the genus *Blautia* (PN21 and PN49), Supporting Information Table S1. Decreased proportions of less abundant clades included the genera *Bilophila* (G17), *Butyricicoccus, Coprobacillus*, and *Dorea* (G17 and PN21), *Candidatus* (G17 and PN49) and *Clostridium, Coprococcus*, *Dehalobacterium*, *and Ruminococcus* (all time points), shown in Supporting Information Table S1.

Maternal antibiotic treatment during pregnancy also reduced the gut microbiota α-diversity (Shannon index) in both mothers

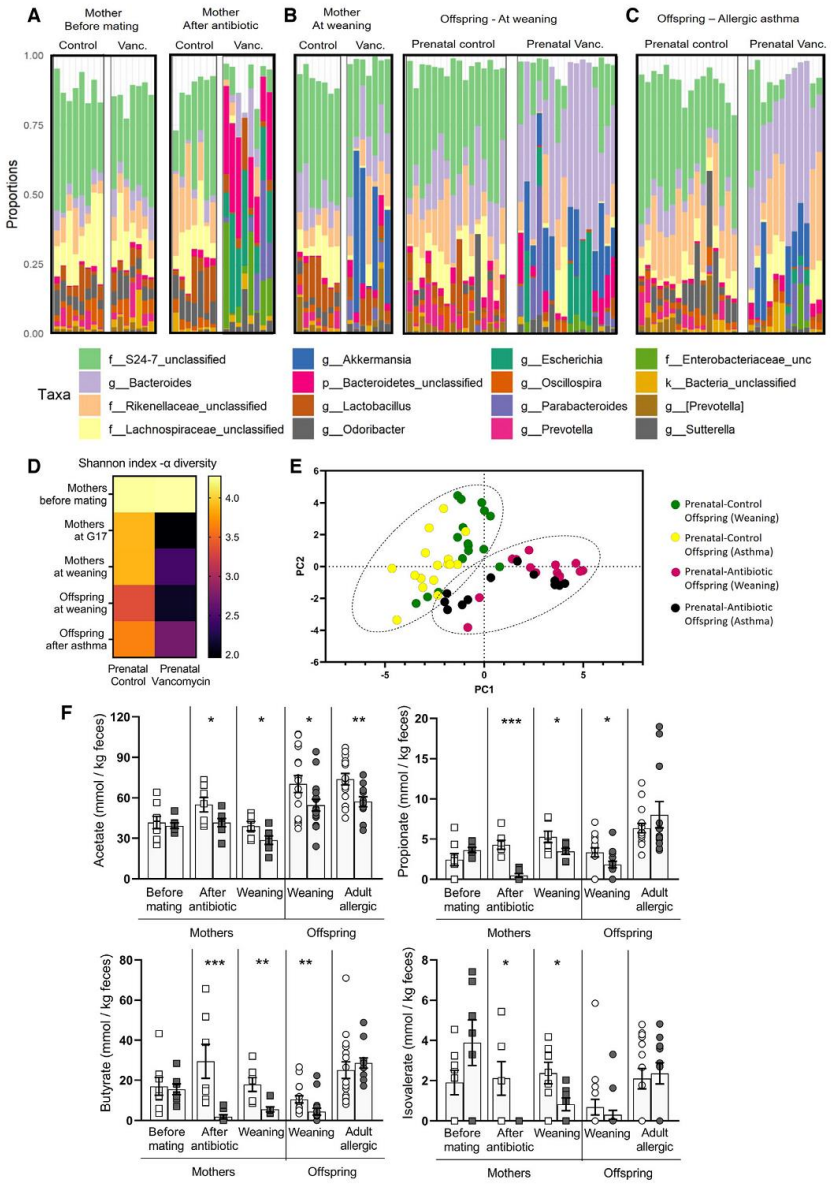

Figure 2. Antibiotic treatment during pregnancy alters the maternal and offspring gut microbiomes as well as fecal SCFA concentrations. Fecal samples were collected from: Mothers (n = 7) before mating, after antibiotic treatment at G17, and at weaning at PN21; Offspring (n = 16) at weaning PN21 and after allergic asthma induction at PN49 (prenatal-control n = 16, prenatal-antibiotic n = 12). **(a-c)** taxonomic bar plots of 16S rRNA gene frequencies in feces. White space on top of a bar represents lower-abundance taxa. Classification: k - kingdom; p - phylum; f - family; g - genus. Each bar represents one mouse. **(d)** Shannon index (α-diversity) of the fecal gut microbiota from mothers and offspring. **(e)** Principal component analysis comparing fecal bacterial communities in prenatal-control and prenatal-antibiotic offspring at weaning and after allergic asthma induction. **(f)** Short-chain fatty acid concentrations in maternal and offspring feces: acetate, propionate, butyrate, and isovalerate. Means ± SEM are shown. Data shown is pooled from two replicated experiments showing the same trends and significance is represented by $^{*}P < .05$, $^{**}p < .01$, $^{***}p < .001$. Student's t-test or Mann–Whitney test of antibiotic exposed animals compared against control animals at each specific time point.

and their offspring at all time points, shown in Fig. 2D. Principal component analysis of the offspring at weaning and after allergy induction revealed that prenatal-control offspring grouped together regardless of age and asthma induction; likewise, prenatal-antibiotic offspring grouped together at both of these time points. Antibiotic treatment during pregnancy was more of a determining factor for gut microbiome composition than asthma induction, showing a large shift in community composition when compared to prenatal-control offspring (Fig. 2E).

Finally, we sought to investigate if the antibiotic-induced changes to the intestinal bacterial community were associated with temporal changes in fecal SCFA concentrations. We showed that antibiotic treatment during pregnancy resulted in significantly reduced acetate, propionate, butyrate, and isovalerate in the feces of G17 antibiotic-treated mothers when compared with control mothers, shown in Fig. 2F. These decreased SCFA concentrations persisted until weaning at PN21 and were also observed in the offspring (with the exception of isovalerate). In adult allergic offspring at PN49, though propionate and butyrate levels in prenatal-antibiotic offspring returned to similar levels as prenatal-control offspring, acetate still remained significantly decreased in the antibiotic exposed group (Fig. 2F). In summary, maternal antibiotic treatment during pregnancy resulted in a low diversity, dysbiotic maternal gut microbiota that was transferred to the offspring. This was associated with significant reductions in fecal SCFA concentrations in the mothers and offspring that persisted until weaning and, in the case of acetate, into adulthood.

PN15 prenatal-antibiotic offspring have increased IgA, intestinal inflammation, and decreased weight

During the postnatal period, a dysbiotic maternal gut microbiota could influence maternal intestinal adaptations to lactation as well as breast milk composition, with possible effects on offspring weight, gut health, and subsequent immune system development. The maternal intestine adapts to the demands of lactation by increasing in length and area for nutrient absorption [32], thus, we first assessed if the dysbiotic maternal gut microbiota in our model was associated with changes to intestinal growth of lactating mothers at PN15. As shown in Fig. 3A and B, we observed no differences in intestinal length or villi-crypt length in prenatal-control versus prenatal-antibiotic treated mothers. Next, to investigate if maternal gut microbial dysbiosis was associated with changes in immunological components in the breast milk, we obtained milk from lactating mothers at PN15. Measurement of 23 cytokines in PN15 milk revealed that of the detectable cytokines (IL-1α, eotaxin, G-SCF, KC, RANTES, and TNF-α) no differences were observed in milk from lactating mothers, shown in Fig. 3C. Additionally, examination of SCFAs revealed that though acetate, propionate, and butyrate were measurable in the milk, there were no differences between prenatal-control and prenatal-antibiotic mothers, Fig. 3D.

Finding no changes in breast milk cytokines or SCFAs, we next examined if vancomycin treatment during pregnancy could influence maternal or offspring IgA concentrations. As shown in Fig. 3E, prenatal-antibiotic mothers had significantly higher serum IgA and milk sIgA concentrations compared to prenatal-control mothers. Further, we observed increased serum IgA concentrations and increased fecal sIgA concentrations in prenatal-antibiotic PN15 offspring (Fig. 3F). Intestinal inflammation at PN15 was evidenced by significantly increased fecal lipocalin-2 concentrations compared to controls, shown in Fig. 3G. Finally, we observed decreased weight in PN15 offspring from antibiotic-treated mothers as compared with the control group (Fig. 3H). These results show that maternal antibiotic use during pregnancy and the ensuing gut dysbiosis transferred to the offspring is associated with increased IgA concentrations and intestinal inflammation in both PN15 mothers and their offspring, as well as decreased offspring weight, compared to control animals.

Prenatal-antibiotic offspring have gut dysbiosis, barrier disruption, and changes in ILC3 subtypes

As intestinal inflammation could influence mucosal immune system development, we next immunophenotyped the offspring's small intestinal lamina propria (SI-LP), both in early life and after asthma induction. Flow cytometric analysis showed no changes in the absolute number of SI-LP CD45$^+$ intestinal leukocytes, however, increased percentages of these cells were observed in both PN15 and PN49 prenatal-antibiotic offspring compared with prenatal-control offspring, shown in Fig. 4A. Examination of Th cells revealed that CD4$^+$ T-cell percentages were increased in PN15 prenatal-antibiotic offspring and decreased in PN49 adult allergic offspring, (Fig. 4B). Though maternal antibiotic treatment did not influence the T-bet$^+$ or RORγt$^+$ percentages at PN15, GATA3$^+$ CD4 T cells were significantly decreased in prenatal-antibiotic offspring in comparison to controls (Fig. 4C). Examination of CD4$^+$ T-cell transcription factors in adult allergic offspring revealed that prenatal-antibiotic allergic offspring SI-LP had global reductions in T-bet, GATA3, and RORγt percentages. Reductions in the RORγt populations were observed in both RORγt$^+$ FoxP3$^-$ Th17 cells and RORγt$^+$ FoxP3$^+$ CD25$^+$ Tregs (Fig. 4C).

We additionally assessed SI-LP ILC populations, due to their importance in the maintenance of gut homeostasis and the establishment of gut lymphoid structures [33, 34]. ILC analysis revealed a reduction in total ILC percentages at both PN15 and PN49 in prenatal-antibiotic offspring. Though percentages of ILC subtypes ILC1 and ILC3 were not affected in general, ILC2 percentages were slightly increased in the small intestine of PN49 prenatal-antibiotic allergic offspring, Fig. 4D. Subpopulation analysis of SI-LP ILC3s showed significantly decreased percentages of NCR+ ILC3s (CCR6$^-$ T-bet$^+$), accompanied by significantly increased percentages of NCR- ILC3s (CCR6$^+$ T-bet$^-$), shown in Fig. 4E, mimicking disproportions already observed in inflammatory bowel diseases [35].

Finally, to assess if the intestinal inflammation observed in prenatal-antibiotic PN15 offspring was associated with changes in

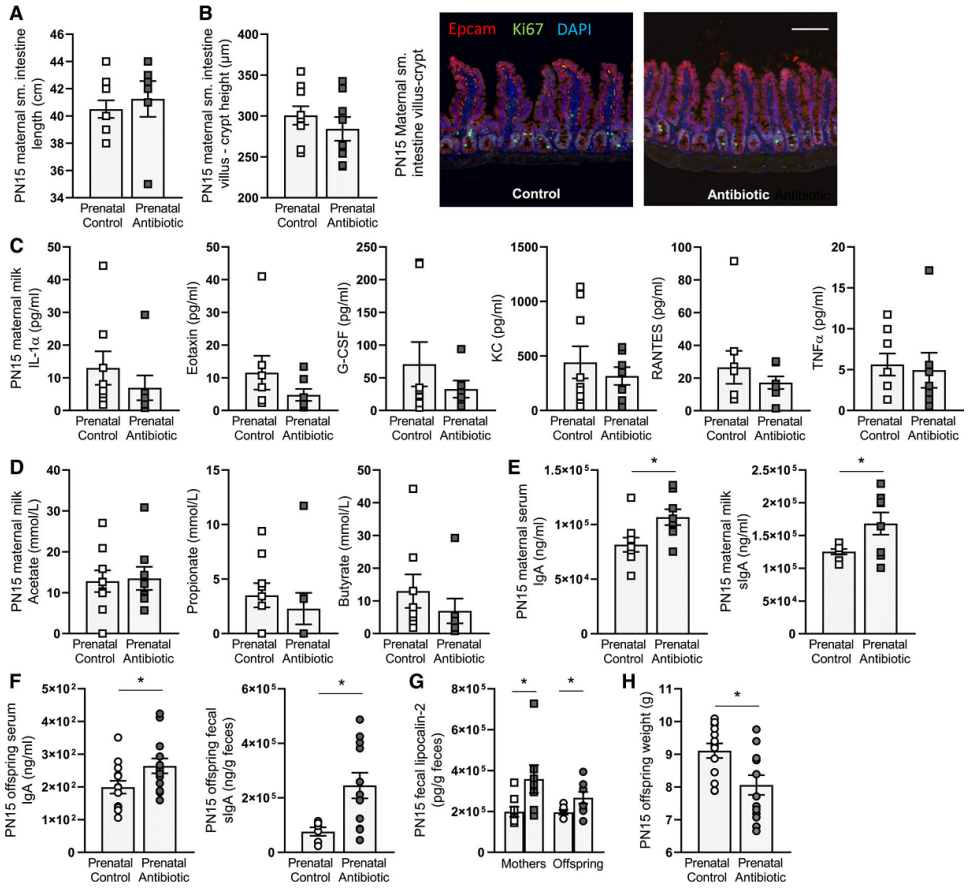

Figure 3. Antibiotic treatment during pregnancy is associated with increased IgA concentrations, intestinal inflammation, and decreased offspring weight during lactation at PN15. (**a**) Maternal small intestine length during lactation. (**b**) Maternal small intestine villus–crypt length during lactation and representative Epcam, Ki67 and DAPI staining. Scale bar = 100 μm. (**c**) Measurable cytokines in breastmilk from control- and antibiotic-treated mothers: IL-1α, eotaxin, G-CSF, KC, RANTES, and TNF-α. (**d**) SCFA concentrations in maternal milk from control and antibiotic-treated animals: Acetate, propionate, and butyrate. (**e**) IgA concentrations in maternal serum and milk (sIgA) from control and antibiotic treated animals. (**f**) Serum IgA and fecal sIgA concentrations of PN15 prenatal-control and prenatal-antibiotic offspring. (**g**) Fecal lipocalin-2 concentrations from control and antibiotic mothers and their offspring. (**h**) Weight of PN15 offspring. **a-e** Mothers: Prenatal-Control n = 9, Prenatal-Antibiotic n = 8. (**f and h**) Offspring: prenatal-control and prenatal-antibiotic n = 13. **g** All groups n = 8. Means ± SEM are shown. Data shown is pooled from two replicated experiments showing the same trends and significance. Significance is represented by $^*p < .05$. Student's *t*-test or Mann–Whitney test of antibiotic exposed compared against control at each specific time point.

gut barrier integrity, we next performed a FITC-dextran intestinal permeability assay. As shown in Fig. 4F, PN15 prenatal-antibiotic offspring serum contained significantly higher concentrations of FITC-dextran, indicating barrier disruption in these animals compared to prenatal-control animals. Allergic offspring were also tested in this manner, and though there was a trend towards increased serum FITC-dextran in the serum of allergic offspring from antibiotic-treated mothers, it was not significant (Fig. 4F). Taken together, these results show that early-life gut microbial dysbiosis is associated with increased inflammatory markers on SI-LP ILC3 subsets, accompanied by a significant reduction in gut barrier integrity in prenatal-antibiotic offspring in early life.

Measurable endotoxin and increased Th17-cell percentages in prenatal-antibiotic offspring blood

Since maternal vancomycin treatment led to the expansion of Gram-negative bacterial clades, increased intestinal inflammation, and reduced gut barrier integrity, we next assessed

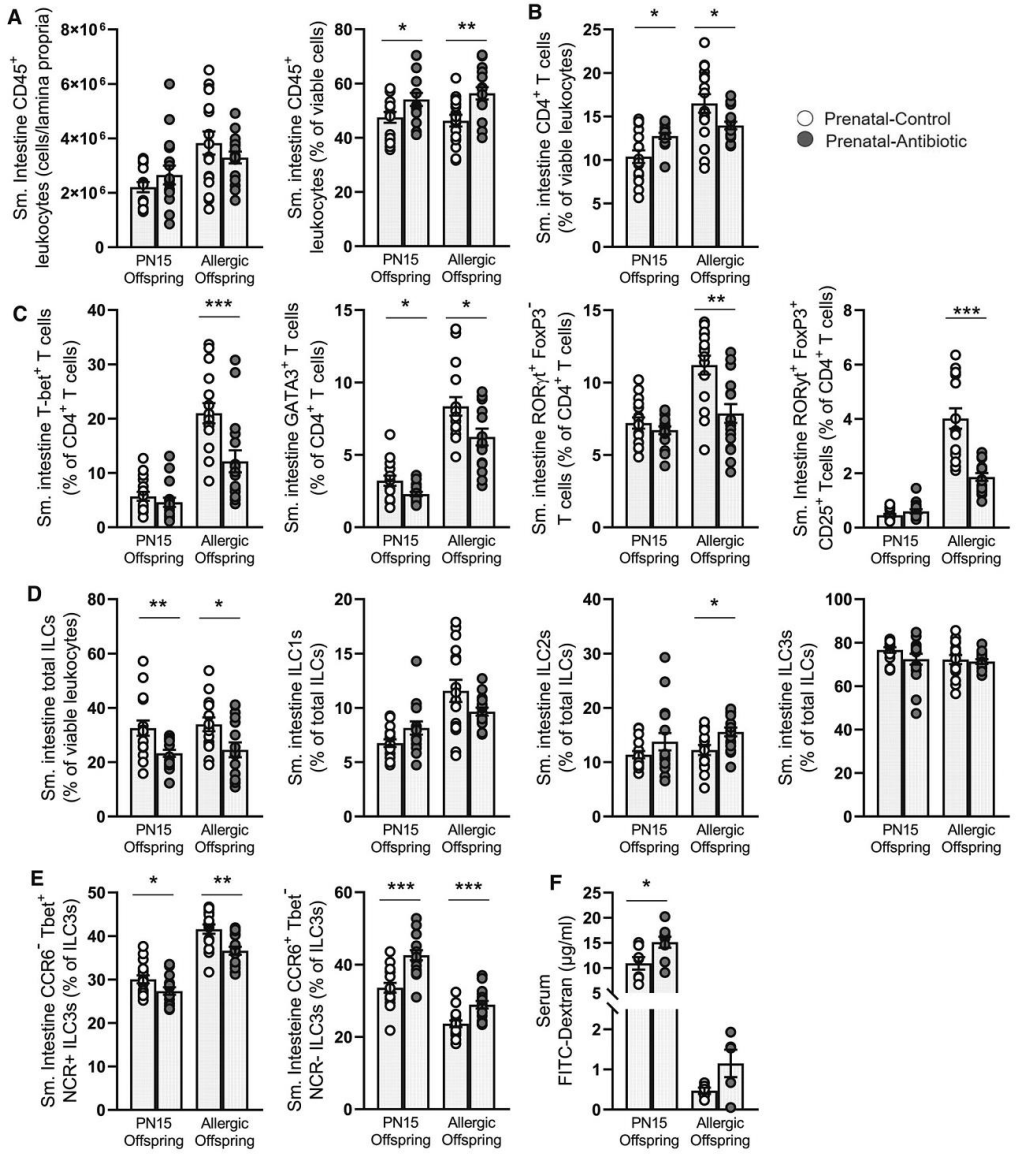

Figure 4. Antibiotic use during pregnancy is associated with significant changes to ILC3 subsets in the SI-LP and gut barrier disruption in early life. Comparison of prenatal-control versus prenatal-antibiotic offspring in early life at PN15 and after allergy induction at PN49. (**a**) Absolute number and percentage of $CD45^+$ leukocytes. (**b**) Percentages of: $CD4^+$ T cells (from viable leukocytes). (**c**) $T\text{-}bet^+$, $GATA3^+$, $ROR\gamma t^+$ $FoxP3^-$ (Th17) cells and $ROR\gamma t^+$ $FoxP3^+$ $CD25^+$ ($ROR\gamma t$ Tregs) (from $CD4^+$ T cells). (**d**) Percentages of: total ILCs (from viable leukocytes) and ILC1s, ILC2s, and ILC3s (from total ILCs). (**e**) CCR^- $T\text{-}bet^+$, NCR+ ILC3s (percent of ILC3s), CCR^+ $T\text{-}bet^-$, NCR- ILC3s (percent of ILC3). (**f**) Serum FITC concentration as measured by a FITC-dextran intestinal permeability assay. (**a-e**) All groups n = 16. (**f**) PN15 Prenatal-control and PN15 Prenatal-antibiotic n = 8, allergic offspring all groups n = 5 Mean ± SEM are shown. Data shown is pooled from two replicated experiments showing the same trends and significance. Significance is represented by $^*p < .05$, $^{**}p < .01$, $^{***}p < .001$. Student's *t*-test or Mann–Whitney test of antibiotic exposed compared against control at each specific time point.

the possibility that microbial compounds, such as LPS, might have been disseminated to the circulatory system. As shown in Fig. 5A, prenatal-antibiotic G17 mothers and PN15 (but not PN49) offspring had significant concentrations of LPS in the blood when compared with prenatal-control samples. As this observed LPS increase could also influence blood immune cell populations, we next performed a flow cytometric analysis of lymphoid and myeloid cell types in the blood. Examination of circulating immune cell populations revealed fewer leukocytes in prenatal-antibiotic offspring at PN15, although no differences were observed in CD45 cell percentages. These differences resolved in adult offspring after asthma induction at P49, Fig. 5B. Myeloid cell analysis revealed no differences in the percentage of Ly6C^{hi} monocytes, Ly6G^{+} neutrophils, or SiglecF^{+} eosinophils (Fig. 5C), however, MFI analysis revealed significantly increased expression of eosinophil activation markers SiglecF and CD11b in prenatal-antibiotic offspring blood, both during early life and after allergy induction (Fig. 5D). Finally, supporting the fact that LPS is a known inducer of the transcription factor RORγt and the differentiation of naïve CD4^{+} T cells into Th17 cells [36], transcription factor analysis revealed though there were no changes in the total CD4^{+} T-cell population (Fig. 5E) or the T-bet and GATA3 subpopulations (Fig. 5F), we observed a marked increase in Th17 cells in the blood of prenatal-antibiotic offspring compared with prenatal-control offspring at both PN15 and PN49 (Fig. 5F). No changes were observed in the CD4^{+} FoxP3^{+} CD25^{+} population at any time point and RORγt Tregs were not detectable in the blood of any group (Supporting Information Figure S1). This analysis demonstrates that offspring from antibiotic-treated mothers have circulating LPS in early life, which is in turn associated with a sustained increase in Th17 cell percentages in the blood of offspring from early life until adulthood.

Prenatal-antibiotic offspring lungs exhibit increased RORγt T cells and more severe asthma

To complete our assessment of the gut–lung axis, we immunophenotyped lung tissue from offspring at both the early life (PN15) and allergic adult (PN49) time points. As shown in Fig. 6A, lung tissue from PN15 prenatal-antibiotic offspring had significantly higher leukocyte numbers compared with prenatal-control offspring. No differences were seen in absolute leukocyte numbers in allergic animals or leukocyte cell percentages in any of the groups. Examination of lung tissue ILCs revealed that though there were no differences in total ILC percentages at PN15 or PN49, prenatal-antibiotic allergic offspring had significantly increased ILC2 percentages (Fig. 6B). Analysis of myeloid cells revealed that only neutrophils were significantly reduced in prenatal-antibiotic offspring at PN15. As expected, allergic offspring from antibiotic-treated mothers had increased lung tissue macrophages and eosinophil percentages compared to allergic offspring from control mothers, indicating a more severe asthma phenotype (Fig. 6C). Finally, examination of T-cell populations in the lung tissue revealed a significant increase in both Th17 and RORγt^{+} Treg percentages in the offspring lung tissue, both in early life and after allergy induction. No differences were seen in CD4^{+}, T-bet^{+}, or GATA3^{+} T-cell percentages (Fig. 6D). Confirming our previous observations of increased asthma severity in prenatal-antibiotic offspring [15], we also demonstrate increased airway reactivity (Supporting Information Fig. S2A), increased eosinophils, and lymphocytes in the bronchoalveolar lavage (BAL) (Supporting Information Fig. S2B) as well as increased serum total IgG, OVA-specific IgG1, and OVA-specific IgE in prenatal-antibiotic offspring compared to their prenatal-control counterparts (Supporting Information Fig. S2C).

Discussion

Using a mouse model, we show that antibiotic use during pregnancy resulted in maternal gut microbial dysbiosis and decreased SCFA concentrations that were also observed in the next generation. Offspring gut dysbiosis in early life was associated with decreased fecal SCFA concentrations as well as increased IgA and lipocalin-2 concentrations, which is indicative of intestinal inflammation [25, 37]. Decreased gut barrier integrity in PN15 prenatal-antibiotic offspring was shown using both a FITC-dextran permeability assay and measurement of significant levels of LPS in offspring serum. Finally, increased CD4^{+} RORγt^{+} T-cell percentages were found in offspring blood and lung tissue in both early life and after allergy induction. We propose that the dysbiotic gut microbiota, intestinal inflammation, and disruptions to intestinal integrity that we observed during early life, reveal a potential gut–lung axis pathway that merits further investigation with regard to the offspring asthma severity previously observed in this model [15].

During the postnatal time period, the maternal gut microbiota, breast milk sIgA, and SCFAs play a major role shaping bacterial populations in the neonatal intestine. Breast milk sIgA promotes intestinal homeostasis in the progeny by directly binding to bacteria [38], and it was shown in 12-month-old children that decreased binding to *Bacteroides* and *E. coli* in the gut was associated with increased childhood asthma risk [26]. Increased fecal sIgA concentrations are a marker of intestinal inflammation and barrier dysfunction [25], and in our model, we observed increased fecal sIgA in the progeny of antibiotic-treated mothers. With regard to intestinal integrity, mouse studies demonstrate that disruption of IgA was associated with Proteobacteria overgrowth and inflammation [39], as well as translocation of bacteria across the intestinal epithelium in nursing mice [40]. We also observed Proteobacteria overgrowth and increased IgA in the neonatal intestine, accompanied by increased fecal lipocalin-2 concentrations suggesting intestinal inflammation. Furthermore, sIgA binding to commensal bacteria is promoted by the SCFA acetate [24, 41] and we also observed decreased fecal acetate in our prenatal-antibiotic offspring. Since evidence suggests that mice with low SCFA concentrations have impaired antibody responses [42], examination of IgA-commensal bacteria binding specificity warrants further study. Taking into account this information, we propose that the

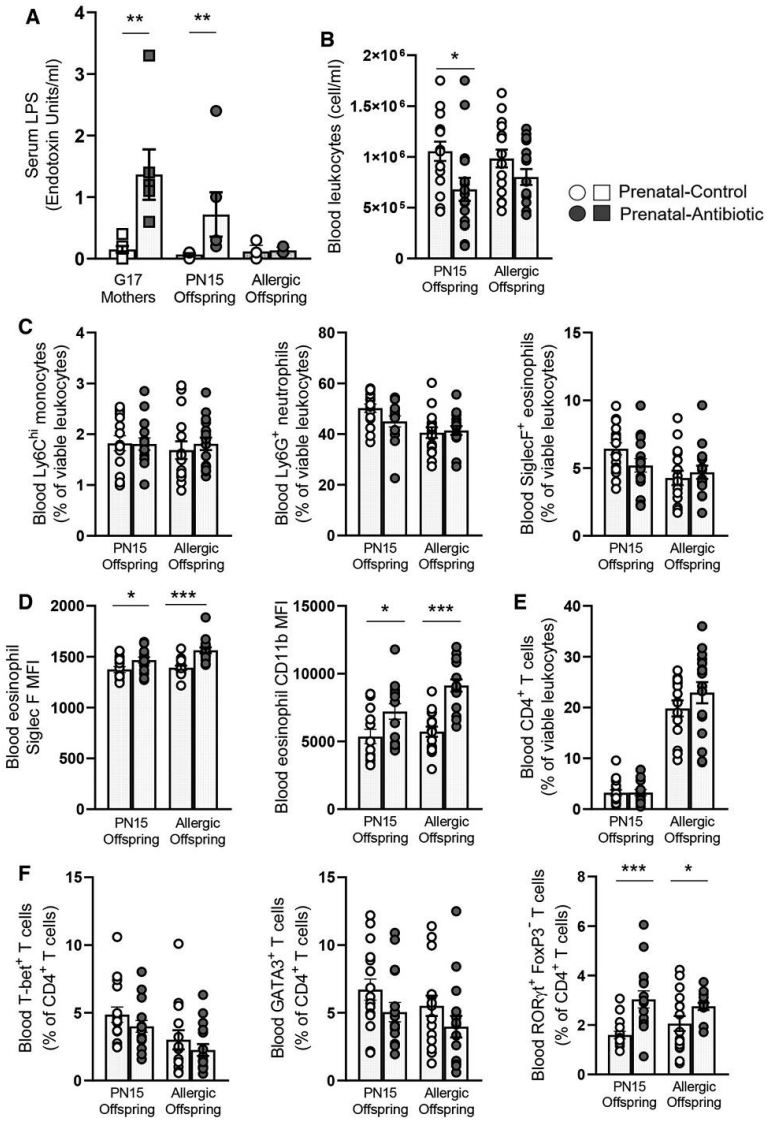

Figure 5. Antibiotic use during pregnancy is associated with increased serum LPS concentrations and increased RORγt T-cell percentages in the blood of prenatal-antibiotic offspring. Comparison of prenatal-control versus prenatal-antibiotic offspring in early life at PN15 and after allergy induction at PN49. (**a**) Maternal and offspring serum LPS measurements. (**b**) Absolute numbers of leukocytes. (**c**) Percentages of Ly6C^{hi} monocytes, Ly6G^{+} neutrophils and SiglecF^{+} eosinophils (from viable leukocytes). (**d**) MFI of SiglecF and CD11b on eosinophils. (**e**) Percentages of: CD4^{+} T cells (from viable leukocytes). (**f**) T-bet^{+}, GATA3^{+}, and RORγt^{+} FoxP3^{-} (Th17) cells (from CD4^{+} T cells). (**a**) Prenatal-control and prenatal-antibiotic mothers and offspring n = 6. (**b-f**) Prenatal-control offspring and prenatal-antibiotic offspring n = 16. Mean ± SEM are shown. Data shown is pooled from two replicated experiments showing the same trends. Significance is represented by $^{*}p < .05$, $^{**}p < .01$, $^{***}p < .001$. Student's *t*-test or Mann–Whitney test of antibiotic exposed compared against control at each specific time point.

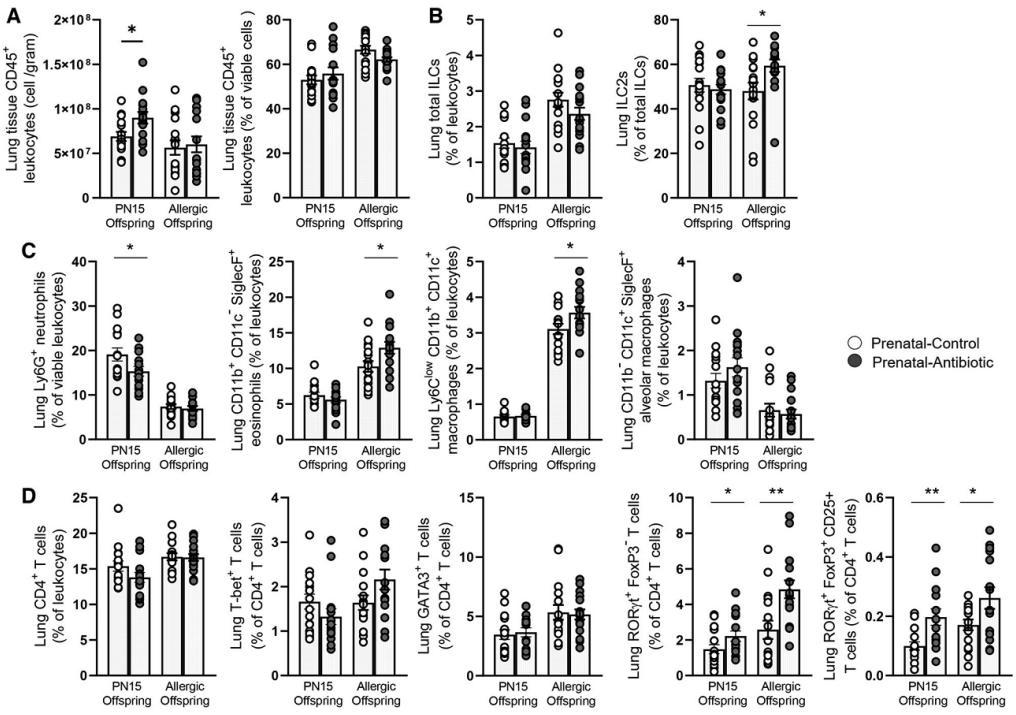

Figure 6. Antibiotic use during pregnancy is associated with altered lung tissue immune cell populations in PN15 and adult allergic offspring. (**a**) Absolute numbers and percentages of CD45+ leukocytes. (**b**) Total ILC percentages (% of leukocytes), ILC2 percentages (% of total ILCs). (**c**) Percentages of neutrophils, eosinophils, macrophages, and alveolar macrophages (from viable leukocytes). (**d**) Percentages of: CD4+ T cells (from viable leukocytes), as well as T-bet+, GATA3+, RORγt+ FoxP3- (Th17) cells, and RORγt+ FoxP3+ CD25+ (RORγt Tregs) (from CD4+ T cells). (**a-d**) Prenatal-control n = 16, Prenatal-antibiotic n = 16. Data shown is pooled from two replicated experiments showing the same trends and significance. Mean ± SEM are shown. Significance is represented by $^{*}p < .05$, $^{**}p < .01$, $^{***}p < .001$. Student's *t*-test or Mann—Whitney test of antibiotic exposed compared against control at each specific time point.

increased relative abundance of Proteobacteria observed in our model combined with decreased acetate and increased sIgA concentrations contribute to intestinal inflammation in early life.

An additional interesting finding from our study was the changes in ILC3 populations observed in prenatal-antibiotic compared to prenatal-control offspring. We observed dysregulation of ILC3 subtypes, characterized by increased NCR- ILC3 (CCR6+, T-bet-) and a concurrent decrease in NCR+ ILC3 (CCR6-, T-bet+) percentages at both time points. ILC3s are essential for maintaining mucosal homeostasis in the intestine [29], and we propose that a combination of intestinal inflammation and alteration of ILC3 subsets may have contributed to a disrupted intestinal barrier in early life. Indeed, an FITC-dextran intestinal permeability assay revealed loss of intestinal integrity in prenatal-antibiotic offspring, and further detection of LPS in the circulation of these offspring indicates the systemic dissemination of Gram-negative microbial components from the dysbiotic intestine. Increased concentrations of bacterial components in the blood have previously been associated with gut microbial dysbiosis in both humans [43] and mice [44, 45]. LPS is a strong mediator of immunity and is associated with several systemic inflammatory effects, the most prominent of which is the generation of CD4+ RORγt+ T cells [46, 47]. We propose that systemic LPS dissemination from a disrupted intestinal barrier in early life is an important pathway that merits further study.

In our model, examination of lung tissue from prenatal-antibiotic offspring showed increased CD4+ RORγt+ T cells (both Th17 and FoxP3) and decreased neutrophil percentages in early life. After allergy induction in these animals, we observed a more severe asthma phenotype, evidenced by increased eosinophil and ILC2 percentages, and significantly higher airway reactivity compared to allergic prenatal-control animals. This is in line with our previous results demonstrating more severe asthma in offspring from mothers treated with antibiotics during pregnancy [15]. Though allergic responses are primarily associated with Th2 cells, recent studies indicate that Th17 cell responses are more interconnected in the allergic process than previously thought [48]. Th17 cells are associated with increased asthma severity in human

patients [49] and Na et al. (2018) recently demonstrated that mice deficient in either IL-17A, IL-17F, or RORγt showed attenuated Th2 and Th17 responses in a mouse model of allergic asthma [50]. It was further shown *in vitro* that blockade of RORγt limited the differentiation of human naïve CD4 T cells into Th2 or Th17 cells, indicating a close linkage between these cell types . The increased Th17 and RORγt Treg percentages observed in the blood and lung tissue of prenatal-antibiotic offspring indicate a possible, previously underestimated participation of these cell types in the establishment of lung mucosal immunity in early life and contribution to asthma exacerbation.

In summary, we show that maternal treatment with antibiotics during pregnancy resulted in gut microbial dysbiosis that was transferred to the next generation. Offspring gut microbial dysbiosis was associated with dysregulation of immunity along the gut–lung axis in early life, beginning with intestinal inflammation and gut barrier disruption, LPS dissemination to the circulation and cumulating in significantly increased percentages of Th17 cells in the blood and Th17 cells and RORγt Tregs in the lung. We propose that these processes represent a major pathway for future research regarding how antibiotics during pregnancy can contribute to increased offspring asthma susceptibility.

Materials and Methods

Animals

A 12-week-old BALB/c mice were obtained from Janvier Labs (Le Genest-Saint-Isle).and housed under specific pathogen-free conditions, five animals per cage, with a 12/12 light/dark cycle and food and water available ad libitum. The animal experiment was approved by the Berlin authorities (Landesamt für Gesundheit und Soziales-LAGeSo) and performed according to German and international regulatory guidelines.

Experimental design

Mice were mated, and the presence of a vaginal plug was denoted as gestation day G(0) of pregnancy. From G8–G17, pregnant mice received a daily oral dose of the antibiotic vancomycin (Sigma–Aldrich, 20 mg/kg body weight) mixed with Ora-Sweet syrup (Paddock Laboratories). The mixture was freshly prepared (25 μL vancomycin solution + 15 μL Ora-Sweet) and a 40 μL volume was delivered through drops from a pipet that were voluntarily consumed by the mice. Control mice were sham treated with water and Ora-Sweet. At PN15, breast milk was collected from the mothers, then mothers and pups were euthanized for organ collection. The remaining pups were weaned from their mothers at PN21 and female pups were subjected to an adjuvant-free experimental asthma protocol [51]. Sensitization was performed at offspring age 21, 28, and 35 days, by subcutaneous injection of 10 μg OVA VI (Sigma) in 200 μL PBS. Asthma exacerbation in the lungs was provoked by a 20-min daily aerosol challenge with 1% OVA V (Sigma) at offspring age 46, 47, and 48. On day 49 of the protocol, airway reactivity was measured in allergic animals, then they were euthanized for organ harvesting and analysis. The protocol is shown in Fig. 1.

Fecal intestinal microbiota, SCFA, and lipocalin-2 analyses

16S rRNA sequencing

To assess the microbial composition of the maternal and offspring gut microbiota, fecal samples were collected at the following time points: maternal (before mating, after antibiotic treatment at G17, and at weaning PN21), offspring at weaning (PN21) and after allergic asthma induction (PN49). Feces were flash frozen with liquid nitrogen and stored at −80°C until analysis. 16S rRNA sequencing was performed by Microbiome Insights Inc. as per the following procedure. A PowerSoil for KingFisher kit (MO Bio) was used to extract DNA, then 16S rRNA gene fragments from the V4 region were amplified with the following bar-coded primers (5′-3′): fwd: GTGCCAGCMGCCGCGGTAA, rev: GGACTACHVGGGTWTCTAAT. PCR amplicons were pooled and diluted to 20 ng/mL and a MiSeq 2000 bidirectional Illumina sequencing and Cluster Kit v4 (Macrogen) was used for sequencing. A TruSeq DNA Sample Prep v2 Kit (Illumina) was used for Library preparation (100 ng DNA/sample) and Qubit (Thermo Fisher Scientific) was used to quality check and quantify the library. A modified MOTHUR standard operating procedure was used to trim, quality filter, and cluster sequence data into operational taxonomic units (97% identity) [52]. Per sample, an average of 31 554 quality-filtered reads were generated, totaling 8631 operational taxonomic units that were taxonomically annotated with the SILVA database [53]. Phyloseq was used to generate global community structure comparisons [54].

Analysis of maternal and offspring fecal SCFA concentrations

Fecal samples from the previously mentioned time points were also analyzed for SCFA concentrations. Measurements were performed using an HP 5890 series II gas chromatograph (Hewlett-Packard) with an HP-20 M column and a flame ionization detector. Feces were diluted and centrifuged, then the supernatant was mixed with 1 M NaOH, 0.36 M $HClO_4$, and 2-ethylbutyric acid as an internal standard. This was then lyophilized overnight, then redissolved in 5 M formic acid plus 400 μL acetone. The resulting mixture was centrifuged, then 1 mL of supernatant was injected into the gas chromatograph.

Lipocalin-2 analysis

PN15 fecal samples were weighed, homogenized, and resuspended in 1 mL PBS + 0.05% TWEEN20, then centrifuged at 12 000 rpm for 10 min. Supernatant was diluted 1:100 and analyzed using a lipocalin-2 ELISA (BioLegend) according to the manufacturer's instructions.

Collection of PN15 maternal milk

To allow for milk accumulation in PN15 lactating mothers, offspring were separated from their mothers 4 h prior to milk harvest. Lactating mice from control- and antibiotic-treated groups were injected intraperitoneally with 1 IU of oxytocin (Sigma–Aldrich) in 50 μL PBS to stimulate milk flow. For milk collection, mice anesthetized with ketamine and xylazine were placed on a heating pad and breast milk was collected for 20 min using a specially constructed breast pump, protocol adapted from Ref. [55]. After milk collection, mother mice were sacrificed, blood was collected from the orbital sinus and serum was frozen at −80°C.

Collection of PN15 and PN49 offspring tissues

Blood samples

Offspring were euthanized and blood samples were collected from the orbital sinus of either PN15 or PN49 allergic offspring. One blood sample was used immediately for flow cytometry (undergoing RBC lysis, followed by staining with antibodies) and one sample was centrifuged for serum isolation, then stored at −80°C.

Small intestine

Small intestine lamina propria was harvested according to a protocol adapted from Ref. [56]. In short, the small intestine was dissected (removing the Peyer's patches), cleaned, cut into pieces, and digested in Hanks balanced salt solution with collagenase D (Sigma), DNase1 (Roche), dispase (Sigma), and FBS (Sigma). Immune cells were purified on a Percoll gradient and subsequently stained and analyzed by flow cytometry as previously described [56].

Lungs

In PN49-allergic offspring, BAL was performed via a tracheal canula using 1 mL of PBS, containing a complete protease inhibitor cocktail (Roche). Both PN15 and PN49 lungs were removed and digested following the protocol from Ref. [57]. Briefly, lungs were cut into pieces and digested with collagenase and DNase 1 (Roche) in RPMI medium with FBS. After digestion and straining, cells were subjected to red cell lysis and then analyzed by flow cytometry.

Small intestine, blood, and lung flow cytometry in PN15 and PN49 offspring

Intestine staining antibodies

Isolated cells from the small intestine were stained with a Zombie aqua viability kit (BioLegend) and then with the following antibodies (CCR6, CD4, IL-17RB, CD25, FoxP3, CD45, CD127 (IL-7Rα), EOMES, GATA3, Ki-67, KLRG1, Live dead, NKp46, RORγt, ST2, T-bet, CD90.2 and lineage (CD3e, CD5, CD19, Gr1, TCRβ, TCRγδ). CD4 T cells were checked later for CD3 positivity.

Blood staining antibodies

After RBC lysis, blood leukocytes were stained with a Zombie aqua viability kit (BioLegend) and then with the following antibodies for lymphocytes (B220, CD3, CD4, CD8), myeloid cells (Ly6C, Ly6G, CD11b, CD11c, SiglecF), and transcription factors (RORγt, T-bet, GATA3, and FoxP3).

Lung staining antibodies

After staining with a viability dye, samples were stained with antibodies for myeloid cells (CD11b, CD11c, CD45, CD49b, FcεR1α, Ly6C, F4/80, Ly6G and SiglecF), ILC2s (CD45, CD90.2, GATA3, KLRG1, RORγt, ST2), and lineage (B220, CD3, CD4, CD11b, CD11c, CD19, FcεR1a, Ly6G, NK1.1, TCRβ, TCRγδ, TER119). Lungs were also stained with the previously mentioned lymphoid and transcription factor blood panels.

Stained cells were analyzed using a BD LSR Fortessa X-20 (BD Biosciences) or MACSQuant Analyzer 10 (Miltenyi Biotech). Gating strategies for all panels are located in Supporting Information Fig. S3–5.

BAL and differential cell counts in PN49 allergic offspring

BAL was centrifuged, the supernatant was stored at −80°C, and total leukocytes were counted with a Neubauer chamber. Differential cell counts were performed on cytospin preparations stained with Diff-Quick (Merz & Dade) using standard morphological criteria for cell type identification. Two hundred cells were counted per cytospin by a researcher blinded to the sample names.

Serum and breast milk antibody measurement

Sandwich ELISA was used to measure breast milk sIgA in PN15 mothers, serum IgA in PN 15 mothers and offspring, and fecal sIgA concentrations in PN15 offspring. Additionally, total IgG, OVA-specific IgG, and OVA-specific IgE were measured in the serum of PN49 allergic offspring by ELISA (BD Bioscience).

Serum LPS (endotoxin) measurement

Serum samples from G17 mothers, PN15 offspring, and PN49 offspring were diluted 1:100 in LAL (endotoxin-free) water and heat treated for 10 min at 80°C. Endotoxin concentration was measured using a kinetic turbidimetric test by Mikrobiologisches Labor Dr. Michael Lohmeyer GmbH.

Measurement of airway reactivity

Airway reactivity was measured in allergic offspring at PN49 by using a FlexiVent ventilator (SCIREQ). Mice were anesthetized and mechanically ventilated with a tidal respiratory rate of 150/min and a tidal volume of 10 mL/kg. Assessment of lung function was performed at baseline, followed by aerosolized methacholine (Sigma–Aldrich) at increasing doses (0.625, 1.25, 2.5, 5, 10, 20, and 40 mg/mL). Airway resistance is reported as Newtonian resistance.

FITC-Dextran intestinal permeability assay

Pregnant mice were treated from G8 to G17 orally with 25 μL of either vancomycin (20 mg/kg) or water mixed with 15μL Ora-Sweet. On PN15, female offspring were separated from their mothers for 1.5 h and then gavaged with 500 mg/kg of 4 KDa FITC-Dextran (Sigma). Food and water were removed for 1.5 h, then the animals were euthanized, and blood was collected from the retro-orbital sinus. Serum samples were diluted at 1:4, loaded on a black 96-well plate, and measured with the plate reader (Infinite® 200 PRO) at an excitation wavelength of 485 nm and an emission wavelength of 530 nm.

Statistical analysis

Samples were tested for normal distribution using a Shapiro-Wilk normality test. Parametric or nonparametric data were analyzed using either Student's *t*-test or a Mann–Whitney U test, respectively. Graphing and statistical tests were performed using the software GraphPad Prism 9.

Acknowledgments: We would like to thank the staff at the animal research facility of the Charité–Universitätsmedizin Berlin for their excellent animal work. Thank you to Dr. Patrick Maschmeyer for his assistance in creating the mouse flow cytometry panels. Finally, we thank Mireia Puig and Thordis Hohnstein for their excellent technical assistance. This work was supported through the Deutsche Forschungsgemeinschaft (DFG: grant CO 1058 3-2) as well as the Konrad Adenauer Foundation. The graphical abstract and Fig. 1 were created with BioRender.com.
Open access funding enabled and organized by Projekt DEAL.

Conflict of interest: The authors declare no commercial or financial conflict of interest.

Author contributions: MMA designed and conducted experiments, analyzed and interpreted data, and wrote the article; YA conducted experiments; WWM analyzed the microbiota and SCFA data; OH, CD, SH, and SG conducted flow cytometry experiments and analysis; NB and AP performed intestinal histology analysis; DL and JG performed airway reactivity analysis; MLC and GB conceived the study, provided funding, oversaw the research program and wrote the article.

Ethics approval statement: These experiments were approved by the Berlin authorities (Landesamt für Gesundheit und Soziales - LAGeSo) and were performed according to German and international regulatory guidelines.

Data availability statement: The data that support the findings of this study are available from the corresponding author upon reasonable request.

Peer review: The peer review history for this article is available at https://publons.com/publon/10.1002/eji.202350394

References

1 **Cait, A., Wedel, A., Arntz, J. L., Duinkerken, J., Datye, S., Cait, J., Alhasan, M. M. et al.**, Prenatal antibiotic exposure, asthma, and the atopic march: A systematic review and meta-analysis. *Allergy: Eur. J. Allerg. Clin. Immunol.* 2022. **77**: 3233–3248.

2 **Arrieta, M.-C., Stiemsma, L.1 T., Dimitriu, P. A., Thorson, L., Russell, S., Yurist-Doutsch, S., Kuzeljevic, B. et al.**, Early infancy microbial and metabolic alterations affect risk of childhood asthma. *Sci. Transl. Med.* 2015. 7:307ra152.

3 **Olin, A., Henckel, E., Chen, Y., Lakshmikanth, T., Pou, C., Mikes, J., Gustafsson, A. et al.**, Stereotypic immune system development in newborn children. *Cell.* 2018. **174**: 1277–1292.e14.

4 **Abrahamsson, T. R., Jakobsson, H. E., Andersson, A. F., Björkstén, B., Engstrand, L. and Jenmalm, M. C.**, Low gut microbiota diversity in early infancy precedes asthma at school age. *Clin. Exp. Allergy.* 2014. **44**: 842–850.

5 **Gensollen, T., Iyer, S. S., Kasper, D. L. and Blumberg, R. S.**, How colonization by microbiota in early life shapes the immune system. *Science.* 2016. **352**: 539–544.

6 **Zheng, D., Liwinski, T. and Elinav, E.**, Interaction between microbiota and immunity in health and disease. *Cell. Res.* 2020. **30**: 492–506.

7 **Kalbermatter, C., Fernandez Trigo, N., Christensen, S. and Ganal-Vonarburg, S. C.**, Maternal microbiota, early life colonization and breast milk drive immune development in the newborn. *Front. Immunol.* 2021. **12**: 1768.

8 **Martin, R., Nauta, A., Ben Amor, K., Knippels, L., Knol, J. and Garssen, J.**, Early life: Gut microbiota and immune development in infancy. *Benef. Microbes.* 2010. **1**: 367–382.

9 **Fujimura, K. E., Sitarik, A. R., Havstad, S., Lin, D. L., Levan, S., Fadrosh, D., Panzer, A. R. et al.**, Neonatal gut microbiota associates with childhood multisensitized atopy and T cell differentiation. *Nat. Med.* 2016. **22**: 1187–1191.

10 **Round, J. L. and Mazmanian, S. K.**, The gut microbiome shapes intestinal immune responses during health and disease. *Nat. Rev. Immunol.* 2009. **9**: 313.

11 **Herbst, T., Sichelstiel, A., Schär, C., Yadava, K., Bürki, K., Cahenzli, J., Mccoy, K. et al.**, Dysregulation of allergic airway inflammation in the absence of microbial colonization. *Am. J. Respirat. Crit. Care Med.* 2012. **184**: 198–205.

12 **Zhao, D., Su, H., Cheng, J., Wang, Xu, Xie, M., Li, K., Wen, L. et al.**, Prenatal antibiotic use and risk of childhood wheeze/asthma: A meta-analysis. *Pediatr. Allergy Immunol.* 2015. **26**: 756–764.

13 **Rantala, A. K., Tapia, G., Magnus, M. C., Stene, L. C., Jaakkola, J J.K., Størdal, K., Karlstad, Ø. et al.**, Maternal antibiotic use and infections during pregnancy and offspring asthma: The Norwegian Mother, Father and Child Cohort Study and a nationwide register cohort. *Eur. J. Epidemiol.* 2022. **37**: 983–992.

14 **Russell, S. L., Gold, M. J., Willing, B. P., Thorson, L., Mcnagny, K. M. and Finlay, B. B.**, Perinatal antibiotic treatment affects murine microbiota, immune responses and allergic asthma. *Gut. Microbes.* 2013. **4**: 158–164.

15 **Alhasan, M. M., Cait, A. M., Heimesaat, M. M., Blaut, M., Klopfleisch, R., Wedel, A., Conlon, T. M., Yildirim, A. O., Sodemann, E. B., Mohn, W. W., Bereswill, S. and Conrad, M. L.**, Antibiotic use during pregnancy increases offspring asthma severity in a dose-dependent manner. *Allergy.* 2020. **75**: 1979–1990.

16 **Bookstaver, P. B, Bland, C. M., Griffin, B., Stover, K. R., Eiland, L. S. and Mclaughlin, M.**, A review of antibiotic use in pregnancy. *Pharmacother. J. Hum. Pharmacol. Drug Ther.* 2015. **35**: 1052–1062.

17 **Momen, N. C. and Liu, X.**, Maternal antibiotic use during pregnancy and asthma in children: Population-based cohort study and sibling design. *Eur. Respir. J.* 2021. **57**: 2000937.

18 **Frati, F., Salvatori, C., Incorvaia, C., Bellucci, A., Di Cara, G., Marcucci, F. and Esposito, S.**, The role of the microbiome in asthma: The gut-lung axis. *Int. J. Mol. Sci.* 2018. **20**: 123.

19 **Sokolowska, M., Frei, R., Lunjani, N., Akdis, C. A. and O'Mahony, L. M**, Microbiome and asthma. *Asthma Res. Pract.* 2018. **4**: 1–9.

20 **Chen, C. M., Chou, H. C. and Yang, Y. C. S. H.**, Maternal antibiotic treatment disrupts the intestinal microbiota and intestinal development in neonatal mice. *Front. Microbiol.* 2021.**12**: 1356.

21 **Enaud, R., Prevel, R., Ciarlo, E., Beaufils, F., Wieërs, G., Guery, B. and Delhaes, L.**, The gut-lung axis in health and respiratory diseases: A place for inter-organ and inter-kingdom crosstalks. *Front. Cell Infect Microbiol.* 2020. **10**: 9.

22 **Budden, K. F., Gellatly, S. L., Wood, D. L. A., Cooper, M. A., Morrison, M., Hugenholtz, P. Hansbro, P. M. et al.**, Emerging pathogenic links between microbiota and the gut–lung axis. *Nat. Rev. Microbiol.* 2016. **15**: 55–63.

23 **Roduit, C., Frei, R., Ferstl, R., Loeliger, S., Westermann, P., Rhyner, C., Schiavi, E. et al.**, High levels of butyrate and propionate in early life are associated with protection against atopy. *Allergy* 2019. **74**: 799–809.

24 **Wu, W., Sun, M., Chen, F., Cao, A. T., Liu, H., Zhao, Y., Huang, X. et al.**, Microbiota metabolite short-chain fatty acid acetate promotes intestinal IgA response to microbiota which is mediated by GPR43. *Mucosal. Immunol.* 2016. **10**: 946–956.

25 **Ghosh, S. S., Wang, J., Yannie, P. J. and Ghosh, S.**, Intestinal barrier dysfunction, LPS translocation, and disease development. *J. Endocr. Soc.* 2020. **4**: bvz039.

26 **Dzidic, M., Abrahamsson, T. R., Artacho, A., Björkstén, B., Collado, M. C., Mira, A. and Jenmalm, M. C.**, Aberrant IgA responses to the gut microbiota during infancy precede asthma and allergy development. *J. Allergy Clin. Immunol.* 2017. **139**, 1017–1025.e14.

27 **Wagner, C., Torow, N., Hornef, M. W. and Lelouard, H.**, Spatial and temporal key steps in early-life intestinal immune system development and education. *FEBS J.* 2022. **289**: 4731–4757.

28 **Huang, Y., Mao, K., Chen, Xi, Sun, M.-A., Kawabe, T., Li, W., Usher, N. et al.**, S1P-dependent interorgan trafficking of group 2 innate lymphoid cells supports host defense. *Science* 2018. **359**: 114–119.

29 **Zeng, B., Shi, S., Ashworth, G., Dong, C., Liu, J. and Xing, F.**, ILC3 function as a double-edged sword in inflammatory bowel diseases. *Cell. Death Dis.* 2019. **10**: 1–12.

30 **Pu, Q., Lin, P., Gao, P., Wang, Z., Guo, K., Qin, S., Zhou, C. et al.**, Gut microbiota regulate gut–lung axis inflammatory responses by mediating ILC2 compartmental migration. *J. Immunol.* 2021. **207**: 257–267.

31 **Jarade, A., Garcia, Z., Marie, S., Demera, A., Prinz, I., Bousso, P., Di Santo, J. P. et al.**, Inflammation triggers ILC3 patrolling of the intestinal barrier. *Nat. Immunol.* 2022. **23**: 1317–1323.

32 **Hammond, K. A.**, Adaptation of the Maternal Intestine During Lactation. *J. Mammary Gland Biol. Neoplasia* 1997. **2**: 243–252.

33 **Poggi, A., Benelli, R., Venè, R., Costa, D., Ferrari, N., Tosetti, F. and Zocchi, M. R.**, Human gut-associated natural killer cells in health and disease. *Front. Immunol.* 2019. **10**: 961.

34 **Ganal-Vonarburg, S. C. and Duerr, C. U.**, The interaction of intestinal microbiota and innate lymphoid cells in health and disease throughout life. *Immunology* 2020. **159**: 39–51.

35 **Chang, Y., Kim, Ju W, Yang, S., Chung, D. H., Ko, J. S., Moon, J. S. and Kim, H. Y.**, Increased GM-CSF-producing NCR-ILC3s and neutrophils in the intestinal mucosa exacerbate inflammatory bowel disease. Wiley. https://doi.org/10.1002/cti2.1311

36 **Wang, L., Xiao, W., Zheng, Y., Xiao, R., Zhu, G., Wang, M., Li, Y. et al.**, High dose lipopolysaccharide triggers polarization of mouse thymic Th17 cells in vitro in the presence of mature dendritic cells. *Cell. Immunol.* 2012. **274**: 98–108.

37 **Chassaing, B., Srinivasan, G., Delgado, M. A., Young, A. N., Gewirtz, A. T. and Vijay-Kumar, M.**, Fecal lipocalin 2, a sensitive and broadly dynamic non-invasive biomarker for intestinal inflammation. *PLoS One* 2012. **7**: e44328.

38 **Huus, K. E., Petersen, C. and Finlay, B. B**, Diversity and dynamism of IgA–microbiota interactions. *Nat. Rev. Immunol.* **21**: 514–525.

39 **Mirpuri, J., Raetz, M., Sturge, C. R., Wilhelm, C. L., Benson, A., Savani, R. C., Hooper, L. V. et al.**, Proteobacteria-specific IgA regulates maturation of the intestinal microbiota. *Gut. Microbes.* 2013. **5**: 28–39.

40 **Rogier, E. W., Frantz, A. L., Bruno, M. E. C., Wedlund, L., Cohen, D. A., Stromberg, A. J. and Kaetzel, C. S.**, Secretory antibodies in breast milk promote long-term intestinal homeostasis by regulating the gut microbiota and host gene expression. *Proc. Natl. Acad. Sci. U. S. A.* 2014. **111**: 3074–3079.

41 **Takeuchi, T., Miyauchi, E., Kanaya, T., Kato, T., Nakanishi, Y., Watanabe, T., Kitami, T. et al.**, Acetate differentially regulates IgA reactivity to commensal bacteria. *Nat.* 2021. **595**: 560–564.

42 **Kim, M., Qie, Y., Park, J. and Kim, C. H.**, Gut microbial metabolites fuel host antibody responses. *Cell. Host Microbe.* 2016. **20**: 202–214.

43 **Salguero, M. V., Al-Obaide, M. A. I., Singh, R., Siepmann, T. and Vasylyeva, T. L.**, Dysbiosis of Gram-negative gut microbiota and the associated serum lipopolysaccharide exacerbates inflammation in type 2 diabetic patients with chronic kidney disease. *Exp. Ther. Med.* 2019. **18**: 3461.

44 **Phillippi, D. T., Daniel, S., Pusadkar, V., Youngblood, V. L., Nguyen, K. N., Azad, R. K., Mcfarlin, B. K. et al.**, Inhaled diesel exhaust particles result in microbiome-related systemic inflammation and altered cardiovascular disease biomarkers in C57Bl/6 male mice. *Part. Fibre. Toxicol.* 2022. **19**: 1–29.

45 **Zhou, S-Yi, Gillilland, M., Wu, X., Leelasinjaroen, P., Zhang, G., Zhou, H., Ye, Bo et al.**, FODMAP diet modulates visceral nociception by lipopolysaccharide-mediated intestinal inflammation and barrier dysfunction. *J. Clin. Invest.* 2018. **128**: 267–280.

46 **Park, J-H., Jeong, So-Y, Choi, Ah-J and Kim, S-J**, Lipopolysaccharide directly stimulates Th17 differentiation in vitro modulating phosphorylation of RelB and NF-κB1. *Immunol. Lett.* 2015. **165**: 10–19.

47 **Ohnmacht, C., Park, J-H., Cording, S., Wing, J. B., Atarashi, K., Obata, Y., Gaboriau-Routhiau, V. et al.**, The microbiota regulates type 2 immunity through RORγt+ T cells. *Science* 2015. **349**: 989–993.

48 **Luo, W., Hu, J., Xu, W. and Dong, J.**, Distinct spatial and temporal roles for Th1, Th2, and Th17 cells in asthma. *Front. Immunol.* 2022. **13**: 4598.

49 **Zhao, Y., Yang, J., Gao, Ya-D and Guo, W.**, Th17 immunity in patients with allergic asthma. *Int. Arch. Allergy Immunol.* 2010. **151**: 297–307.

50 **Na, H., Lim, H., Choi, G., Kim, B-K., Kim, S-H., Chang, Y-S., Nurieva, R. et al.**, Concomitant suppression of TH2 and TH17 cell responses in allergic asthma by targeting retinoic acid receptor–related orphan receptor γt. *J. Allergy Clin. Immunol.* 2018. **141**: 2061–2073.e5.e5.

51 **Conrad, M. L., Yildirim, A. Ö., Sonar, S. S., Kılıç, A., Sudowe, S., Lunow, M., Teich, R. et al.**, Comparison of adjuvant and adjuvant-free murine experimental asthma models. *Clin. Exp. Allergy* 2009. **39**: 1246–1254.

52 **Schloss, P. D., Westcott, S. L., Ryabin, T., Hall, J. R., Hartmann, M., Hollister, E. B., Lesniewski, R. A. et al.**, Introducing mothur: Open-source, platform-independent, community-supported software for describing and comparing microbial communities. *Appl. Environ. Microbiol.* 2009. **75**: 7537–7541.

53 **Pruesse, E., Quast, C., Knittel, K., Fuchs, B. M., Ludwig, W., Peplies, J. and Glockner, F. O.**, SILVA: A comprehensive online resource for quality checked and aligned ribosomal RNA sequence data compatible with ARB. *Nucleic Acids Res.* 2007. **35**: 7188–7196.

54 **Mcmurdie, P. J. and Holmes, S.**, An R package for reproducible interactive analysis and graphics of microbiome census data. *PLoS One* 2013. **8**: e61217.

55 **Gómez-Gallego, C., Jaakkola, U. M., Salminen, S., Periago, M. J., Ros, G., Frias, R. and Iio**, A method to collect high volumes of milk from mice. *An. Vet. Murcia.* 2013. **29**: 55–61.

56 **Gronke, K., Kofoed-Nielsen, M. and Diefenbach, A.**, Isolation and flow cytometry analysis of innate lymphoid cells from the intestinal lamina propria. *Methods Mol. Biol.* 2017. **1559**: 255–265.

57 **Duerr, C. U. and Fritz, J. H.**, Isolation of group 2 innate lymphoid cells from mouse lungs. *Methods Mol. Biol.* 2017. **1656**: 253–261.

Abbreviations: **BAL**: bronchoalveolar lavage · **G**: Gestation day · **PN**: Postnatal day · **SCFA**: Short-chain fatty acids · **sIgA**: secretory immunoglobulin A · **SI-LP**: Small intestine lamina propria

Full correspondence: Dr. Melanie Conrad, Charité–Universitätsmedizin Berlin, Institute of Microbiology, Infectious Diseases and Immunology, Hindenburgdamm 30, 12203 Berlin, Germany
e-mail: conradml@gmail.com

Received: 13/1/2023
Revised: 16/5/2023
Accepted: 21/6/2023

Supplementary Tables and Figures

Supplementary Table 1: Phylogenetic classification of bacterial clade changes in the faeces from antibiotic treated versus control mothers (time points G17 and PN21), as well as their Prenatal-Antibiotic compared with Prenatal-Control offspring (time points PN21 and PN49). Measured by 16S rRNA sequencing. Classification: k - kingdom; p - phylum; o – order; f - family; g - genus. Grey highlighted cells represent the most abundant clades. Student's t-test or Mann Whitney test of antibiotic exposed compared against control at each specific time point. A blank cell = no difference between control and antibiotic treated groups. *P < .05, **P < .01, ***P < .001. ****P < 0.0001.

	Mother after antibiotics (G17)	Mother weaning (PN21)	Offspring weaning (PN21)	Offspring asthma (PN49)
g_Akkermansia		Inc*	Inc****	Inc**
g_Bacteriodes			Inc****	Inc****
p_Bacteroidetes	Inc***	Inc*		
g__Blautia		Inc*	Inc****	Inc*
f__Desulfovibrionaceae	Inc**			
f__Enterobacteriaceae	Inc*			
g__Escherichia	Inc**		Inc****	
g__Parabacteroides	Inc**	Inc*		Inc****
p__Proteobacteria	Inc**			
p_Proteobacteria	Inc****	Inc*	Inc****	
g__Sutterella	Inc***	Inc***	Inc**	Inc*
p_Verrucomicrobia		Inc*	Inc****	Inc**
o__Bacteroidales		Dec*	Dec****	Dec****
g__Bilophila	Dec**			
g__Butyricicoccus	Dec***	Dec**	Dec*	
g__Candidatus_Arthromitus	Dec***			Dec**
g__Clostridium	Dec***	Dec*	Dec*	
g__Clostridium	Dec***		Dec**	Dec**
g__Clostridium		Dec***	Dec**	Dec***
g__Coprobacillus	Dec**	Dec*		Dec**
g__Coprococcus	Dec***	Dec**	Dec****	Dec**
g__Dehalobacterium	Dec***	Dec***	Dec****	Dec**
g__Dorea	Dec***	Dec***	Dec*	
f__F16	Dec***		Dec**	Dec*
p__Firmicutes	Dec***	Dec*	Dec****	Dec**
p_Firmicutes	Dec****	Dec***	Dec***	
f__Lachnospiraceae	Dec***	Dec**	Dec**	
g__Lactobacillus			Dec*	
f__Mogibacteriaceae			Dec*	Dec**
g__Oscillospira	Dec***	Dec**	Dec***	
g__Odoribacter	Dec****	Dec****	Dec****	Dec****
g__Prevotella	Dec**	Dec***	Dec****	Dec****
g__Prevotella	Dec***		Dec****	Dec****
o__RF39	Dec ***	Dec*		Dec***
f__Rikenellaceae	Dec**		Dec*	
f__Ruminococcaceae	Dec****	Dec**	Dec****	Dec**
g__Ruminococcus	Dec****	Dec**	Dec**	Dec***
f__S24-7 p_(o_Bacteriodales)	Dec***	Dec*	Dec****	Dec***

Supplementary Figure 1

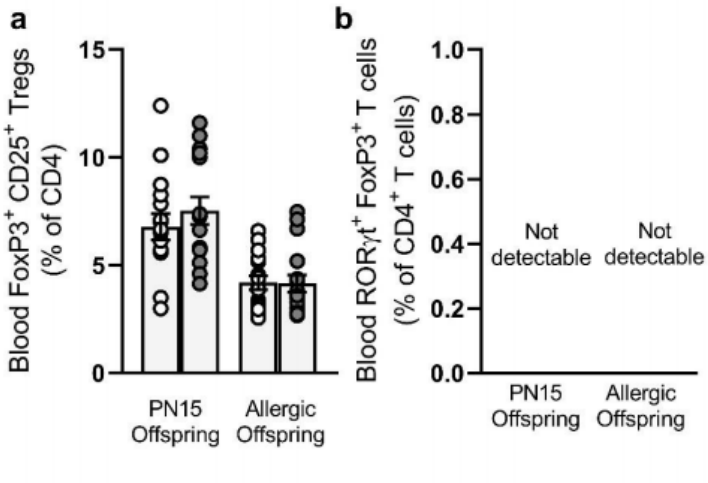

Supplementary Figure 1

Analysis of Treg and RORγt Treg populations in the blood of Prenatal-Control versus Prenatal-Antibiotic offspring in early life at PN15 and after allergy induction at PN49. **a** FoxP3+ CD25+ Tregs (from CD4+ T cells). **b** RORγt+ FoxP3+ Tregs (from CD4+ T cells). **a-b** Prenatal-Control offspring and Prenatal-Antibiotic offspring n = 16. Means ± SEM are shown. Data shown is pooled from two replicated experiments showing the same trends. Student's t-test or Mann Whitney test found no significant difference between antibiotic exposed compared against control at each specific time point.

Supplementary Figure 2

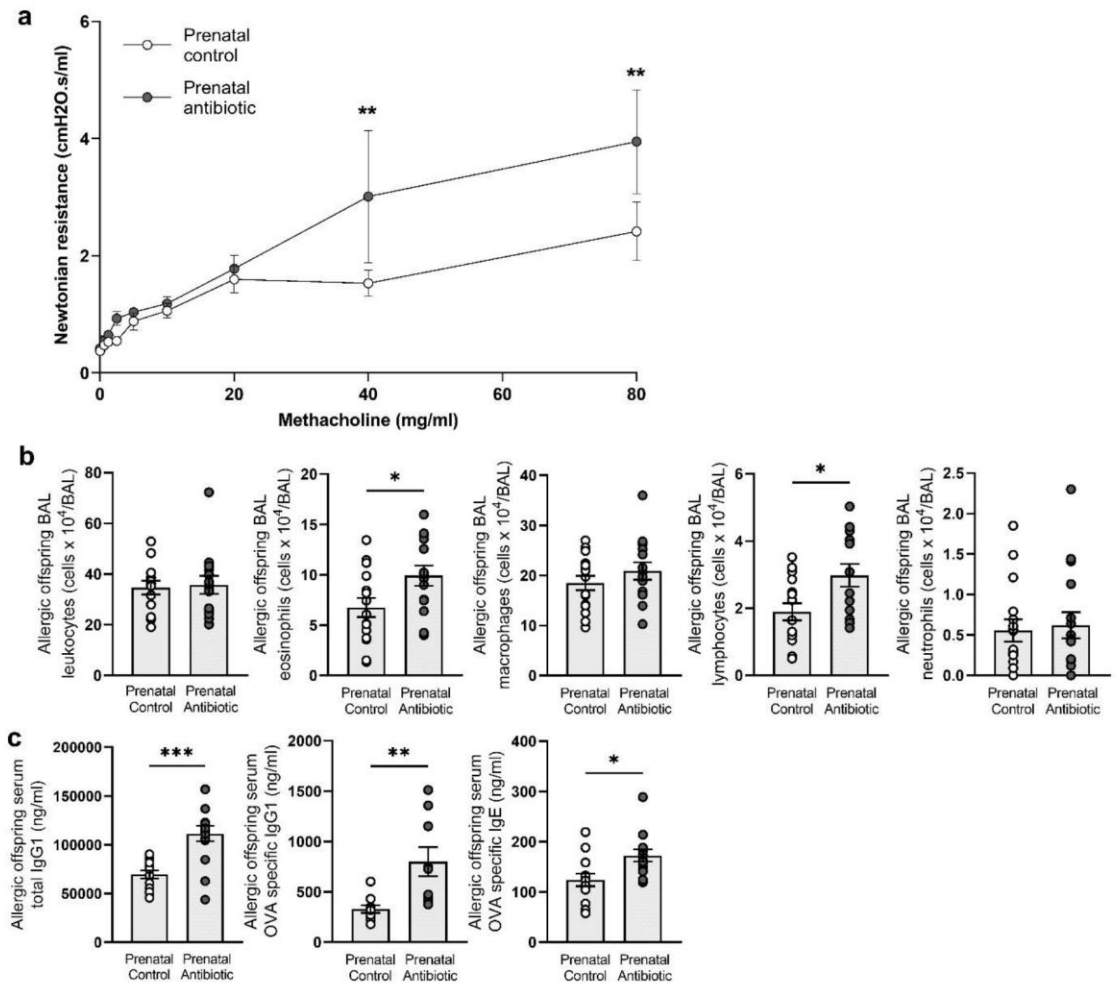

Supplementary Figure 2

Antibiotic treatment during pregnancy results in a more severe asthma phenotype in the offspring. **a** Methacholine Dose-response curve demonstrates a significant increase in airway hyperreactivity (expressed via Newtonian resistance) in Prenatal-Antibiotic allergic offspring. **b** Differential cells count of bronchoalveolar lavage (BAL) cytospins of allergic offspring; Leukocytes, eosinophils, macrophages, lymphocytes, and neutrophils. **c** Allergic offspring serum antibody measurements via ELISA; Total IgG1, OVA specific IgG1, OVA specific IgE. Means ± SEM are shown, Airway reactivity test (n = 12), Cytospins (n=16), total IgG1 and OVA IgE measurements (n=13), OVA IgG1 (n=9). Significance is represented by *P < .05, **P < .01, ***P < .001, Student's t-test or Mann Whitney test of prenatal-Antibiotic offspring compared against Prenatal-Control.

Supplementary Figure 3

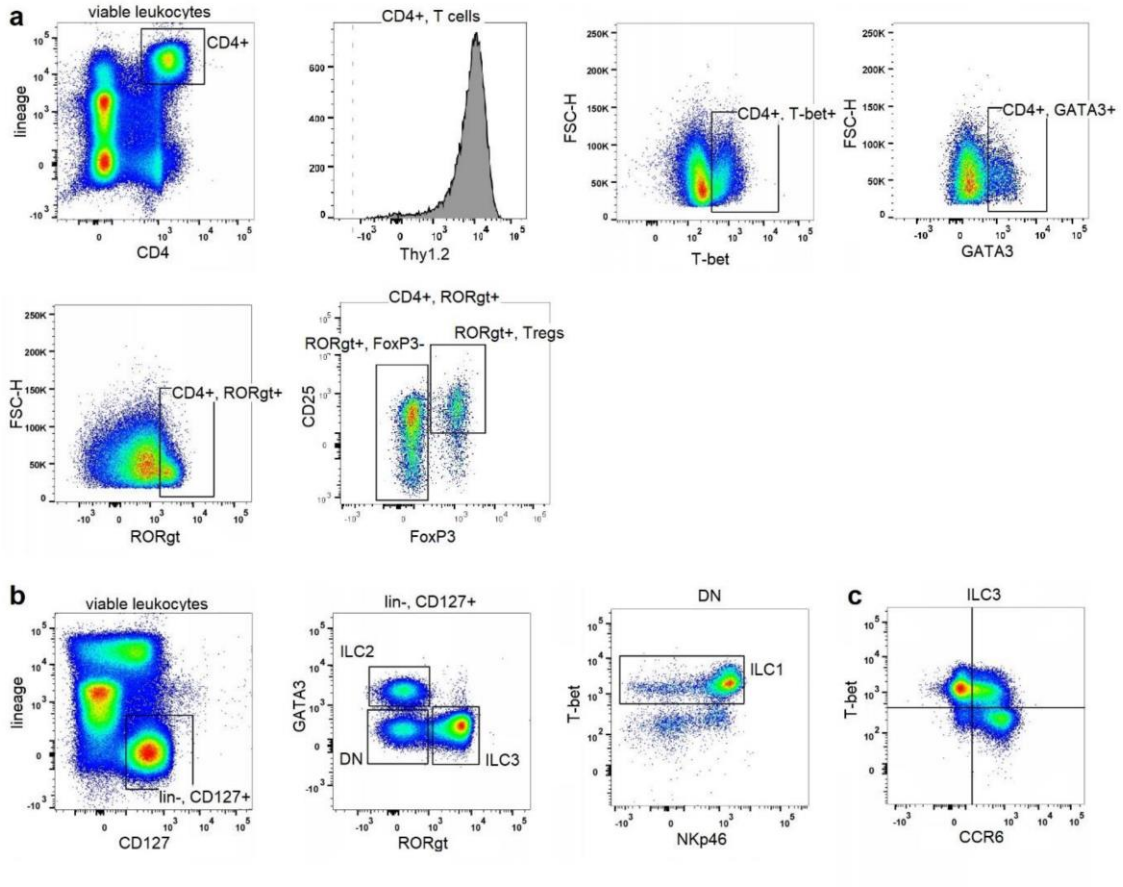

Supplementary Figure 3

Flow cytometry gating strategy for the small intestine lamina propria. **a** After removing doublets and dead cells, leukocytes were isolated via CD45 and three groups were examined. CD4+ T cells and the subpopulations T-bet+, GATA3+ and RORγt+. **b** Total ILCs were defined as Lin- CD127 then from this gate, ILC subgroups were identified as follows: ILC1 (T-bet+ GATA3-, RORγt-), ILC2 (GATA3+, RORγt-) and ILC3 (RORγt+, GATA3-). **c** ILC3 subpopulations were identified as NCR- (CCR6+, T-bet-), NCR+ (CCR6-, T-bet+), and CCR6+, T-bet+. Lineage mix contained (CD3e, CD5, CD19, Gr1, TCRβ, TCRγδ).

Supplementary Figure 4

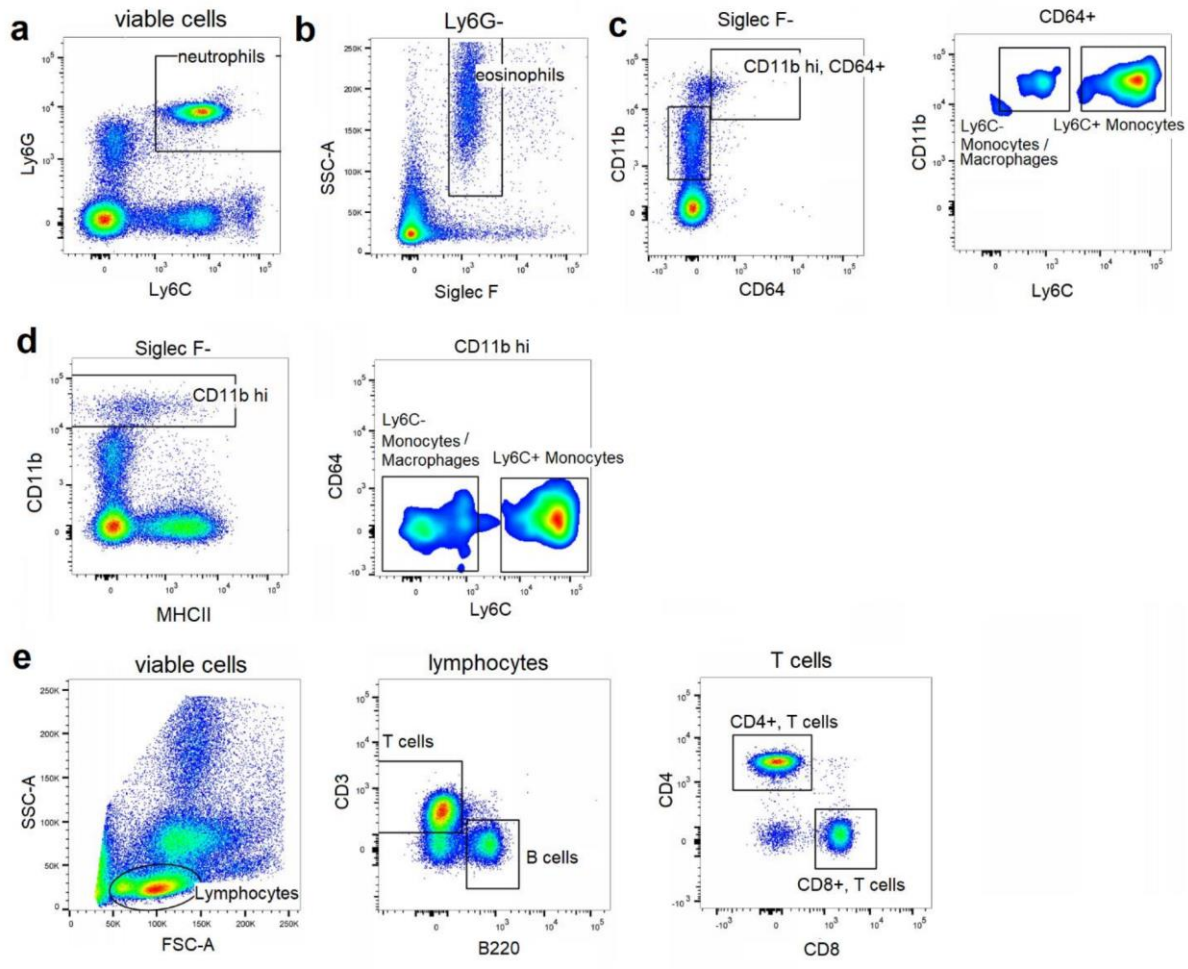

Supplementary Figure 4

Flow cytometry gating strategy for the lung and blood lymphoid cells and blood myeloid cells. First doublets and dead cells were removed then leukocytes were gated as flowing **a** Ly6G+ neutrophils. **b** Siglec F+ SSC hi eosinophils. **c** CD64+ Ly6C+/- monocytes. **d** CD11b hi Ly6C+/- monocytes. **e** B and T lymphocytes were gated as SSC low, FSC low. B220+ defined B cells and CD3 defined T cells. T cells were also gated further for CD4+ T cells and CD8+ T cells.

Supplementary Figure 5

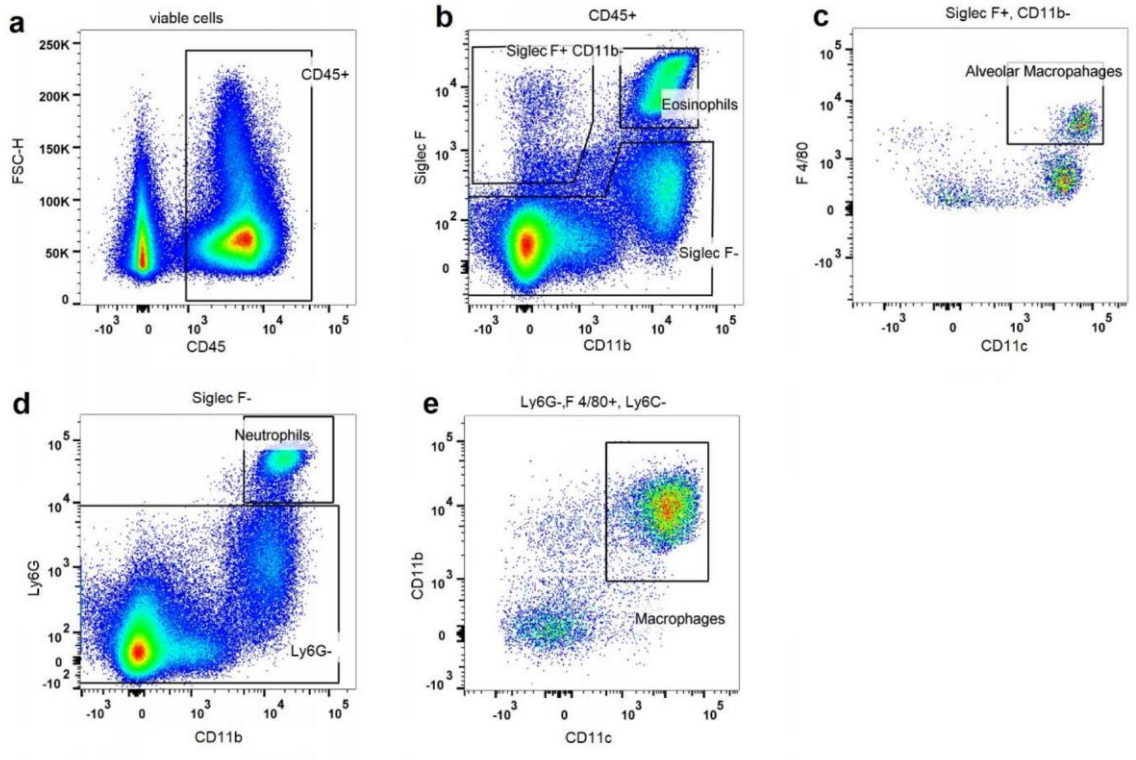

Supplementary Figure 5

Flow cytometry gating strategy for lung myeloid cells. **a** Viable leukocytes were gated for CD45+. **b** Eosinophils were defined as SiglecF+ CD11b+. **c** From the SiglecF+ CD11b- population, alveolar macrophages were defined as CD11c+ F4/80+. **d** From the Siglec F- population, neutrophils were defined as Ly6G+ CD11b+. **e** From the Ly6G- Ly6C- F4/80+ population, macrophages were defined as CD11b+ CD11c+.

Curriculum Vitae

Mein Lebenslauf wird aus datenschutzrechtlichen Gründen in der elektronischen Version meiner Arbeit nicht veröffentlicht.

Publication list

1. **Alhasan MM**, Hölsken O, Duerr C, Helfrich S, Branzk N, Philipp A, Leitz D, Duerr J, Almousa Y, Barrientos G, Mohn WW, Gamradt S, Conrad ML. Antibiotic use during pregnancy is linked to offspring gut microbial dysbiosis, barrier disruption, and altered immunity along the gut-lung axis. Eur J Immunol. 2023 Oct;53(10):e2350394. doi: 10.1002/eji.202350394. Epub 2023 Jul 10. PMID: 37431194.

2. Arntz JL, **Alhasan MM**, Datye S, Kahhaleh FG, Almousa Y, Barrientos G, Schwiertz A, Conrad ML. Low-dose perinatal supplementation with Enterococcus faecalis increases concentrations of short-chain fatty acids in the offspring but does not protect against allergic asthma. Int Immunol. 2023 Oct 6;35(10):475-482. doi: 10.1093/intimm/dxad025. PMID: 37464466.

3. **Alhasan MM**, Habazin S, Kahhaleh FG, Lauc G, Conrad ML, Novokmet M. Mouse milk immunoglobulin G Fc-linked N-glycosylation nano-LC-MS analysis in a model of vancomycin exposure during pregnancy. Anal Bioanal Chem. 2023 May;415(12):2239-2247. doi: 10.1007/s00216-023-04635-5. Epub 2023 Mar 14. Erratum in: Anal Bioanal Chem. 2023 Mar 30;: PMID: 36914840.

4. Cait A, Wedel A, Arntz JL, Duinkerken J, Datye S, Cait J, **Alhasan MM**, Conrad ML. Prenatal antibiotic exposure, asthma, and the atopic march: A systematic review and meta-analysis. Allergy. 2022 Nov;77(11):3233-3248. doi: 10.1111/all.15404. Epub 2022 Jun 27. PMID: 35689800.

5. **Alhasan MM**, Cait AM, Heimesaat MM, Blaut M, Klopfleisch R, Wedel A, Conlon TM, Yildirim AÖ, Sodemann EB, Mohn WW, Bereswill S, Conrad ML. Antibiotic use during pregnancy increases offspring asthma severity in a dose-dependent manner. Allergy. 2020 Aug;75(8):1979-1990. doi: 10.1111/all.14234. Epub 2020 Mar 11. PMID: 32064643.

6. Sodemann EB, Dähling S, Klopfleisch R, Boiarina E, Cataldo D, **Alhasan MM**, Yildirim AÖ, Witzenrath M, Tabeling C, Conrad ML. Maternal asthma is associated with persistent changes in allergic offspring antibody glycosylation. Clin Exp Allergy. 2020 Apr;50(4):520-531. doi: 10.1111/cea.13559. Epub 2020 Jan 28. PMID: 31912551.

Acknowledgments

“He who does not thank the people is not thankful to God.”

Muhammad, 570 CE.

My sincere gratitude and acknowledgment are extended to everyone who helped me along the way. My greatest thanks go to my supervisor, Dr. Melanie Conrad, who gave me a chance and believed in a refugee whose dreams were completely stolen and destroyed at the hands of a dictator. Her support is a debt that I will never be able to repay. Additionally, I am grateful to Dr. Markus Heimesaat for his support, and to all my lab colleagues (Yahia, Fariz, Jeanne, and Swarali) with whom I spent some of my best years. Lastly, I want to express my gratitude to my parents, Mahmoud and Samer; my siblings Abdulrahman, Eman, Islam, and Momena; my wife, Nour; and my children Mahmoud, Marya, and Josef for their patience, understanding, and unwavering support. I could not have accomplished anything without you.